Universidade do Minho
Escola de Engenharia

João Pedro Mendes Lopes

Towards a Human-in-the-Loop Control for a Smart Orthotic System

Dissertação de Mestrado

Mestrado Integrado em Engenharia Biomédica

Ramo de Eletrónica Médica

Trabalho efetuado sob a orientação do(s)

Professora Doutora Cristina Manuela Peixoto Santos

Doutora Joana Sofia Campos Figueiredo

Universidade do Minho

Doutora Elena Garcia Armada

Consejo Superior de Investigaciones Científicas

Universidad Politécnica de Madrid

dezembro de 2019

AGRADECIMENTOS

O final de uma importante etapa chega hoje ao fim. Há cinco anos atrás ingressei na *mui nobre* Universidade do Minho para me graduar em Engenharia Biomédica. Confesso que não foi a minha primeira opção pois sempre quis estudar no meu Porto, manter-me junto dos meus familiares e dos meus grandes amigos de vida. No entanto, quis o destino que eu viesse formar-me em Braga. Passados estes cinco anos, hoje posso dizer que foi o melhor que me poderia ter acontecido. Esta universidade ensinou-me a ser a pessoa independente que hoje sou. Aqui, conheci aqueles que serão também eternamente meus amigos. Foram anos repletos de grandes convivências e de muita felicidade. Foram, também, anos de muito estudo, em que vivemos momentos de muita tensão e cansaço. Enganem-se os que julgam que a vida de estudante é o melhor que se pode ter. É uma etapa muito importante na vida profissional e pessoal que deve ser encarada com muito empenho e dedicação. Estudar não é um fardo, mas sim um investimento. Hoje, sinto-me pronto para dar o meu contributo à sociedade.

Restam-me, por isso, os agradecimentos. Os meus maiores agradecimentos vão para os meus pais e irmão, três pessoas fundamentais na minha vida. Agradeço aos meus pais pelo seu incansável esforço, por me apoiarem sempre nos bons e nos maus momentos. Sem eles, estes cinco anos não seriam possíveis. Agradeço ao meu irmão por todos momentos fraternos que vivemos e pelos três anos conjuntos de vida universitária que recordarei com muito carinho. Aos meus pais, desejo que a vida os sorria sempre e que possam, agora, viver um pouco mais, aproveitar a vida ao máximo que o tempo não volta. Ao meu irmão, desejo tudo do melhor que o mundo possa oferecer e que estude muito, reforço, para que seja o Engenheiro bem-sucedido que eu vejo nele. Agradeço, também, aos meus companheiros de vida e amigos eternos, por todo o apoio, carinho e amizade que sempre senti na vossa presença. Cátia, Fábio, Rafaela, Patrícia, Paula, Ana Luís, o meu muito obrigado pelos mais de 10 anos de amizade. É uma década de amizade verdadeira e de momentos inesquecíveis. Aos meus amigos universitários, também eles eternos, agradeço por estes cinco anos maravilhosos que, juntos, vivemos em Braga. Luís, Margarida, Cristiana, Luciana, Pedro, Ana e Carla, o meu sincero obrigado pela vossa amizade, dedicação e apoio nesta jornada.

Por fim, agradeço à minha orientadora, professora Doutora Cristina Santos, pela orientação e oportunidade de trabalhar neste projeto. À minha colega Doutora Joana Figueiredo, agradeço pelo seu apoio e visão na realização desta dissertação, e aos meus colegas de laboratório o meu muito obrigado por prontamente me ajudarem sempre que necessitei.

Um bem-haja a todos vós.

STATEMENT OF INTEGRITY

I hereby declare having conducted this academic work with integrity. I confirm that I have not used plagiarism or any form of undue use of information or falsification of results along the process leading to its elaboration.

I further declare that I have fully acknowledged the Code of Ethical Conduct of the University of Minho.

RESUMO

O AVC é uma das maiores causas de paralisia. Esta patologia, cada vez mais com maior incidência nos jovens, tem provocado um aumento considerável de pessoas com problemas de mobilidade. Com uma terapia focada a cada caso clínico, a recuperação total ou parcial pode ser conseguida. As ortóteses ativas têm vindo a ser desenvolvidas com o propósito de promover uma recuperação eficaz, baseada em treinos repetitivos e numa participação ativa dos utilizadores. Várias abordagens de controlo têm vindo a ser desenvolvidas para controlar estes dispositivos, mas nenhuma delas promove uma estratégia orientada às necessidades do utilizador. Na tentativa de solucionar este problema, uma nova abordagem, designada por *Human-in-the-loop* está a emergir. Baseada no custo energético, esta estratégia permite adaptar parâmetros da assistência, promovendo uma terapia focada e direcionada a cada utilizador. No entanto, para estimar o custo energético, recorre-se ao uso de sensores que não são adequados para contexto clínico. Assim, torna-se necessário estudar novas formas de estimar o custo energético.

Nesta dissertação são apresentados os primeiros passos para introduzir o controlo *Human-in-the-loop* numa ortótese ativa. Para isso, duas estratégias foram apresentadas: uma estratégia que permite adaptar a trajetória angular da ortótese, em tempo real, e outra que promove a adaptação da complacência do sistema ao longo do ciclo da marcha. Ambas foram validadas com sujeitos saudáveis. Relativamente à primeira abordagem, a ortótese foi capaz de modificar a sua assistência em microssegundos, e os utilizadores foram capazes de a seguir com um erro mediano inferior a 10%. No que diz respeito à segunda abordagem, os resultados mostram que a ortótese promoveu uma alteração eficaz da complacência de interação, promovendo uma participação ativa do utilizador durante a sua assistência.

O impacto energético do uso do sistema robótico é, também, apresentado. Promovendo um aumento do custo energético em mais de 30%, a necessidade da estratégia *Human-in-the-loop* foi realçada. Na tentativa de encontrar uma técnica para estimar o custo energético, recorreu-se ao uso de *machine learning*. Os resultados, obtidos com uma MLP e uma LSTM, provam que é possível estimar o custo energético com um erro médio próximo dos 11%.

Trabalho futuro passa pela implementação do modelo em tempo real e a recolha de mais dados com as abordagens de controlo apresentadas, de forma a construir um modelo mais robusto.

PALAVRAS-CHAVE

Controlo de trajetória adaptativa, Controlo de impedância *assisted-as-needed*, Controlo *Human-in-the-loop*, Ortóteses ativas, Reabilitação de AVC

Abstract

Stroke is the main cause of paralysis. This pathology has provoked a considerable increase of persons with motor impairments. With a therapy focused on each clinical case, the total or partial recovery can be achieved. Powered orthoses have been developed to promote an effective recover, based on repetitive gait training and user's active participation. Many control approaches have been developed to control these devices, but none of them promotes an user-oriented strategy focused to the user's needs. In an attempt of solving this issue, a new approach named Human-in-the-loop is emerging. This strategy allows the adaptation of some assistive parameters based on the user's energetic cost, promoting a therapy tailored to each end-user needs. However, to estimate the energy expenditure, the use of non-ergonomic sensors, not suitable for clinical context, is required. Thus, it is necessary to find new ways of estimating energy expenditure using wearable and comfortable sensors.

In this dissertation, the first steps to introduce the Human-in-the-loop strategy into a powered orthosis are presented. For this purpose, two strategies were developed: a strategy that allows the angular trajectory adaptation in real-time and other that promotes a stiffness adaptation all over the gait cycle. Both strategies were validated with healthy subjects. In the first strategy, the orthosis was able to modify its assistance in a fraction of microseconds, and the end-users were able to follow her with a median error below 10%. Regarding the second strategy, the results show that the orthosis allowed an effective change in the systems' interaction stiffness, promoting an active participation of each user during its assistance.

The energetic impact of using the robotic assistive device is also presented. As it promotes an energy expenditure augmentation in more than 30% in comparison to walk without the device, the necessity of implementing the Human-in-the-loop strategy was highlighted. In an attempt of finding an ergonomic technique to estimate the energetic cost, the use of machine learning algorithms was tested. The results, obtained with a MLP and a LSTM, prove that it is possible to estimate the energy expenditure with a mean error close to 11%.

Future work consists in the implementation of the model in real-time and the collection of more data with the aforementioned control approaches, in a way of constructing a more robust model.

Keywords

Adaptive Trajectory Control, Assisted-as-needed impedance control, *Human-in-the-loop* control, Powered Orthoses, Stroke Rehabilitation

TABLE OF CONTENTS

INDEX OF FIGURES

INDEX OF TABLES

List of Abbreviations and Acronyms

AAN – Assisted-as-needed;

AEE – Activity Energy Expenditure;

AFO – Ankle-Foot-Orthosis;

ANN – Artificial Neural Network;

APP – Application;

BEE – Basal Energy Expenditure;

BF – *Bicep Femoris*;

BMR – Basal Metabolic Rate;

BR – Breath rate;

CCU – Central Controller Unit;

CNN – Convolutional neural network;

DOF – Degree-of-freedom;

EDA – Electrodermal activity;

EE – Energy Expenditure;

EMG – Electromyography;

FF – Flat foot;

FSR – Force-sensing resistor;

GL – *Gastrocnemius Lateralis*

HKAF – Hip-Knee-Ankle-Foot orthosis;

HK – Hip-Knee orthosis;

HO – Heel off;

HR – Heart rate;

HS – Heel strike;

IMU – Inertial measurement unit;

KAF – Knee-Ankle-Foot orthosis;

LLOS – Low-level orthosis system;

MLP – Multilayer perceptron;

MSt – Mid-Stance;

MSw – Mid-Swing;

MV – Minute ventilation;

MVC – Maximum voluntary contraction;

PCC – Pearson Correlation Coefficient;

PD – Proportional-derivative;

PI – Proportional-integral;

PID – Proportional-integrative-derivative;

PAFO – Powered Ankle-Foot orthosis;

PHO – Powered Hip orthosis;

PKO – Powered Knee orthosis;

RMSE – Root Mean Squared Error;

ROM – Range of motion;

ROT – Range of torque;

RNN – Recurrent Neural Network;

RQ – Research questions;

SPC – Spearman Correlation Coefficient;

TA – *Tibialis Anterior*;

TO – Toe off;

VL – *Vastus Lateralis*;

$\dot{V}O_2$ – Carbon dioxide flow;

$\dot{V}O_2$ – Oxygen flow;

WHO – World Health Organization;

WML – Wearable motion lab;

1. INTRODUCTION

This dissertation presents the work developed since February of 2019 in the scope of the fifth year of the degree in Biomedical Engineering, aiming to obtain the master's degree in the field of Medical Electronics. The work was performed in the Biomedical Robotic Devices Laboratory (BiRD Lab) of the Centre for Microelectromechanical Systems (CMEMS), at the University of Minho, Portugal, in agreement with the Smart Wearable Orthotic System (SmartOs) project.

This dissertation was the culminate of a project started in the second semester, since an Erasmus Internship was made between September of 2018 and February of 2019 at Marsi-Bionics enterprise, in Madrid, Spain. The work developed in Marsi-Bionics was related with the one presented in this dissertation since, during the internship, knowledge in human locomotion was achieved. There, the modulation of the human body as a three-link inverted pendulum was performed, studying the human gait and more precisely, the standing position. Also, the main advances in exoskeletons and assistive orthoses was followed closely, allowing for deepening the knowledge in the field of human locomotion and rehabilitation with orthotic devices.

In this first chapter, the motivation and problem statement of this dissertation will be presented, as well as the dissertation goals, contributions and outline.

1.1 Motivation and Problem Statement

According to WHO, almost one billion persons suffer from a disability. This represents nearly 15% of the world's population and the number tends to increase since the average life expectancy is rising and the population is aging, making disability a recurring term in daily life [1]. Considering disability due to mobility impairments, the population affected drops to 1% of the world's population. Around 60 million persons are affected by mobility injuries, either caused by the simple process of aging (36 million citizens) or by health disorders (24 million citizens). Many health conditions, as Post-Polio Syndrome, Cerebral Palsy, Neurofibromatosis, Traumatic Brain injury, Spinal Cord injury, Multiple Sclerosis, Stroke, and others, are becoming to be one of the leading causes of motor disabilities through the younger population [2].

Stroke, a worldwide and ageless cerebrovascular disorder, is the world's third cause of death [3]. It affects more than 15 million persons per year of which 6 million do not survive. Stroke is the main cause of death in Portugal (leader among the European countries), affecting more than two hundred Portuguese

citizens per one hundred thousand habitants. This disease, classified as haemorrhagic or ischemic, depending if it is caused by, respectively, a disruption of a brain vessel or an embolic occlusion [4], cause several disorders on brain tissues, such as sensory or memory deficits, motor aphasia, facial paralysis and, among others, lower and/or upper limbs hemiparesis [4], [5]. Stroke survivors also commonly present impaired motor coordination, muscular morbidity, high articulation stiffness and the walking pattern highly corrupted [5], particularly on the ankle articulation [6]. As such, these persons need a complete and rigorous plan of rehabilitation.

With the astonishing incidence of cardiovascular and neurodegenerative disorders on the world's population and in specific in Portugal's population, the biomedical search has been focusing on the use of robotic assistive devices, such as powered orthoses, aiming for the time-effective recovery of subjects with motor impairments. Many control approaches, as electromyography-based control, trajectory tracking control and impedance control, have been proposed to promote a therapy sustained in the user's participation, effort and in a repetitive gait training [7]. Most of the current powered orthoses accomplished with success these three principals. However, most of them do not use these assistive strategies to promote an user-oriented therapy, where the assistance could be timely modified and tailored to each end-user needs.

In an attempt to solve this problem, the investigators are now focusing in another fundamental question: the energetic cost that these orthotic devices can represent when used by impaired persons. A new strategy termed Human-in-the-loop control is being investigated, by means of using the energy expenditure as a way of adapting the assistance to each user [6]. However, estimating the energy expenditure is challenging task. Energy expenditure is frequently evaluated through indirect calorimetry, which is a reliable technique but not suitable for daily live and clinical usage. It is dependent on a team of experts, is an expensive technique, and it also presents a very noisy signal. Thus, new ways of estimating energy expenditure using wearable and ergonomic sensors are being studied, addressing machine learning-based models. With a reliable model for estimating the energy expenditure, it is possible to successfully apply the Human-in-the-loop control; thus, leading to a more effective and efficient recovery, where the assistance can be modified for each end-user.

1.2 Dissertation Goals

The main goal of this dissertation addresses the first advances of a new control strategy, named Human-in-the-loop control, for a Smart Orthotic system - SmartOs. This strategy makes use of a physiological

signal, namely the energy expenditure, to adapt the assistance for each user, allowing an user-oriented assistance and rehabilitation based on the effort that the subject is spending.

Towards a Human-in-the-loop control strategy, the modulation, implementation, and/or validation of control approaches, such as **(i)** the Adaptive User-Oriented Trajectory Tracking control, where the angular trajectory can be real-time modified, and **(ii)** the Adaptive User-Oriented Impedance control, where the virtual stiffness of the joint can be real-time modified, in a smart, standalone orthotic system was performed. The integration of these control strategies into robotic assistive devices allows personalized and specific assistance for each end-user, leading to a more effective and less energy-consuming rehabilitation.

For the first control strategy, new modular trajectories applied to the users' needs are created as a reference for a low-level controller. The main goal is that these different trajectories can be used to automatically adjust the assistance in real-time concerning the effort that the end-user is performing, i.e., user's energy expenditure. As a modular approach, the strategy was developed to be used by the physiotherapists in order to change and adapt the trajectory in real-time during the rehabilitation therapy, maintaining the integrity and the continuity of the movement.

For the second control strategy, the main goal is to adapt the interaction between human-orthosis to achieve a compliant assistance and assist-as-needed approach. This dissertation aims to extend the implemented adaptive impedance control for the ankle joint. A linear model was used to estimate the *quasi*-stiffness values per gait phases from the user-orthosis interaction torques and ankle angles. Once the *quasi*-stiffness values are found, these values will be used to produce an assisted-as-needed interaction torque, used as a reference trajectory for a low-level controller.

At last, it is studied the effect of using the orthotic device into the subjects' effort by evaluating the oxygen consumption and carbon dioxide production, to quantify the energy that the end-user is spending. In an attempt of eliminate the use of indirect calorimetry to evaluate the energy consumption, different measurements obtained with wearable and ergonomic devices, such as standard physiologic measurements, as heart rate (HR), electromyography (EMG), among others, and kinetic measurements, as angular velocity and segments' acceleration, were studied together with artificial intelligence to predict the energy expenditure of subjects while walking with the orthotic device. This study aims to propose a reliable energy consumption estimation, such that indirect calorimetry with non-portable and non-ergonomic sensor systems is no longer required.

To achieve these ultimate goals, it is necessary to pursue the following objectives.

Objective 1: To investigate the *state-of-the-art* of powered exoskeletons and orthotic systems for gait rehabilitation and assistance; analyse how these powered devices are controlled, focusing in trajectory tracking control and impedance control strategies; study how the energy expenditure is being used to investigate the effects of robotic gait assistance; and how artificial intelligence could be used to predict the energy expenditure of users while walking.

Objective 2: To implement and validate the adaptive user-oriented trajectory tracking control as a high-level controller, fostering a time-effective and simple strategy to create different trajectories tailored to the user needs. These trajectories will be used as the real-time references for a proportional-integrative-derivative (PID) low-level controller responsible for the SmartOs system control. This control approach is validated in a laboratory context, performing experiences with healthy users. This strategy was evaluated in terms of the trajectory integrity and continuity of the movement, and considering its latency, time-response and magnitude errors.

Objective 3: To study the human-orthosis interaction torque when the system is working closely to a passive device, analysing the strength each user is applying to perform the healthy trajectory; apply a linear model to the interaction torque *vs* angle curve to estimate the *quasi*-stiffness of the ankle joint considering the phases of the gait cycle; adapt and validate with healthy subjects the adaptive impedance control strategy for the ankle orthosis, using the values of *quasi*-stiffness estimated with the linear model.

Objective 4: To study the applicability of *Human-in-the-loop* control for the SmartOs, analysing the energy expenditure that the orthosis produces in a trajectory tracking control approach, and applying machine learning tools to predict the energy expenditure of users while walking at different speeds using easy-to-obtain measurements, as EMG, HR, angular velocity, segments' acceleration, among others. For this study, the correlations between the ground truth and the predictors are assessed in order to select the best features.

1.3 Research Questions

For the work developed, four research questions (RQ) were formulated and answered during the present dissertation, as follows.

RQ 1: *Can the energy expenditure be used to study the gait efficiency enabled by powered assistive devices, and to exploit the Human-in-the-loop control?* This RQ is answered in Chapter **2**.

RQ 2: *Is it possible to adapt the existing control strategies as a way to introduce the Human-in-the-loop control in the SmartOs?* This RQ is answered in Chapter **4** and **5**.

RQ 3: *Is there differences in the user's energy expenditure when assisted by the SmartOs at slow walking speeds?* This RQ is answered in Chapter **6**.

RQ 4: *Are the machine learning-based models able to evaluate the energy expenditure in the SmartOs, minimizing the use of non-ergonomic systems?* This RQ is answered in Chapter **6**.

1.4 Scientific Contributions

The work developed for this dissertation aims the applicability of Human-in-the-loop control for a smart orthotic system through user-oriented and assist-as-needed control strategies. In the scope of this dissertation, four-main scientific contributions can be pointed:

(i) A literature review on the use of energy expenditure in powered orthosis for lower limb gait assistance and rehabilitation (chapter 2);

(ii) An adaptive trajectory tracking control strategy for further use in Human-in-the-loop control that creates different trajectories tailored to the user's needs in real-time. So far, it is the first orthotic system with an adaptive trajectory control based on the joint angle that allows a position trajectory adaptation in real-time, intended to aid persons with motor impairments to have a better rehabilitation therapy, focused on his/her degree of disability (chapter 4);

(iii) An adaptive impedance control strategy for the ankle orthosis and further use in Human-in-the-loop control, allowing the stiffness modulation of the human-orthosis interaction in real-time, using the user-friendly mobile application, encouraging the users to interact with the system, providing a rehabilitation sustained in training, effort and interaction (chapter 5);

(iv) An empirical study of the use of easy-to-obtain measurements, as HR, EMG, angular velocity and angular acceleration, to predict the energy expenditure of users while walking with the orthotic system; and two machine learning tools for estimating the energy expenditure of users while walking at slow speeds with the orthotic device in assistance mode (chapter 6).

With the work developed during this academic year, three scientific publications, one as first author and two as co-author, were published on a conference and one paper is submitted in a journal:

(i) **João M. Lopes**, Luís Moreira, Cristiana Pinheiro, Daniel Sanz-Merodio, Joana Figueiredo, Cristina P. Santos, and Elena Garcia, "Three-Link Inverted Pendulum for Human Balance Analysis: A Preliminary Study," 2019 IEEE 6th Portuguese Meeting on Bioengineering (ENBENG), Lisbon, Portugal, 2019, pp. 1-4. doi: 10.1109/ENBENG.2019.8692531

(ii) Cristiana Pinheiro, **João M. Lopes**, Luís Moreira, Daniel Sanz-Merodio, Joana Figueiredo, Cristina P. Santos, and Elena Garcia, "Kinematic and kinetic study of sit-to-stand and stand-to-sit movements towards a human-like skeletal model," 2019 IEEE 6th Portuguese Meeting on Bioengineering (ENBENG), Lisbon, Portugal, 2019, pp. 1-4. doi: 10.1109/ENBENG.2019.8692569

(iii) Luís Moreira, Cristiana Pinheiro, **João M. Lopes**, Daniel Sanz-Merodio, Joana Figueiredo, Cristina P. Santos, and Elena Garcia, "Study of Gait Cycle Using a Five-Link Inverted Pendulum Model: First Developments," 2019 IEEE 6th Portuguese Meeting on Bioengineering (ENBENG), Lisbon, Portugal, 2019, pp. 1-4. doi: 10.1109/ENBENG.2019.8692451

(iv) **João M. Lopes**, Joana Figueiredo, Elena Garcia, and Cristina P. Santos, "Energy expenditure use on gait rehabilitation and assistance driven by powered assistive devices: A Review," Topics Stroke Rehabilitation (submitted).

1.5 Dissertation Outline

This dissertation is organized as follows:

Chapter 2 presents the *state-of-the-art* of this dissertation, including the current state of lower limb assistive devices, such as exoskeletons and orthoses responsible for assisting humans in their daily living tasks. As one of the main goals of this dissertation is to develop a control strategy capable of adapt the trajectory and the joint impedance according to the user's needs, an overview of control strategies will be exploited, focusing mainly on trajectory tracking control and joint impedance control. Also, although the control strategy will not be totally closed, a literature review of Human-in-the-loop control and energy use on powered assistive devices is presented, aiming to study how the investigators are introducing humans into the loop system and which are the main changes to the assistive strategies to decrease the energy expenditure of users.

Chapter 3 introduces an overview of the system used in the scope of this dissertation – the Smart Wearable Orthotic System. Here, it will be presented a general description of the system, presenting both orthoses for ankle and knee assistance, describing the embedded sensors and the system mechanism, as well as the wearable sensors used to perform gait analysis and monitorization.

Chapter 4 describes the Adaptive User-Oriented Trajectory Tracking Control, detailing the strategy developed to create adaptive, personalized and user-oriented trajectories, maintaining always the integrity and continuity of the movement. This chapter is divided into two main sections, one for the powered ankle orthosis device and another for the powered knee orthosis, where both methods and validation are stated.

Chapter 5 presents the Adaptive User-Oriented Impedance Control strategy. This chapter defines the concept of *quasi*-stiffness, obtained through a modulation of a linear model to the human-orthosis interaction torque *vs* angle curve. The implementation and validation using the ankle orthosis are exploited.

Chapter 6 introduces the first steps towards the Human-in-the-loop control strategy. This chapter presents an empirical study of the impact of using the orthotic system in healthy users in terms of energy, performing a comparison of walking with and without the assistive device; also, it addresses techniques of machine learning to predict the energy expenditure using easy-to-obtain measurements from each user while walking with the orthotic device.

At last, in **Chapter 7**, the conclusions of this dissertation and the future perspectives are pointed out.

2. *STATE-OF-THE-ART*

2.1 Introduction

In the last decades, the high incidence of neurodegenerative and cardiovascular disorders through the world population had led to an augmentation of disabilities concerning mobility malfunctions. The use of assistive devices for gait rehabilitation and assistance have been studied for the last 20 years and the main results are positive. With one or two degrees of freedom, these powered devices help to restore the gait pattern, decreasing the lower-limbs asymmetry, and giving support. When the rehabilitation is performed with a powered device, new strategies as user-oriented therapies, adapted to the users' needs, can be developed, enhancing the users' recovery [7].

In the following sub-chapters, the current *state-of-the-art* of lower limb assistive devices is presented, as well as a review of the use of energy expenditure in robotic gait assistance.

2.2 Lower Limb Assistive Devices

In the world of robotic assistive devices, two main terms are recursively used: *exoskeleton* and *orthosis*. According to [8], an **exoskeleton** comprehends a single or multi-joint segment capable of augmenting the force of healthy users, while the term **orthosis** is referred to a single or multi-joint that assists the user's limb with a certain injury. In medical terms, there is no consensus between authors to describe the terms *exoskeleton* and *orthosis*. In some studies, these two terms appear to have the same meaning and, in others, the *exoskeleton* term is referred as a multi-segment device, e.g. in [7], while an *orthosis* is a single-segment device, aiming to recover a part of the limb one at a time. Nevertheless, both devices have the same purpose when applied to medicine: aid persons with motor impairments to restore their daily-live activities.

The exoskeletons have been widely used in the military industry, improving soldiers' strength and transferring the load-carrying weight to the ground [2], [8]. The first exoskeleton remounts the year of 1965, when General Electrics, in the United States of America, started to build the first approach to an exoskeleton [9]. The exoskeleton was built and design to assist the soldiers, enhancing their physical capabilities [10]. By the other side, the first orthosis intended to provide locomotion to non-ambulatory persons was developed in Serbia, by Mihailo Pupin Institute, in 1969. This orthosis was endowed with artificial pneumatic "muscles", capable of produce a pattern of walking close to the healthy one [11].

These two assistive devices, each one with its purpose, were the first step into the huge development of humanoid technology during the last decades.

The powered assistive devices can be divided into two categories: the multi-segment devices, that assist more than one joint at the same time, and the single-segment devices, which assist assistance a specific joint.

2.2.1 Multi-segment devices

The multi-segment devices are a category of powered assistive devices. As it provides assistance to the total lower limbs or to parts of it, these powered devices are usually subdivided into three groups: the hip-knee-ankle-foot devices (HKAF), that gives assistance to the full lower-limbs, the hip-knee (HK) devices, that give assistance to the hip and knee joint at the same time, or knee-ankle-foot (KAF) devices, that give assistance to the knee and ankle joints [7].

When applied to the military and industry, the powered devices commonly developed are the HKAF devices. These are used to increase the strength of its users, helping them carrying heavy loads or to walk in uneven surfaces, such as the BLEEX, HULC, Sarcos Exoskeleton or HAL. Following [8] and described also in [10], these devices are called *exoskeletons*. Figure **2.1** displays some examples of powered devices built to improve the users' physical capabilities.

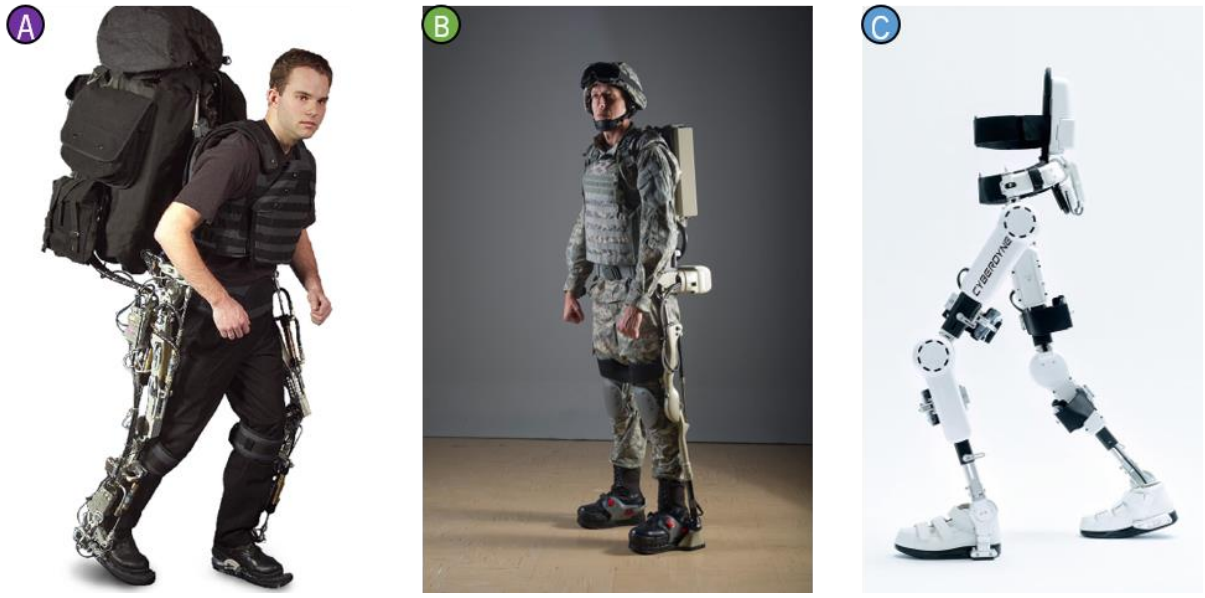

Figure 2.1: Examples of exoskeletons build to improve the users' physical capabilities: (A) BLEEX [12], (B) HULC [13] and (C) HAL [14].

When applied to medicine, the devices are used to help restoring the gait pattern of persons with hemiparesis due to neurological injuries, cardiovascular disorders or muscular weakness, such as the LokoMat and LOPES devices, or to assist handicap persons, with paraplegia or quadriplegia, as the ATLAS and ReWalk devices. As these systems are used to rehabilitate patients, they are *orthoses*. Figure 2.2 displays some examples of powered devices built to assist or recover persons with motor impairments.

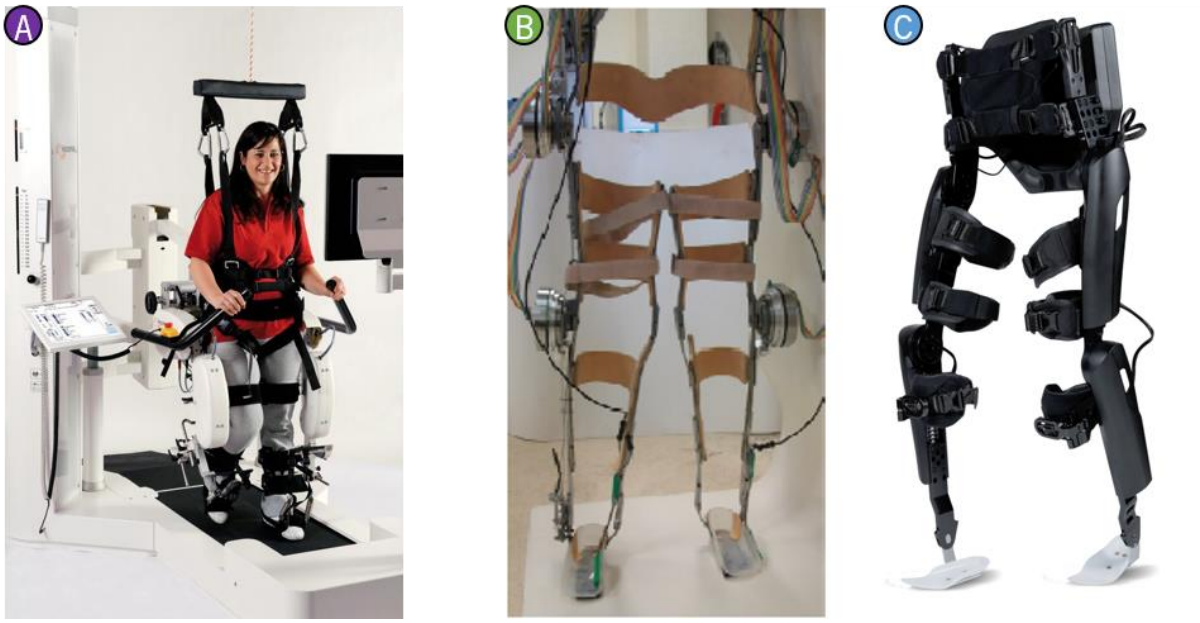

Figure 2.2: Examples of orthoses built to recover an hemiparetic limb or restablishing the gait to non-ambulatory persons: (A) LokoMat [15], (B) ATLAS [16] and (C) ReWalk [17].

Table 2.1 contains some of the many multi-segmented lower limb devices for both military, industry and medicine applications reported by [7]. For each device, the application and a general description is presented.

Table 2.1: Multi-segment devices reported by [7] (continue)

Study	*Names*	*Type*	*Description*
[12]	BLEEX	HKAF	Intended to give assistance to the full lower-body while carrying loads, having 7-DOF for each leg.
[16]	ATLAS	HKAF	Provides motion for children suffering from quadriplegia. Intended to assist the hip, knee and ankle joint considering healthy patterns.
[14]	HAL	All body, HKAF or single-leg	Intended to either assist persons with gait disorders or to augment the strength of its user.

(continuation)

Study	*Names*	*Type*	*Description*
[17]	ReWalk	HK and unpowered ankle-foot	Intended to assist persons with chronic spinal cord injury. The subjects need to use crutches for more stability.
[18]	Vanderbilt	HK	Intended to assist persons with spinal cord injury. It is compatible with an AFO to ensure the gait.
[19]	IHMC	HK and unpowered ankle-foot	Intended to either assist, in a passive mode, or to augment to users' performance.
[20]	MINA	HK	An evolution from IHMC. It has 2-DOF, one for each joint that assists. Intended to provide gait to paraplegic and paraparesis persons.
[21]	WWH	HKA	It is designed to assist the locomotion of disabled and elderly persons.
[22]	WPAL	HKA	It is designed to assist the locomotion of disabled, elderly persons and after an amputation process.

2.2.2 Single-segment devices

The single-segment devices are often developed to be applied in the rehabilitation field. Indeed, many single-joint devices have been proposed to aid persons with motor impairments. Most of them are considered passive since does not exist an actuator. However, in the past decades, the single-joint powered devices had gain strength, and new studies have been performed. If powered, these systems allow an effective and periodic joint motion, allowing the assistance and, in some cases, the recovery of the hemiparetic joint. These devices are often divided into three types, considering the joint intended to aid: powered hip-orthoses (PHO), powered knee-orthoses (PKO) and powered ankle-foot-orthoses (PAFO) [7].

The literature analysis report that these devices can have electric, pneumatic or cable-based actuators. If the device is electric, usually the orthoses are wearable with a DC motor controlled by smaller central control units (CCU). If pneumatic, the orthoses usually are tethered, meaning that they are attached to an external source of power that controls the system, insufflating air into the "artificial muscles". At last, if the orthoses are cable-based mechanisms, forces are applied and transmitted to the system all over

the cables. Figure **2.3** displays some of the main orthoses for hip, knee and ankle assistance presented in the recent literature.

Figure 2.3: Single joints Lower-limbs devices: (A) Pneumatic hip orthosis [23], (B) Pneumatic AFO orthosis [24], (C) MIT PKO orthosis [25], (D) Pneumatic AFO [26], (E) Pneumatic AFO [27], (F) Cable-based ankle-foot exoskeleton [28], and (G) Cable-based hip orthosis [29].

Most of the orthotic devices presented in the literature are PAFOs since the ankle joint is one of the most affected articulations of persons with motor impairments. Most of them are pneumatically actuated, as the ankle-foot orthoses presented in Figure **2.3 – B**, **2.3 – D** and **2.3 – E**, developed, respectively, by [24], [26], and [27]. These devices are provided with compressed air systems that transform the pneumatic energy into kinetic energy. As it is needed an external source of power to inflate the air into the artificial muscles, these orthotic devices are considered tethered. Another orthosis for ankle assistance was developed by [28] (Figure **2.3 – F**), with a cable-based mechanism that provides 1-DOF to the device. Composed of a brushless DC motor, the system allows the dorsiflexion and plantarflexion movements applying the proper force to the cables. By opposition to the previous devices, this orthotic system is totally wearable since it is controlled by a hardware interface that the subjects carry on their waist.

Similar approaches as those presented above are also applied to PHO orthoses. In fact, an orthotic device for hip assistance (Figure **2.3 – A**) was developed by [23]. This orthotic device consists of a prefabricated hip brace that was modified to include a pneumatic actuator that insufflates a certain quantity of air to

provide the correct pattern of motion. Another orthosis for hip assistance, or exosuit as described by [29] (Figure **2.3 – G**), was recently developed, made of a soft fabric. This orthotic device endows inner cables responsible to create a tension between two strategic points. Pulling the inner cable, the orthosis forces the subject to perform hip extension. Both orthoses ([23] and [29]) are tethered.

At last, an orthosis for knee assistance was developed by [25] (Figure **2.3 – C**). It is an orthotic device placed on the back of the legs with an electric actuator. The motor moves a bar paralell to the leg continuously, promoting the correct gait pattern. Table **2.2** presents the devices displayed on Figure **2.3** and a few more examples of lower limb single-joint devices for gait assistance.

Table 2.2: Single-joint devices for lower-limb assistance (continue)

Study	*Assisted joint*	*Actuator*	*Description*
[23]	**Hip**	Pneumatic	Intended to aid persons with motor impairments. It is provided a gait assistance based on a predefined gait pattern. 1-DOF.
[29]	**Hip**	Cable-based	Intended to give assitance to the hip joint considering the energy the subject is spending. 1-DOF.
[30]	**Hip**	Electric	Intended to aid healthy elderly persons to maintain their daily-live activities, promoting a gait training. 1-DOF.
[25]	**Knee**	Electric	Intended to aid healthy persons to run. 1-DOF, allowing knee flexion and extension.
[31]	**Knee**	Series Elastic Actuator / Eletric	Intended to enhance the user's strength and speed. Allows the user to climb stairs and to perform squads while carrying a load. 1-DOF.
[32]	**Knee**	Electric	Intended to aid persons with disordered gait to regain normal walking and for elderly people to maintain their daily-live activities. 1-DOF.
[24]	**Ankle**	Pneumatic	Intended to give assitance to the ankle joint considering the energy the subject is spending. 1-DOF.

(continuation)

Study	*Assisted joint*	*Actuator*	*Description*
[26]	**Ankle**	Pneumatic	Intended to give assistance to impaired subjects. It consists of a 1-DOF orthosis.
[27]	**Ankle**	Pneumatic	Intended to restore gait symmetry to users with motor impairments. 1-DOF, allowing dorsiflexion and plantarflexion.
[28]	**Ankle**	Cable-based / Electric	Intended to aid persons to walk while carrying a load. It exhibits 1-DOF, allowing dorsiflexion and plantarflexion.

Note: Abbreviations' meaning can be found here.

2.3 Control strategies of powered assistive devices

Findings in the literature of robotic devices for gait assistance shows that many control approaches have been proposed to control the powered devices for lower-limbs assistance. According to [7], [33], and [10], the powered assistive devices are controlled by: **(i)** a predefined gait trajectory control, where a position tracking control is systematically performed based on the periodicity of the gait; **(ii)** an impedance control, where the joint impedance is modelled considering the gait phase; **(iii)** a control based on a predefined action considering the gait pattern; **(iv)** an EMG-based control, where the muscular information is used, usually, to create a joint torque replica to be applied on the systems' motor; and **(v)** kinematic model-based control, where a joint torque pattern is created according to dynamic equations with kinematic and kinetic information. In some cases, the assistance is given with a hybrid control, where more than one control strategy is applied to the system. In these cases, the information about the gait cycle phase can be used to switch between control approaches. Considering the goals of this dissertation, the first two assistive strategies will be discussed with more detail in the following sub-topics.

A recent control approach, named Human-in-the-loop control, caught the attention of the investigators and it is emerging in the present decade. It uses a physiological signal indicator of energy, mainly oxygen consumption and carbon dioxide production for real-time optimization of one or more assistance parameters, such as the torque actuation onset timing or the torque peak magnitude. Thus, the assistance is personalized and specific for each patient, contributing to, possibly, a more efficient recovery

while minimizing the energetic cost of walking [34]. Topic **2.4** presents a literature research of the use of energy in powered assistive devices, introducing this new field of interest.

2.3.1 Trajectory Tracking Control

The trajectory tracking control strategy was firstly applied to the industrial robots, where the position of the end-effector is calculated applying a trajectory generator based on known points that the system must reach. The angle information, for example, is frequently used to describe the trajectory of a manipulator. In order to create a smooth and non-random trajectory, it is necessary to give a more detailed pattern, giving a set of intermediate points, described in [35] as via points. Then, the trajectory can be created using the inverse kinematics, where these via points are converted into joint angles [35].

As a result of the periodicity and repetitive gait pattern for the ankle, knee and hip joints, the applicability of this technique was also studied for gait assistance purposes. According to [7], the trajectory control can be performed either with a joint position, where the reference is the joint angle, or using the joint torque. The kinematic and kinetic information, obtained with gold-standard motion systems, as the VICON or Qualysis systems, or wearable sensors as goniometers, accelerometers, gyroscopes, or IMUs [10], can be used to estimate the reference trajectories. Frequently, the joint angle pattern is estimated with cubic interpolation, adapting the trajectory into the system specifications [7], [32].

Usually, this strategy is more intended to aid persons that lost the walking capability, as paraplegic and quadriplegic persons [7]. This is the case of ATLAS [16], HAL [14], ReWalk [17], Vanderbilt [18] and IHMC [19] orthoses presented earlier. In a pure trajectory tracking control mode, these orthoses impose a gait pattern to their users, providing a cyclic training session. Other example is the investigation carried out by Lai *et al.* [32] that culminated into a single-joint powered orthosis for knee assistance in which the control is performed with a PID controller using the knee angle trajectory as the reference signal. In this study, the knee kinematics are calculated considering the hip's angular velocity, which is linearly correlated with the knee angle at the swing phase, through a polynomial equation [32]. For the stance phase, the knee orthosis is locked at 13° since the trajectory variation for this phase is quite small when compared to the swing phase. Dao *et al.* [36] created a pneumatic robotic orthosis for gait rehabilitation in which the control is performed with the angle trajectory of knee and hip, using for that a proportional-integrative (PI) controller. In this way, the air pressure of the artificial muscles that compose the orthotic system is controlled, and the specific amount of air needed to perform the imposed trajectory can be delivered [36].

Considering the aforementioned studies, this control strategy is well suited for the first rehabilitation sessions of persons with a highly corrupted gait pattern and weak muscular activity.

2.3.2 Joint Impedance Control

The joint impedance control is a frequently used assistive strategy where the joint impedance is modulated with the main goal of decrease the subjects' effort [37]. According to Huo *et al.* [37], reducing the subjects' effort is still a very demanding challenge. The fact of using a wearable orthosis with friction, produces inertia to the movement, that adds mass to the limb, conditions the effort that the subject is performing. These constraints, as inertia, as mass, produce gravitational components, and the stiffness are considered the lower limb impedances [37].

In general, the studies presented in the literature turn their focuses into adapting the joint stiffness. In this way, the joint compliance can be adjusted, transforming the orthosis into a truly assistive device [38]. The use of these systems in impaired subjects can improve their recovery, providing repetitive training sessions and a user-oriented assistance. In the current decade, assist-as-needed (AAN) control strategies have been developed in an attempted of providing interactive assistances, encouraging the subjects' participation and interaction [36], [37].

LOPES (LOwer-extremity Powered ExoSkeleton) is one impedance-controlled orthosis that modulates the compliance of the joint as a way to allow an assisted-as-needed strategy control that provides more freedom to the movement, promotes user's participation and allows an assistance modulation considering the user's needs [39]. The orthosis uses a series elastic actuator and allows two modes of assistance: the *patient-in-charge*, where the stiffness is null and the user commands the system, and a *robot-in-charge*, in which the stiffness is set to high, imposing a trajectory to the end-user [40]. Another device that modulates the joint stiffness is the Lokomat orthosis [15]. This orthotic device allows an user-oriented assistive strategy in a way that it is possible to adapt the assistance, passing from a more stiff behaviour, where the system is purely trajectory tracking control, to a more compliant one. The error in angular position produced by the subject considering a reference trajectory is multiplied by a virtual stiffness value (K), designated as linear elastic coefficient, and its first derivative, the angular velocity, is multiplied by a coefficient B, named linear viscous coefficient. Therefore, a reference torque can be created and sent to a proportional-derivative (PD) controller with negative feedback [15].

Additionally, Hussain *et al.* [41] applied the same principals of Lokomat and LOPES orthoses to adjust the joint stiffness, allowing the subject to deviate from the reference gait trajectory. The effort, measured through a human-orthosis interaction torque, was used to adjust the impedance of the robotic orthosis,

giving more freedom to the subject. As it is user-dependent, the strategy is also considered an assisted-as-needed approach. A similar approach was implemented by Rajasekeran *et al.* [42], where a virtual stiffness was evaluated considering the positions errors and the human-orthosis interaction torque. As the virtual stiffness is systematically changed all over the gait cycle and the assistance is given considering the position error, the strategy is considered assisted-as-needed. At last, another work, presented in [43], followed the same principal as the previous works, presenting an adaptive impedance control law for a knee orthosis that modulates the virtual stiffness in real-time and promotes a robotic gait assisted-as-need assistance based in the subject's motion intention.

2.4 Energy use on powered assistive devices: towards Human-in-the-loop Control

Impaired gait function affects the persons' walking economy, promoting an augmentation of energy expenditure [44], [45]. Considering the muscular activation on post-stroke individuals, that is compromised, it is important that these assistive devices not only contribute to the gait recovery, but also to decrease the energy dispended while walking.

Energy expenditure is one of the main outcomes of studies involving exoskeletons built and designed to assist patients with motor impairments, mainly ankle-foot orthosis (AFOs) or exosuits [46], [47]. Most of these studies were conducted with passive orthoses and the results point to a reduction in the energy expenditure and a gait pattern improvement [47]. With the introduction of powered devices, either with pneumatic, cable-based mechanical power transmitters or electric actuators, as presented earlier, new studies have been performed and the energy expenditure is starting to be used for further purposes, as to promote a more efficient gait for its users, allowing user-oriented assistances.

Table 2.3 shows a representative sample of studies that used the energy expenditure to evaluate the energetic cost of assisted walking with powered devices.

According to Table 2.3, Seo *et al.* [48] and Martini *et al.* [30] reported both powered orthosis for hip assistance that allowed a reduction in the energy cost of walking. A higher reduction on the metabolic cost was obtained in [30], ranging between 20% and 27%, comparing to [48], that reported an energy reduction of 13%. For both studies, the decreasing on energy consumption was statistically significant, meaning that the assistive devices may have clinical potential to reduce the patients' energetic walking cost.

Awad *et al.* [6], Mooney *et al.* [28] and Malcom *et al.* [27] reported that the use of powered devices for ankle assistance decreased the energy expenditure of its end-users. These studies reported a decreasing

on the metabolic energy consumption while walking with the orthotic device, ranging between 6% and 15% of power saving, when compared to unpowered condition ([6], [28] and [27]), and the absence of robotic assistance ([28]). Despite of that, this decreasing was only statistically significant on studies [6], [28] and in the second condition of [27]. Moreover, in [6], the subjects were post-stroke patients. Although the energy consumption was almost 32% higher than the normal walking, the exosuit allowed a metabolic cost reduction of 0.0721 mL O2/m/kg considering the reported value for hemiparetic gait, which is, according to [49], approximately 0.270 mL O2/m/kg. According to these findings, the robotic gait assistance can reduce the energetic cost of human walking when it is used in the assistive mode.

In the current decade, the energy expenditure is not only used to assess the effectiveness of powered assistive devices upon gait assistance. The energy expenditure is being used as a means to change the assistance. For instance, torque parameters, mainly on ankle-foot orthoses and exosuits, are tuned to promote a more personalized and specific assistance to each user. This optimization can be either **(i)** offline and **(ii)** online. If offline, a set of control parameters are tested, and the energy expenditure is assessed to verify which are more effective. In online optimization, torque parameters are changed in real-time according to the measured energy expenditure. The online optimization is considered the Human-in-the-loop control approach.

Table **2.4** presents four studies in which at least one parameter was optimized offline to ensure a correct pattern of walking and a reduction on energy expenditure, and Table **2.5** presents 3 studies where an online optimization of one or more parameters were investigated.

For both offline and online parameter optimization, the actuation onset is the main variable tuned to adjust the assistance aiming the minimal energy effort from the user. According to Table **2.4**, Malcom *et al.* [50] and Galle *et al.* [51] reported studies of ankle-foot orthoses in which they tuned offline the actuation onset for an array of values pointed as candidates. Both found similar values of optimal actuation onset (43% and 42% of the gait cycle, respectively) with savings on energy consumption of, respectively, 17% and 21%, considering unpowered conditions, and 6% and 12%, respectively, without the assistive device. Moreover, in [51], an average power level of 0.4 W/kg was found to be helpful in reducing the energetic cost of walking with the assistive device. Ding *et al.* [52] studied the actuation onset timing and the maximum peak timing of torque of an exosuit for hip extension assistance. The authors found that, although all powered conditions produced a more efficient gait relatively to the unpowered condition (more than 5% efficient), the differences between powered conditions were not significant.

Table 2.3: Studies in which the energy expenditure was used as a performance metric of gait assistance with powered orthosis

Study	*No. Subjects*	*Assistive device*	*Signal*	*Sensor device*	*Experimental protocol*	*Observed effects*
[6]	9 stroke	Tethered exosuit for ankle joint with cable-based	$\dot{V}O_2$ and $\dot{V}CO_2$ [mL/min]	K4b² (COSMED, Italy)	2 days of protocol. The experimental set consisted of two 8-minute bouts on a treadmill at a preferred walking speed. Users performed two trials: one with exosuit unpowered and other with exosuit powered.	**(i)** Metabolic cost was reduced by 10.0 ± 3.0% (p-value = 0.009) with powered assistance comparing to unpowered conditions; **(ii)** Energy preservation of 32 ± 9% (p-value = 0.009) closer to the normal walking cost.
[48]	5 healthy	Wearable electric hip actuator	$\dot{V}O_2$ and $\dot{V}CO_2$ [mL/min]	K4b² (COSMED, Italy)	1-day protocol. Stand for 5 minutes; then walk for 10 minutes without and with the device with a 5-min period of rest between; then, walk 10 minutes without the device and finish with a 5-min standing.	Metabolic cost was reduced by 13.2 ± 4.3% (p-value = 0.0024) in comparison with walking without the device.
[28]	6 healthy	Wearable electric ankle-foot orthosis	$\dot{V}O_2$ and $\dot{V}CO_2$ [mL/min]	K4b² (COSMED, Italy)	1-day protocol. 1 trial standing and 1 trial walking. 10 minutes walking without the device, then 20 minutes walking with it, 20 minutes with exoskeleton unpowered and 10 minutes walking without it.	Metabolic cost reduced by 11.0 ± 4.0% (p-value = 0.019) compared to the cost of walking without the exoskeleton and 14.0 ± 3.0% (p-value < 0.01) considering unpowered condition.
[27]	11 healthy	Tethered pneumatic ankle-foot orthosis	$\dot{V}O_2$ and $\dot{V}CO_2$ [mL/min]	K4b² (COSMED, Italy)	Habituation trial for 5 minutes for each 4 conditions (two unilateral assistances and two bilateral assistances). Subjects walked for 4 minutes for each condition with a resting period of 2 minutes between each evaluation.	Metabolic cost, compared to unpowered condition, was reduced by: **(i)** 6.4 ± 3.3% for assistance in dominant leg (p-value = 0.066); **(ii)** 7.9 ± 2.2% for non-dominant leg assistance (p-value = 0.003); **(iii)** 11.3 ± 1.5% for bilateral assistance (sum of both legs); **(iv)** 14.9 ± 2.5% per leg with bilateral assistance.
[30]	20 healthy elderly	Wearable electric hip actuator	$\dot{V}O_2$ and $\dot{V}CO_2$ [mL/min/kg] Heart rate [min^{-1}]	Oxycon Mobile (JAEGER, Germany)	2-months protocol. Subjects walked on a treadmill at increasing speeds every 2 minutes. The subjects walked until they reached 75% of the maximum heart rate allowed (210 – Age x 0.65).	Energy expenditure was reduced by: **(i)** 26.6 ± 16.1% (p-value < 0.01) 4-weeks after baseline (with the subjects standing still); **(ii)** 20.2 ± 19.7% (p-value < 0.01) 2-months after baseline.

Note: Abbreviations' meaning can be found here.

Table 2.4: Studies in which the energy expenditure was used for an offline control parameter(s) optimization to allow gait efficiency

Study	*No. Subjects*	*Assistive device*	*Signal*	*Sensor device*	*Control parameter(s)*	*Experimental protocol*	*Observed effects*
[50]	18 healthy	Tethered pneumatic ankle-foot exoskeleton	$\dot{V}O_2$ and $\dot{V}CO_2$ [mL/min]	Oxycon Pro (JAEGER, Germany)	Actuation onset timing	1-day protocol. 5 minutes of habituation. 4 minutes standing still. 5 minutes walking.	Metabolic cost reduced by: **(i)** 6 ± 2% (p-value = 0.019) vs walking without the exoskeleton; **(ii)** 17 ± 1% (p-value < 0.001) versus unpowered conditions. It was found that the actuation onset at 43% of GC was optimum.
[52]	8 healthy	Tethered exosuit for hip with cable-based power transmission	$\dot{V}O_2$ and $\dot{V}CO_2$ [mL/min]	K4b² (COSMED, Italy)	Actuation onset and torque peak timing	2 days protocol. 5 minutes standing still. 4 minutes warmup (1-minute per condition). Rest for 5 minutes. 6 minutes data collection with 5 minutes of resting period between each condition.	Metabolic cost was reduced in more than 5% p-value < 0.015 in powered assistance vs unpowered assistance. No significant differences were found between different powered conditions, i.e., between the tested actuations onset and torque peak timings.
[51]	10 healthy	Tethered pneumatic ankle-foot exoskeleton	$\dot{V}O_2$ and $\dot{V}CO_2$ [mL/min]	K4b² (COSMED, Italy)	Actuation onset timing and power level	1 habituation session and 1 collecting session separated in a week. 3 minutes of habituation and 2 minutes resting. 4 minutes walking.	It was found an optimal actuation onset at 42% of GC and a power level of 0.4 W/kg. Optimal assistance reduced the metabolic cost by: **(i)** 21% vs to the exoskeleton unpowered; **(ii)** 12% vs without the exoskeleton.
[53]	7 healthy	Tethered multiarticular soft exosuit	$\dot{V}O_2$ and $\dot{V}CO_2$ [mL/min]	K4b² (COSMED, Italy)	Torque peak magnitude	1 training session and 1 assessment session. 6 conditions (powered off and 5 powered on). 8 min of warmup. 2 continuous trials of 20 minutes (5 minutes per condition + 5 minutes without the device).	Optimal conditions were found with the torque peak magnitude at 0.707 ± 0.053 Nm/kg, reducing the energy expenditure by 22.83 ± 3.17% (p-value = 0.0002) comparing powered vs unpowered condition.

Note: Abbreviations' meaning can be found here.

Table 2.5: Studies in which the energy expenditure was used for an online control parameter(s) optimization to allow gait efficiency

Study	*No. Subjects*	*Assistive device*	*Signal*	*Sensor device*	*Control parameter(s)*	*Experimental protocol*	*Observed effects*
[24]	9 healthy	Tethered pneumatic ankle-foot orthosis	$\dot{V}O_2$ and $\dot{V}CO_2$ [mL/min]	Oxycon Pro (JAEGER, Germany)	Actuation onset timing	3-days protocol. Standing for 4 minutes. 10 conditions (powered off + 9 powered conditions). 6 minutes per condition (random except first and last condition).	The optimal actuation onset timing, specific for each subject, allowed a reduction in energy expenditure of 19.6 ± 3.2% considering the maximum observed during the experiments. The algorithm took a mean of 50 minutes to set the optimal optimization.
[34]	11 healthy	Tethered ankle-foot exoskeleton with cable-based power transmission	$\dot{V}O_2$ and $\dot{V}CO_2$ [mL/min]	K4b² (COSMED, Italy)	Torque peak timing and magnitude, rise and fall time	1-day protocol. Brief period of habituation to the device. Subjects walked with the device in unpowered condition and 4 control laws with 8 periods of two minutes. A validation was performed with the optimal assistance in comparison with unpowered mode.	Metabolic cost was reduced by 24.2 ± 7.4% (p-value = 1.0×10^{-6}) considering unpowered condition and 5.8 ± 6.2% (p-value = 0.01) considering static torque. The optimized parameters were found after a mean of 64 minutes of walking. The best parameters were specific for each subject.
[54]	8 healthy	Tethered exosuit for hip with cable-based power transmission	$\dot{V}O_2$ and $\dot{V}CO_2$ [mL/min]	K4b² (COSMED, Italy)	Force peak timing and offset timing	1-day protocol. 5 minutes standing. 5 minutes without the device. 40-min of optimization with 3 minutes of warmup and 5 minutes of resting period. 5 minutes validation with the best condition. 5 minutes without the device.	With the optimal parameters setting, specific to each subject, the metabolic cost was reduced by 17.4 ± 3.2% comparing to walking without the device. The algorithm took a mean of 21.4 ± 1.0 minutes to find the best parameters.

Note: Abbreviations' meaning can be found here.

Koller *et al.* [24], listed in Table 2.5, performed an optimization of the actuation onset in a powered, pneumatic exoskeleton for bilateral assistance, minimizing the energy expenditure of end-users through a Human-in-the-loop control strategy. Under optimal assistance conditions, after 50 minutes of search, the authors reported a decrease in the metabolic effort of almost 20%. However, this reduction was not about unpowered conditions or walking without the exoskeleton but considering the energy expenditure observed while the parameters were changed in real-time.

Another parameter that is being tuned in both offline and online optimization is the torque peak magnitude. Quinlivan *et al.* [53] found the optimization of the torque peak magnitude fostered by an ankle exosuit reduced the energy expenditure when compared to unpowered conditions. They found that under maximum conditions, i.e., torque magnitude of 0.707 Nm/kg, the energy expenditure could be reduced in more than 20%, being this result statistically significant. Additionally, Zhang *et al.* [34] reported a study in which the torque peak magnitude was adjusted to each user. The authors also studied the best time to reach the maximum peak, and the rise and fall time of torque pattern. In this study, the optimization was accomplished in real-time and conducted with a tethered orthosis for ankle assistance. When compared to [24], the optimization involved more parameters, finding the optimal values, in average, after 64 minutes. Here, the authors performed a comparison with unpowered conditions and with a static pattern of torque hand-tuned. For both situations, the energy cost of walking was significantly reduced by more than 5%.

At last, Ding *et al.* [54] tuned the force applied to the exosuit for hip assistance considering a research area of force magnitudes previously defined. The algorithm was faster comparing to the presented in [24] and [34], finding the best parameters in, more or less, 22 minutes. The authors accomplished a reduction of 17% considering walking without the device. For the three studies that investigated online parameter optimization, the control parameters were optimized for each person, allowing a proper and personalized assistance to each user.

2.5 Energy Expenditure Estimation by machine learning methods

According to Tables 2.3, 2.4 and 2.5, the energy expenditure is evaluated using, manly, respiratory measurements, by measuring the oxygen consumption ($\dot{V}O_2$) and the carbon dioxide production ($\dot{V}CO_2$) through indirect calorimetry. These energetic indicators were measured by a gas analyser. The K4b^2 device (COSMED, Rome, Italy) and Oxycon Mobile device (JAEGER, London, UK) are the most used devices to evaluate the energy expenditure.

Indirect calorimetry is considered a gold standard [55] and an effective method but not very ergonomic to use due to its size and type of sensors, that give noisy and dynamically delayed data. Also, these devices are often expensive and need trained specialists to use it [56]. To overcome this problem, new types of wearable and comfortable sensors are being studied to evaluate the subjects' physiological effort. Heart rate (HR) could be a solution since it was found that, in physical activity conditions, this signal is linearly related to the oxygen consumption [57]. As an alternative strategy, new approaches involving machine learning algorithms are being studied to obtain generalized models that can predict the energy expenditure using easy-to-obtain inputs, such as the angular velocity, the angular acceleration, the electromyography (EMG), the breath rate (BR) and HR, among others. Table **2.6** resumes four recent studies that exploited machine learning algorithms to predict the energy dynamics using wearable sensors.

A recent study, presented by K. Ingraham *et al.* [58], presents a linear regression model to predict the energy expenditure while the subjects perform different tasks. As predictors, the authors used many inputs, such as HR, EMG, electrodermal activity, oxygen saturation, skin temperature, among others. They found that some of these inputs, namely acceleration, EMG and HR, present a high correlation with the ground truth signal [58]. The results show the feasibility of this approach since the predictive performance was considered reasonable, with squared errors rounding 1.0 W/kg. However, this error should be compared with the total range of energy for a specific task to see the error magnitude and if it is significant or not.

A similar approach was implemented by T. Beltrame *et al.* [59] using the oxygen uptake as the predicted variable. In this study, the HR, the minute ventilation (MV), the BR, the hip acceleration and the walking cadence were extracted as features for a random forest regression model. The results reveal that the predicted signal is highly correlated with the ground truth signal ($r > 0.69$), presenting an error that propagates in direction to the equality line, i.e., to null bias. Furthermore, the regression model was able to identify different walking tasks and resting demand.

Additionally, T. Beltrame *et al.* [56] explored the feasibility of a neural network, a multilayer perceptron (MLP) with one hidden layer of 11 neurons, for this purpose. For this study, different features were used to assess the oxygen and energy dynamics. In [56], the sex, the body mass, the time of exercise, the time of recovery, the grade, speed and HR were used as predictors. It was found that this neural network is suitable to predict the oxygen and energy dynamics with easy-to-obtain inputs, revealing a correlation of almost 1 between the ground truth and the predictor.

Table 2.6: Recent studies that used wearable sensors for predicting the energy expenditure

Study	*Method*	*Target Signal*	*Predictors*	*Metrics Used*	*Protocol*	*Observed effects*
[58]	Pseudoinverse regression model	Energy Expenditure [W/kg]	MV, EMG, Acceleration on waist, wrist and ankle, BR, HR, EDA	Correlation Coefficient of Pearson and Root-Mean Squared Error	30 minutes for walking protocol, consisting of 6 minutes of standing still, 6 minutes of walking for each speed and, finally, 6 minutes seated.	The authors found that **filtering is very important**, especially for EMG and acceleration. The best model had an error of 1.25% of the total range of energy (10 W/kg). Calculate the **total EMG** was also beneficial.
[59]	Random forest regression model	Oxygen uptake [mL/min kg]	HR, BR, MV, Hip acceleration, Walking cadence	Correlation coefficient, Bland-Altman plot	13 minutes protocol consisting of 2 pseudorandom ternary sequences in over-ground walking and one sequence of daily live activities.	The predicted data was strongly correlated with the ground truth signal, with a positive correlation higher than 0.69 for all conditions.
[56]	Multilayer perceptron Neural Network	$\dot{V}O_2$ [mL/min] and Energy Expenditure [W/kg]	Sex, Body mass, time on, time off, grade, speed, HR	Correlation Coefficient of Pearson, Bland-Altman plot and t-test	Two separated visits. 1-minute standing, 6-minutes walking and 6-minutes standing and one incremental test of 1-min baseline, 6-min warm-up followed by a new incremental to the maximum velocity and progressive increments of 1%/min.	The authors found that 11 neurons in the hidden layer formed the best predictive model. According to the Bland-Altman plot, there were small deviations of the differences from zero. The predicted energy expenditure was strong correlated with the measured one.
[60]	Convolutional Neural Network	Energy Expenditure [kcall/min]	Acceleration of waist, HR, age, height, weight, BMR	Root Mean Squared Error	Participants were asked to perform a sequence of pre-defined ambulatory tasks. No rest between activities. 30 minutes for each participant.	RMSE was 1.12 kcal/min, which is 30% less then Activity-Specific ANN (1.59 kcal/min) and 35% less then general ANN model (1.73 kcal/min).

Note: The abbreviations' meaning can be consulted here.

A different approach was implemented by Zhu *et al.* [60], that used deep learning, a convolutional neural network (CNN), to predict the energy expenditure. This CNN, very used in imaging processing [60], consists of a two layers of features extractors and a regression MLP with one hidden layer. The authors found a root mean squared error (RMSE) of 1.12 kcal/min. This result was compared to two *state-of-the-art* models of energy expenditure prediction: an activity-specific ANN and a normal regression MLP. In fact, in [60], the authors stated that the use of an artificial neural network for regression with a prior activity recognition is a way to increase the performance of the prediction. Indeed, the authors found that, in comparison with a normal MLP, the activity-specific ANN had better performance, with a RMSE of 1.59 kcal/min. Nevertheless, the error of using a CNN was 30% lower, obtaining better results. When the authors used the model found by the MLP neural network, the RMSE increased 35%, obtaining a RMSE of 1.73 kcal/min.

2.6 General Conclusions

The exoskeletons and orthoses have been developed since the last decades focusing on two main-folds: to augment the humans' strength and to aid persons with motor impairments due to aging or neurological disorders, such as stroke or cerebral palsy.

According to the literature, these devices can be single or multiple segment systems, allowing, respectively, a localized assistance focusing on each joint or on the total lower limb. They can be controlled following five assistive modes, well designed and investigated in the literature, such as the trajectory tracking control, the impedance control, the EMG-based control or the model-based control. The trajectory tracking control and the impedance control were describe with more detail in this chapter. Most of these robotic devices allow an assistance based on repetitive gait patterns, when controlled with trajectory tracking control, and based on the user's participation and effort, when controlled with the impedance control. Nevertheless, these orthotic devices are not prepared to use these strategies to promote an user-oriented assistance. Therefore, these strategies should be tailored to fit to each end-user clinical case.

In this sense, a Human-in-the-loop control strategy was also introduced. This strategy uses the user's energy expenditure to control the assistance delivered by the assistive device. Towards a Human-in-the-loop control strategy, the current *state-of-the-art* of energy use on assistive devices was presented. According to the literature, current research directions aim to reduce the energy expenditure of users while walking with assistive devices. This energy expenditure is calculated manly with indirect calorimetry

that uses non-wearable sensors as gas analysers. In an attempt to solve this problem, new approaches using neural networks and regression models are being studied to allow an effective and non-biased prediction of energy expenditure. The biggest challenge is to find an optimal model that fits well the energy dynamics, allowing the disuse of high cost and non-wearable sensors giving place to small, comfortable, ergonomic and wearable sensors.

3. SmartOs – Smart Wearable Orthotic System

3.1 Introduction

The main goal of this dissertation addresses the implementation of a new control strategy named Human-in-the-loop in a Smart Wearable Orthotic System – SmartOs. For that, one control strategy that modulates the reference trajectory in real-time and another that modulates the orthosis compliance, will be presented. Furthermore, an empirical study of the impact of using SmartOs in healthy subjects in terms of energy, as well as two machine learning techniques for estimating the energetic effort of users while walking with the orthotic device, will be presented. Therefore, it is necessary to present the SmartOs and explain its current state.

In this chapter, an overview to the SmartOs project will be performed, presenting the two orthotic devices that compose the project, as well as its technical aspects and further explanations that are required to proceed to the following chapters.

3.2 SmartOs Description

SmartOs is a wearable, modular, bioinspired, smart and standalone lower-limb orthotic assistive system capable of interacting closely to its users, allowing personalized assistance. Towards an orthotic device intended to aid post-stroke survivors, it allows **(i)** a task-oriented and periodic gait training, **(ii)** an abnormal gait pattern correction, decreasing the asymmetry between the healthy and the hemiparetic limbs, **(iii)** a functional motor rehabilitation and **(iv)** a real-time gait analysis by tracking kinetic, kinematic and muscular information. Being smart and bioinspired, it encourages the user to actively participate in the gait training, allowing a more effective motor recovery.

The system is divided into two orthotic devices, the PKO and the PAFO, powered by a DC motor and controlled by a hierarchical control architecture separated into high-, mid- and low-level stages. The system is fed by a DC battery, making it completely wearable and suitable for clinical usage. Furthermore, it is controlled by an intuitive Mobile Graphical Application, which allows all the system and therapy settings. Also, the therapy data can be displayed and analysed making use of the Desktop Graphical Application. Figure 3.1 presents the conceptual design of SmartOs.

SmartOs is an orthotic gravity compensated system that can be either a multi-segment device or a single-segment device. Consisting of two orthotic devices, the PKO and the PAFO, it allows an effective recovery for persons with motor impairments, as stroke survivors, at the knee and ankle joint.

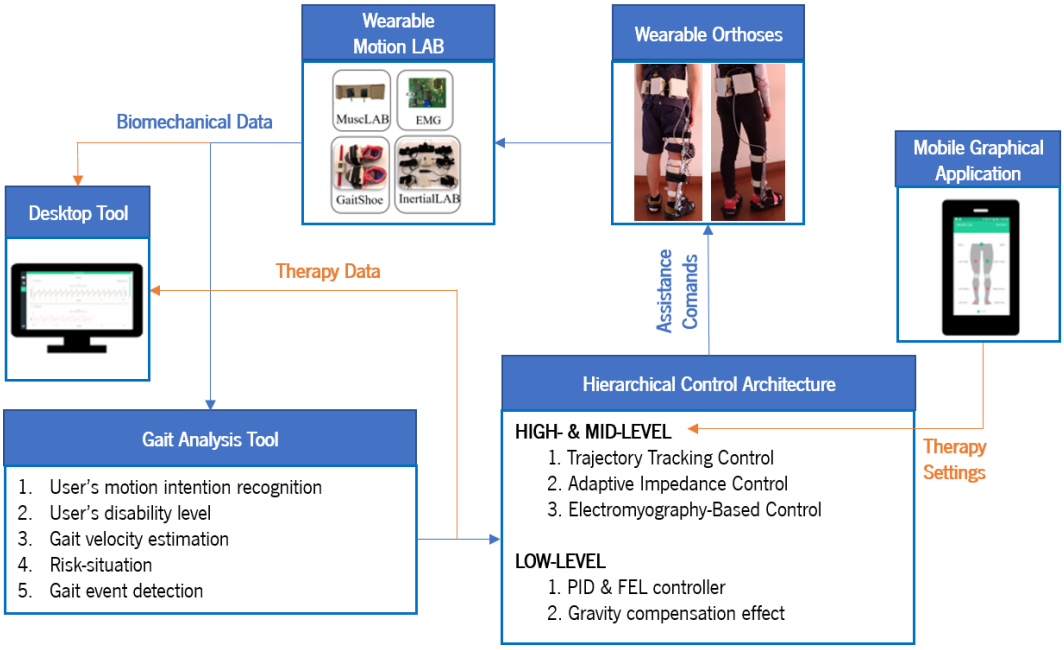

Figure 3.1: SmartOs conceptual design. Adapted from [61].

Following the proposal of Tucker *et al.* [10], the SmartOs is hierarchically controlled, diving the control strategy into high-, mid- and low-level, that work at different rates. The high-level, implemented into a Raspberry Pi 3 (SmartOs CCU), works at 100 Hz. It works closely with the mid-level control, that is implemented STM32F4-Discovery at 1000 Hz. On the high- and mid-level, the system provides four types of control: **(i)** User-Orthosis Interaction Based Control, a strategy based on the interaction torque between the user and the orthotic device, **(ii)** Trajectory Tracking Control, allowing a repetitive gait training with patterns of walking generated through the healthy trajectory, **(iii)** Adaptive Impedance Control, which adapts the stiffness of the joint considering the user's needs assuming more or less control of the therapy and **(iv)** Electromyography-Based Control, allowing a control strategy based on the muscular information during the gait.

The low-level, also known as Low Level Orthotic System (LLOS), is also implemented in a STM32F4-Discovery and it works at 1000 Hz. On the low-level stage, the control law is applied, receiving the reference trajectory from the above stages and controlling the DC motor with a PID controller, and the gravity compensation effect is performed. These four assistive strategies are implemented in the two orthotic devices, except the adaptive impedance control that is not closed for the ankle orthosis.

SmartOs endows a Wearable Motion Lab (WML) that includes three main wearable sensor systems: **(i)** the EMG, **(ii)** the InertialLAB and **(iii)** the GaitShoe. The EMG consists of four PCBs allowing the measurement of muscular activity directly from four muscles at the same time. It is possible to be extended up to eigth PCBs to measure four more muscles.

InertialLAB is formed by wearable IMUs to monitor the biomechanical motion of the lower limbs and the GaitShoe includes FSRs to measure force-ground contacts to perform the gait segmentation. Using the signals from the Wearable Motion Lab, a gait analysis can be performed through the Gait Analysis Tools. With this feature, the SmartOs is capable of recognizing the user's motion intentation, his/her disability level, as well as the gait speed estimation and gait event detection. Figure **3.2** displays the wearable actuation system and the wearable motion lab, including the two orthotic devices that compose the SmartOs.

Figure 3.2: SmartOs system overview. Adapted from [61].

The information gathered through the Gait Analysis tool is transmitted to the hierarchical control, which process this information and adapts the system control. As the brain of the system, the Hierarchical Control Architecture sends the physiological and biomechanial signals into a Desktop Application, giving visual feedback to the user and to the physioterapist. Also, with a brand-new wearable vibrotactile biofeedback system being developed, the SmartOs will be also capable of interacting even more with its users, encouraging his/her participation in the therapy, improving the user's gait recovery. At last, the system provides a user-friendly Mobile Graphical Application used to **(i)** introduce the demographic data, as the age and height; **(ii)** to perform the assistance settings, for example the orthotic device to be used,

the type of desired control, the gait speed, the gravity compensation effect, amoung others; and **(iii)** the monitorization settings, i.e., if the user or therapist want to activate the InertialLAB, the EMG or the GaitShoes/FSRs. Figure **3.3** displays the mobile application and its features, as well as the desktop application intended to monitor the assistance in real-time.

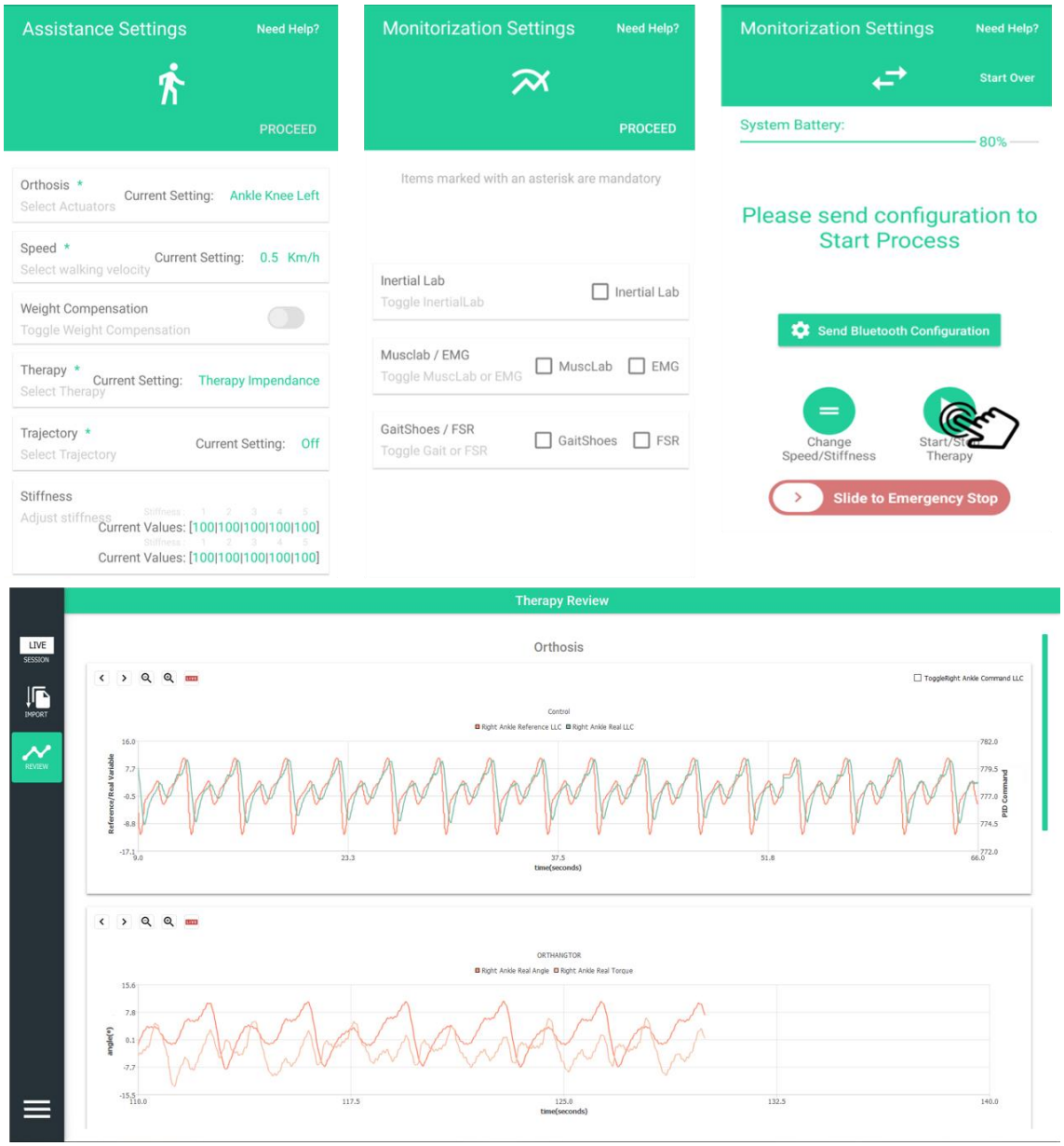

Figure 3.3: Examples of layouts from the mobile (top) and desktop applications (bottom). Adapted from [61].

Considering the technical aspects, the SmartOs consists of two orthotic devices developed for a localized assistance, the powered ankle-foot orthosis and the powered knee orthosis. Both devices are originally part of the H2-exoskeleton from Technaid S.L., Spain. Its velocity can range between 0.5 to 1.6 km/h by a brushlees DC motor coupled to a gearbox, capable of providing an average torque of 35 Nm and peak

torques of 180 Nm. Both PAFO and PKO have three embedded sensors for gait analysis purposes: **(i)** a precision potentiometer, used to estimate the device angle position; **(ii)** four strain gauges performing a full Wheatstone bridge used to estimate the human-orthosis interaction torque; and **(iii)** one hall effect sensor, used to estimate the motor's angular speed, current and torque. The PAFO device is composed by two additional FSRs, at the heel and toe, to measure the ground reaction force.

Table 3.1 presents the main techinal aspects of both orthotic devices, including the gait speed, the allowed angle, the DC nominal current, voltage and the nominal torque.

Table 3.1: Main technical aspects of the SmartOs system [62]

Parameters	*Units*	*Orthotic Device*	*Values*			
			Minimum	**Average**	**Maximum**	**Resolution**
Gait Speed	km/h	PAFO	0.5	—	1.6	0.1
Angle	°	PAFO	-20	—	20	0.5
		PKO	3	—	98	0.5
Nominal Voltage	V	PAFO and PKO	—	24	—	—
Nominal Current	A	PAFO and PKO	—	4.33	—	—
Nominal Torque	Nm	PAFO and PKO	0	35	180	—

3.3 General conclusions

In the current chapter, the SmartOs system was presented. It was performed an overview of the two orthoses that compose the system, as well as its main components and sensor systems. As the work developed in this dissertation addresses the implementation of a strategy that modulates the trajectory of the system and the joint compliance in real-time, some of the components presented in this chapter will be used and modified. The high-level control architecture and the front-end mobile application will be used and updated to fulfil the goals outlined in Chapter 1.

The following chapters present the work developed in this dissertation, as well as the theoretical concepts necessary for its elaboration and the results achieved.

4. Adaptive User-Oriented Trajectory Tracking Control

4.1 Introduction

As reviewed in Chapter 2, one of the main control approaches implemented on orthotic devices intended for gait rehabilitation and assistance is the trajectory tracking control using, for that, a standard gait pattern obtained with empirical studies of the biomechanics of the human body [63]. The main goal of this control strategy is to mimic the gait pattern of a healthy subject, allowing a repetitive training for persons with motor impairments, incapable of performing a smooth trajectory as the humans' one. However, most of the current orthoses do not use this control strategy to promote a *user-oriented* assistance. In hemiparetic patients, especially persons who suffered a neurological disorder as stroke is, the gait is extremely affected and, as natural, the clinic board for each one is different, existing patients with different scales of disability. Considering this, it is important to have a strategy oriented to the user's needs, capable of providing an assistance fitted to their incapacity.

Towards a Human-in-the-loop control, an adapted strategy to the traditional trajectory tracking control is presented in this dissertation, named **Adaptive User-Oriented Trajectory Control**. For each joint composing the SmartOs, a solution to design, build and implement different trajectories tailored to the user's needs was developed. The following subchapters will be divided into the two orthotic systems that compose the SmartOs project, and, for each, it will be presented the strategy that was implemented for creating, in real-time, new and different trajectories, as well as the validation protocol and the respective results.

4.2 User-Oriented Trajectory Adaptation

According to J. Perry [64], the ankle joint presents a repetitive rotation in the sagittal plane which is frequently called **dorsiflexion** and **plantarflexion** that represent, respectively, the upward and downward movement of the foot in relation to the floor. Along the gait cycle, the ankle motion is equally divided into these two rotations, summing four sub-phases during stance and swing. In the stance phase, while the foot is leaning on the floor, the walking pattern presents three of the four sub-phases: a first plantarflexion arc, in which the angle normally strikes the floor with a small angle and performs a downward motion towards negative angles, crossing the neutral angle, i.e., zero degrees, a first time until it reaches again the neutral angle. Afterwards, the ankle regains positive values of angle, reaching its maximum, producing the second arc and the first sub-phase of dorsiflexion. After reaching the maximum value, the angle starts to decrease, crossing the neutral angle for the third time. In this time, the foot is almost leaving the floor,

passing from stance to swing. In this third arc and second sub-phase of plantarflexion, the ankle angle reaches again another extreme and starts to increase, crossing the neutral angle for the fourth time. Finally, the last sub-phase of dorsiflexion starts until another heel strike is performed [64]. Therefore, the ankle joint angle is characterized typically by four passages into the neutral angle, dividing the ankle motion into the dorsiflexion and plantarflexion phases.

Considering the knee joint, the gait cycle is divided into **flexion** or **extension** movements if, respectively, the knee is bending, obtaining a positive angle, or is in full extension, obtaining an angle rounding zero degrees. During the stance phase, the knee angle is almost invariant, with a variation of nearly 5 degrees that, considering the total angle variation, it corresponds to less than 10% of the ROM. However, the same is not valid for the swing phase, in which the joint displays an important role in the gait pattern [64]. In this important phase, where the limb is projected to the front, allowing the execution of a new stride, the joint performs an angle variation of almost 50°, i.e., about 90% of the gait variation.

Figure **4.1** displays the ankle and knee trajectories created by cubic interpolation of healthy subjects that are used as the reference for the SmartOs project and follows the pattern described previously and presented by J. Perry [64].

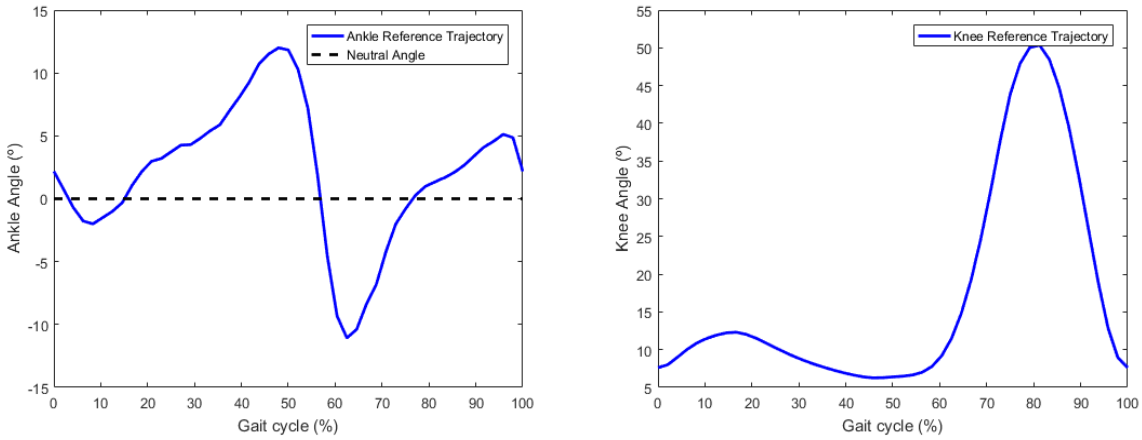

Figure 4.1: Ankle trajectory selected as the reference for a PID controller of the SmartOs project.

The reference is sent to a PID controller with negative feedback that continuously calculates the error *e(t)* between the reference points and the measured variable which is, in this case, the ankle angular position. Subsequently, the error is transformed into a controller's response, considering the proportional, integrative and derivative coefficients, and sent to an actuator which interprets it and performs a correction to the measured variable. Figure **4.2** displays the block diagram of the control strategy.

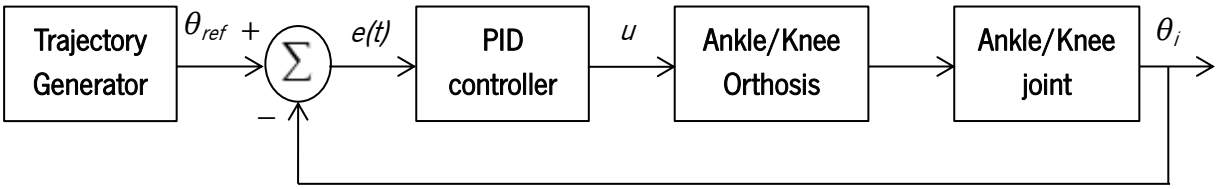

Figure 4.2: Block diagram of the position tracking control implemented in the SmartOs.

A PID controller executes a mathematical equation that conjugates three coefficients: the proportional (K_p), the integrative (K_i) and the derivative (K_d) gains, according to equation **(4.1)**. The weight of these coefficients will influence the response *u(t)* that is sent to the system's actuator.

$$u(t) = \mathrm{K_p} e(t) + \mathrm{K_i} \int_0^t e(\tau) d\tau + \mathrm{K_d} \frac{de(t)}{dt} \qquad \text{Equation (4.1)}$$

The gains should be correctly tuned to provide stability to the system and avoid oscillations that could affect and compromise the actuator's response. Therefore, the coefficients should be properly calculated in order to be suited for the application. In the SmartOs system, the controller's coefficients (listed in Table **4.1**) were tuned using the Ziegler-Nichols method.

Table 4.1: Controller's proportional, integrative and derivative gains found for the SmartOs project

Controller's Coefficients	*Adopted values*
K_p	90
K_i	1.5
K_d	1.5

As the high-, mid- and low-level controls work at different rates, as stated in the previous chapter, and considering the speed that is configurated, the trajectory length is resized. Using an empirical equation previously found to adjust the time of each sample considering the orthosis's speed – Equation (**4.2**) – the number of points that compose the final trajectory is calculated and the resized trajectory is sent to the PID controller, each sample at a time.

$$t\,[ms] = -34.62 \times Gait\ Speed + 107.31 \qquad \text{Equation (4.2)}$$

4.2.1 Ankle Trajectory Adaptation

The fact of creating different trajectories tailored to the user's needs is an important step to provide a more effective and user-oriented rehabilitation to persons with motor impairments. As mentioned in the beginning of section **4.2**, the ankle joint angle is divided into four moments of dorsiflexion and plantarflexion movements, depending on the foot is moving upwards and downwards, respectively.

The strategy developed to create user-oriented trajectories is based on real-time adaptations of the reference trajectory for the four sub-phases of the gait cycle. As the changes are accomplished in real-time, the algorithm should be capable of providing a correct pattern, maintaining always the **integrity** and **continuity** of the ankle angle position. Also, the algorithm should be quick and effective in order to promote, in real-time, a smooth transition, imperceptible to the users. Considering the four sub-phases of ankle angle position, the adaptations can be performed regarding the neutral angle, as shown in Figure **4.3**.

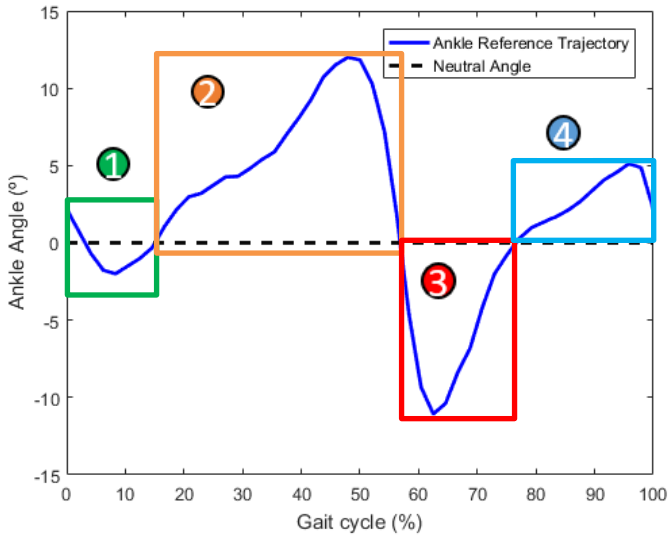

Figure 4.3: Sub-phases of ankle joint angle suited to perform a user-oriented trajectory adaptation: (1) and (3) plantarflexion movements, (2) and (4) dorsiflexion movements.

The joint angle presented in Figure **4.3** consists of a cubic interpolation with $N = 49$ samples of a healthy trajectory, sent each one at the time as a reference to the PID controller. To find the indexes corresponding to the transitions between sub-phases, the points in which the neutral value is achieved must be found. The neutral angle was chosen to be the base of the trajectory adaptation since the approximation of the trajectory to zero will produce the effect of **adaptability** all over the *kernel*. After finding these indexes, a *kernel* of size N was calculated considering the percentual factors to be applied to each sub-phase.

The percentual factors, controlled with the mobile application by the physiotherapist, are an integer between a *minimum* of 60% and a *maximum* value of 100%, with a resolution of 1%, that corresponds to a change in the healthy trajectory. Applying this *kernel* to the array of samples, a new reference trajectory is created. The *minimum* trajectory was found empirically analysing data from post-stroke subjects and considered the minimum trajectory that the user must perform. Nevertheless, this value is passive to be changed considering the degree of disability. As an additional feature, the algorithm must promote a trajectory adaption of the reference as whole, allowing to the physiotherapists to adjust the entire trajectory.

As explained in Chapter **3**, the SmartOs control is divided into three hierarchical levels (high-, mid- and low-level), as introduced by Tucker *et al.* [10]. The algorithm to perform the trajectory adaptations was inserted into the high-level control, as it is the control level responsible to generate the gait pattern trajectories. Furthermore, the mobile application was modified in order to allow a real-time changing of the trajectory. Figure **4.4** shows the block diagram of the high-level trajectory adaptation approach for the ankle orthosis.

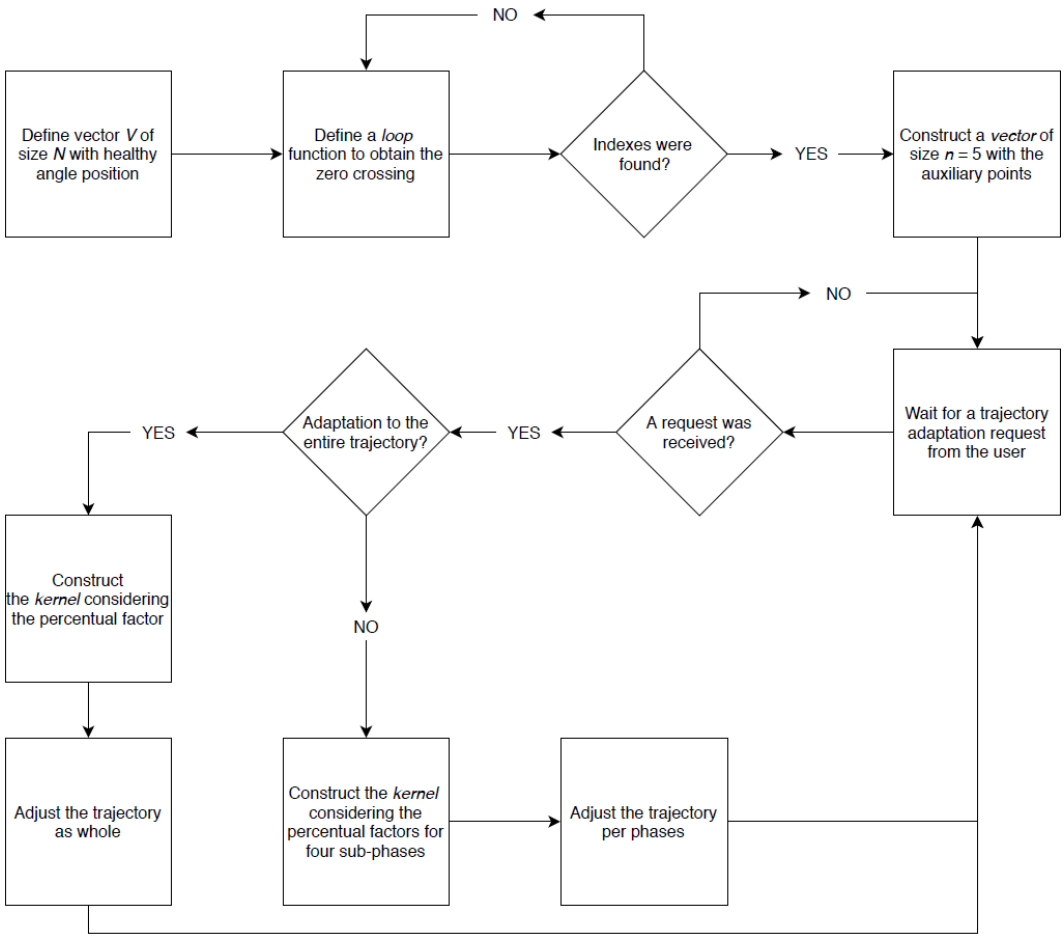

Figure 4.4: Block diagram of the ankle trajectory adaptation algorithm.

As a result of the trajectory adaptations, Figure **4.5** shows the simulation of different trajectories that can be created considering the user's needs. The **dark blue** is the reference trajectory of healthy users used in the current position tracking control, and the **black** is the adapted trajectory proposed in this dissertation.

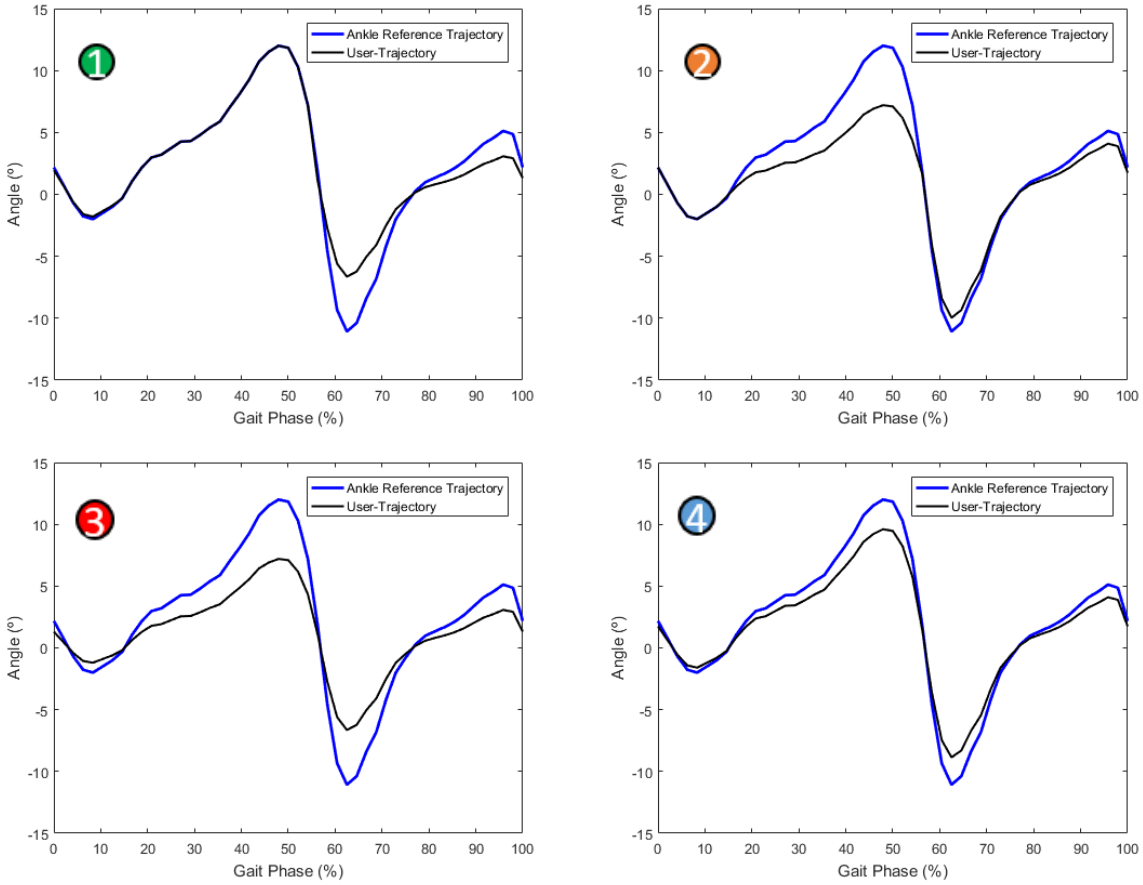

Figure 4.5: User-oriented trajectories simulation following the developed strategy, in which the percentual factors were: (1) 90%, 100%, 60% and 60% of healthy reference for, respectively, the four sub-phases; (2) 100%, 60%, 90% and 80% of healthy reference for, respectively, the four sub-phases; (3) 60% of healthy reference for the entire trajectory; and (4) 80% of healthy reference for the entire trajectory.

As the main goal of this control strategy is to promote an **user-oriented** gait training, it is intended that the physiotherapists change continuously the trajectory that the users are performing at the same time that the patients are improving in the rehabilitation. Considering the proposed strategy, and with a resolution of 1%, the number of different trajectories arises to almost 92 thousand.

In the sub-sections **4.4** and **4.5**, the algorithm's implementation is explained with more detail, as well as the changes that were performed to the front-end mobile application.

4.2.2 Knee Trajectory Adaptation

For the knee trajectory adaptation, the same principle of thought was adopted. However, as described in this chapter and in [64], the knee trajectory is not properly divided into four phases, as the ankle trajectory is. By opposition, the knee is characterized by a single phase of **flexion**. As such, the strategy was designed considering the stance and swing phases, constructing an adaptive *kernel* considering the percentual factors that are attributed by a request of the physiotherapist. Figure **4.6** shows the division of the knee trajectory into the two possible phases of change, i.e., the stance and swing phases.

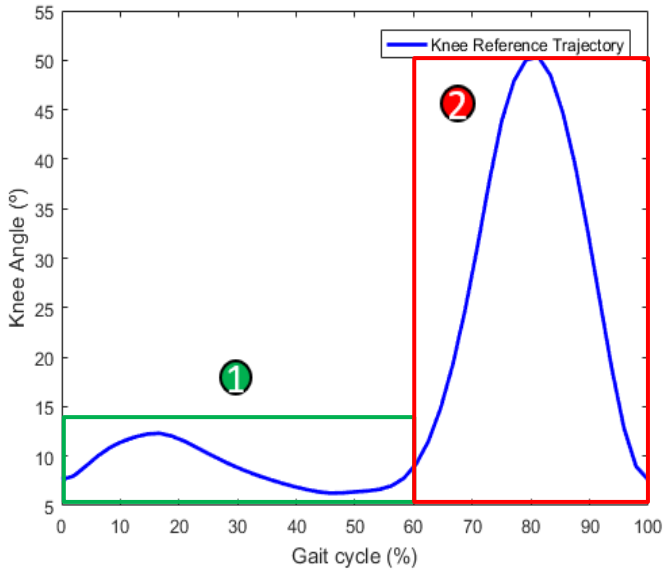

Figure 4.6: Phases in which the knee trajectory will be adapted: (1) stance and (2) swing phases.

In this case, the trajectory cannot be changed considering a fixed angle value (i.e., a basis value), as it was planned for the ankle joint, because it would produce an abrupt change in the transition of the stance phase to the swing phase, i.e., around 60% of the gait cycle. Therefore, an **adaptive *kernel*** considering the percentual factors received for the two phases must be constructed, allowing a smooth transition between them. However, this point alone is not sufficient to adjust the trajectory properly. As such, the inflection points of the stance and swing curve were found as auxiliary points to promote a correct trajectory adaptation. Following this strategy, the percentual factors will be directly applied between the auxiliary points in which the knee extremities are included. The remaining points that compose the *kernel* will be adapted considering the percentual factors for each phase. Figure **4.7** displays the knee reference trajectory with the auxiliary points used to adapt the trajectory.

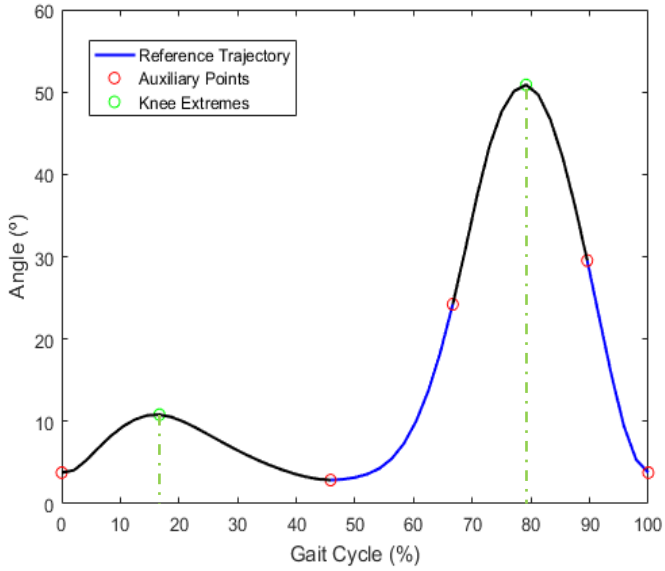

Figure 4.7: Knee reference trajectory auxiliary points used to adjust the trajectory. The green dots correspond to the knee extremes, in which the percentual factors will be directly applied. The red dots consist of the auxiliary points to construct the adapting kernel.

In Figure **4.7** is displayed the knee trajectory divided into two lines: the **black curves** correspond to the *kernel* zone in which the percentual factors received from the mobile application will be directly applied to the trajectory; and the **blue curves** correspond to the *kernel* zone in which the percentual factors must be adapted.

To find the auxiliary points it was developed an algorithm considering the monotony of the knee trajectory. The first step was to calculate the zeros of the first derivative in order to find the angle extremes. Considering this step, the green dots and the red dot around 45% of the gait cycle, represented in Figure **4.7**, were found. Then, the zeros of the second derivative were computed. Thus, the points in which the knee angle changes its concavity were discovered. This step was only applied to the swing phase. As such, the red dots rounding 65% and 90% of the gait cycle were found. Finally, the initial and final points were also considered as auxiliary points since they represent the stride initialization and finalization, respectively. Once the auxiliary points are found and if it is presented a request to change the trajectory, the adaptive *kernel* can be constructed.

Considering an array K of $N = 49$ samples, $K \in \mathbb{R}$, and $\mathbf{F_{ST}}$ and $\mathbf{F_{SW}}$ the percentual factors of stance and swing phases, respectively:

1. Between the first and second red dots, the percentual factor F_{ST} is directly applied;
2. Between the second and third red dots, the *kernel* is adapted considering the difference between $\mathbf{F_{SW}}$ and $\mathbf{F_{ST}}$ and the length of the array section;

3. Between the third and fourth red dots, the percentual factor F_{sw} is directly applied;
4. Between the fourth and fifth red dots, the *kernel* is adapted considering the difference between F_{st} and F_{sw} and the length of the array section.

Figure 4.8 illustrates the block diagram of the developed strategy for the knee angle adaptation.

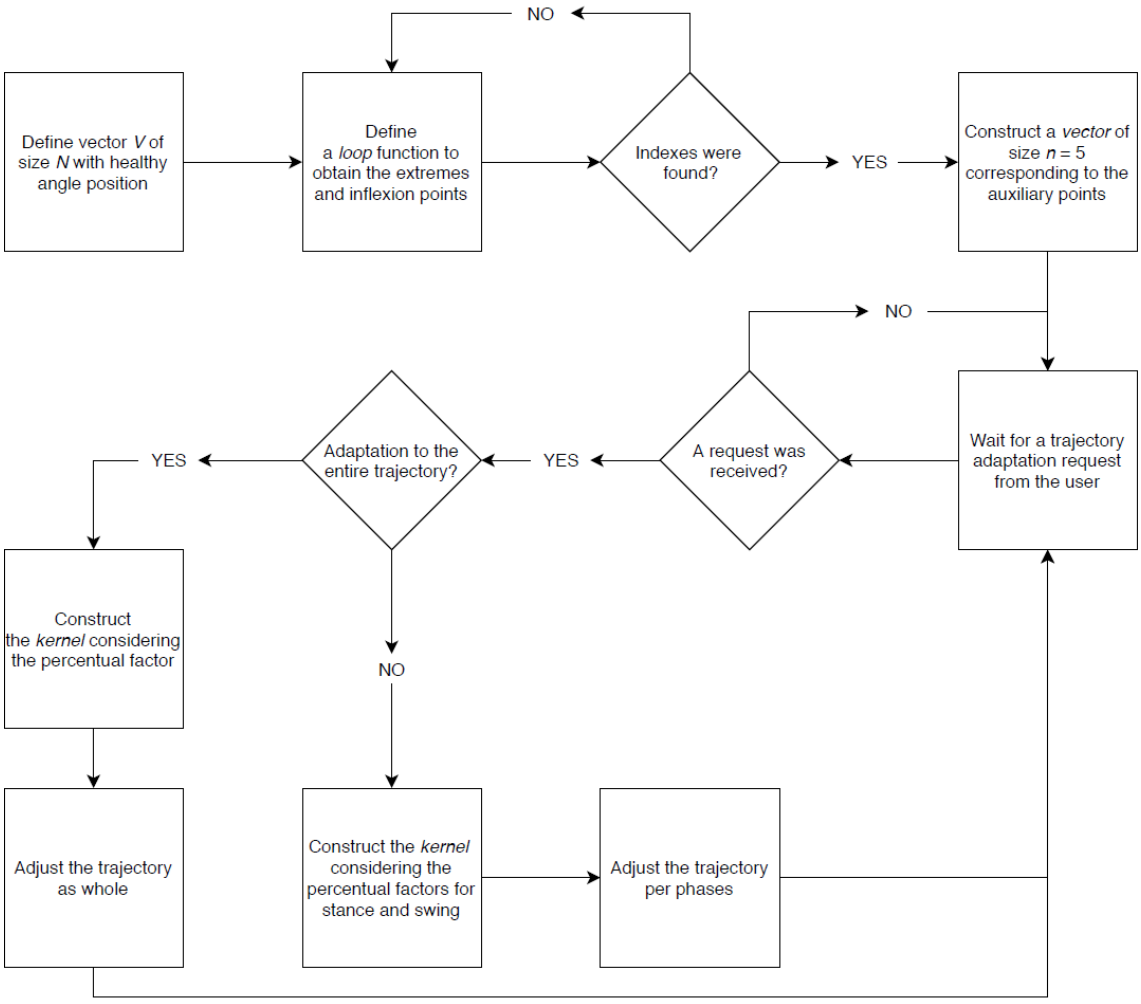

Figure 4.8: Block diagram of the developed strategy for the knee trajectory adaptation.

As for the ankle trajectory, a *minimum* value for the percentual factors was also considered. Analysing the gait pattern of stroke survivors, some patients walk with the knee full extended or with a minor angle, and in some cases, with an extremely high angle in the swing to compensate the ankle impairment. Moreover, a low value of reference would produce very low values in the stance phase, as the knee was completely locked. As such, a *minimum* value of 75% of the healthy reference trajectory was adopted. Nevertheless, this value is passive to be changed considering the degree of disability. The *maximum* value allowed was 100% of the healthy trajectory, as stated for the ankle orthosis.

With the proposed strategy, 300 different modes of assistance are allowed, considering a minimum resolution of 1%.

Figure **4.9** displays four different trajectories tailored to the user's needs constructed with the developed strategy. As can be seen, by the simulations, the trajectory's integrity and continuity is ensured while constructing new references personalized and adjusted to the user's degree of disability.

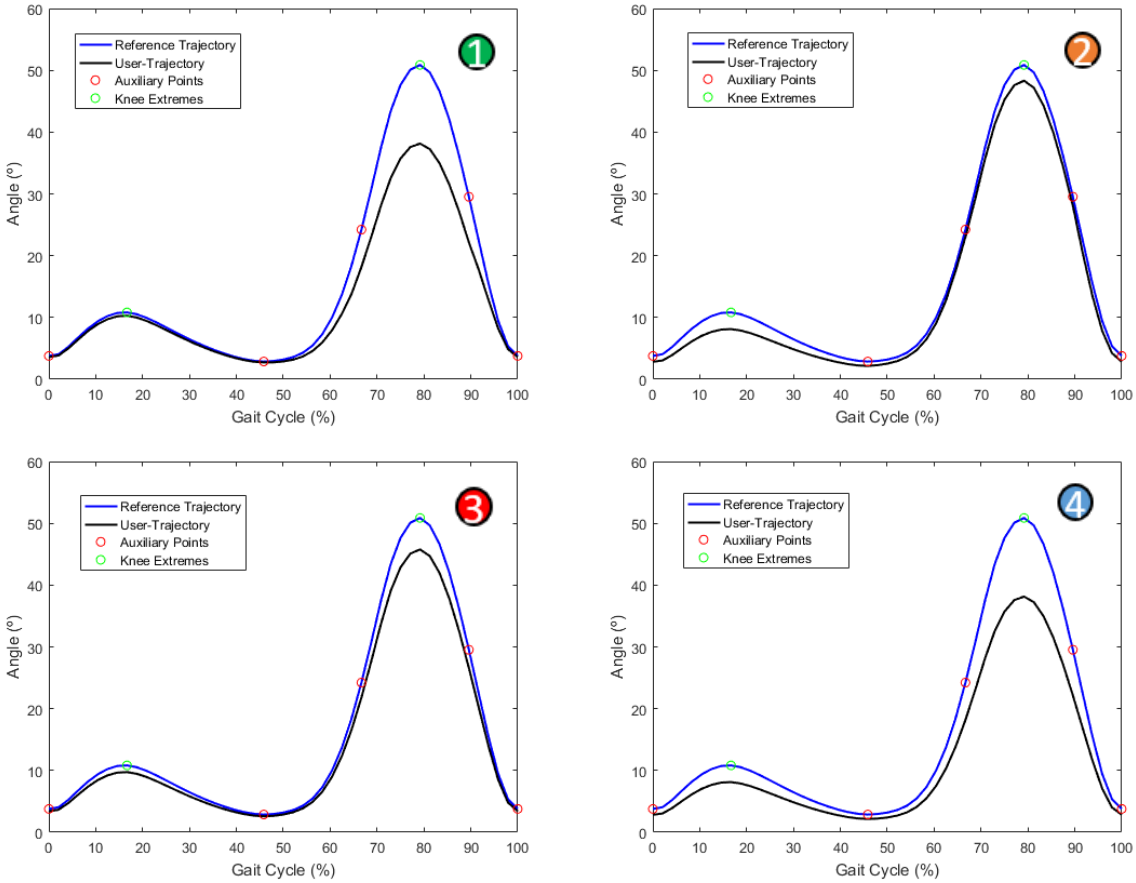

Figure 4.9: User-oriented trajectories simulation following the developed strategy, in which the percentual factors were: (1) 95% of healthy reference for stance and 75% for swing; (2) 75% for stance and 95% for swing; (3) 90% of healthy reference for the entire trajectory; and (4) 75% of healthy reference for the entire trajectory.

4.3 Algorithm Implementation

As stated in the previous sub-sections, the developed strategy to adapt the reference trajectory tailored to the user's needs, was directly implemented into the high-level of the hierarchical control architecture of the SmartOs system.

Figure **4.10** displays the class diagram that explicit the relationship between the classes responsible for creating the reference trajectories.

Figure 4.10: Class diagram that displays the classes responsible to generate the reference trajectories.

In the high-level of the SmartOs control system, a superclass named *TrajectoryGenerator* is responsible for creating the reference trajectories and controlling the assistive strategies for the two orthoses. Two subclasses, the *Passive_ModeTrajectory* and *Healthy_Trajectory* receive by inheritance some of the methods of the superclass, allowing the implementation of each strategy. In order to implement the Adaptive User-Oriented Trajectory Control into the SmartOs system, the same line of thought was followed. Thus, a new subclass, or "child", called *User_Trajectory* was created. In this class, the *kernel*

is constructed every time a new command is received. If the ankle orthosis is chosen, the public methods *crossingValue*, *AnkleLocalExtremes* are invoked to, respectively, find the points in which the alterations will be applied and to find the local extremes in each trajectory's sub-phase. By analogy, if the knee orthosis is chosen, the method *KneeStanceSwing* is invoked to find the points in which the trajectory's adaptation is based-on. Considering the *default_val*, which is the initial default value of the reference, the first trajectory is defined. This initial value, which should be configurated in the mobile application, is defined in the SmartOs using the virtual method *setDefaultValue*. Subsequently, the system waits for new commands from the user. If a trajectory change is requested, the vector *factor* of the superclass will be fulfilled. The algorithm analyses if the change is to be applied to the entire trajectory (if it is received just one value), or per-phases (if more than one value is received) and changes the *type_alteration* variable to "ALL PHASES" or "PHASES", respectively. Regardless of being chosen the adaptation to the entire trajectory or between phases, the methods *KneeKernelConstruction* or *AnkleKernelConstruction* are invoked, creating the *kernels* and applying the changes.

An important fact is that these changes must only be applied to the **next stride**. This aspect aims to minimize sudden changes in gait pattern, ensuring the integrity and continuity of the gait. Consequently, a control system was implemented. The virtual method *prepare_NewReference* is responsible to increase the trajectory index, sending point to point the next position to the mid- and low-level controls. Whenever the index is reset, the size of the vector *factor* is analysed. If the length is different from zero, it means that a trajectory adaptation was requested. It is just in this moment that a trajectory adaptation can be performed. This means that, although a request command is sent, the algorithm will not produce any changes until the index is reset. Finally, due to mechanical constraints, another control system was applied to prevent blockage of the system when an angle outside the allowed ROM is calculated. This feature is more important into the knee orthosis since an alteration in the stance phase can produce lower values of angle, near zero degrees, which is a value that the system cannot support.

As described in Chapter 3, the SmartOs system includes a user-friendly mobile application to set up the orthosis, the assistive strategy, the speed, the gravity compensation effect, among other configurations that the system allows. In order to promote an online trajectory adaptation, the mobile application was updated to introduce the new control strategy. Figure 4.11 displays the adaptations performed to the mobile application in the configuration menu.

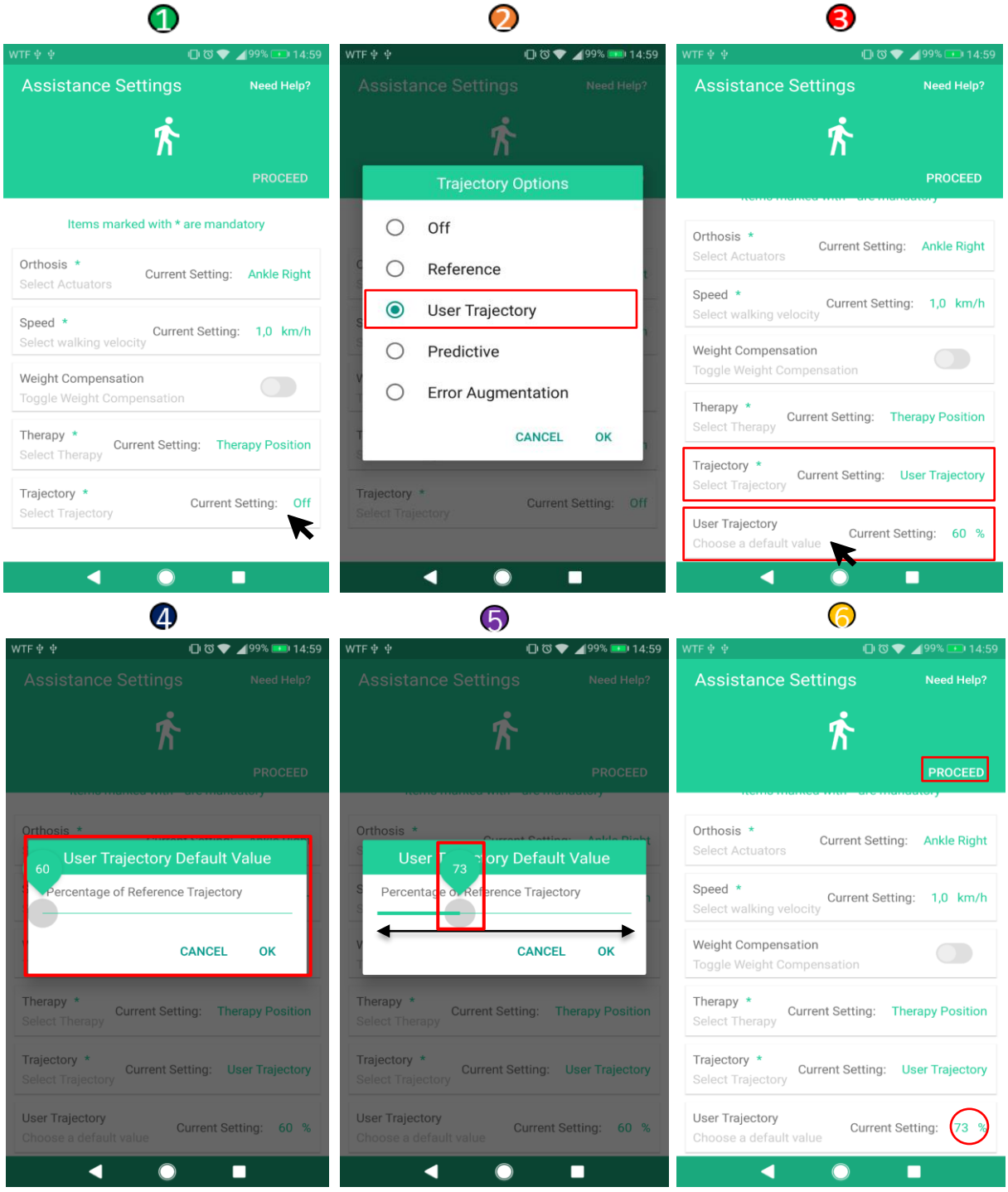

Figure 4.11: Configuration menu adaptations in the SmartOs mobile application.

Once the orthosis and speed are configurated, the physiotherapist must choose the assistive strategy for the rehabilitation session. To choose the Adaptive User-Oriented Trajectory control, first, the user must click the on the therapy option and choose the **Therapy Position**. Afterwards, a new layout will appear (layout **2**) showing four types of assistive strategies which all use the trajectory as the control variable. The user must click in the option ***User Trajectory*** and a new configuration box will appear. This box, shown in layout **3**, is used to choose the initial trajectory considering the healthy reference. As the ankle

orthosis is selected, the value 60% appear per default. However, the user can click on this box and a new layout, named *User Trajectory Default Value*, with a progress bar appears. This progress bar ranges between 60% and 100%, allowing the physiotherapist to choose the adequate value for his/her patients considering their disability and degree of locomotion. If the knee orthosis is chosen, the default value will be 75%, as described in the previous sub-sections of the current chapter.

Once the adequate value is chosen, in layout **5**, the user must click in the OK button to proceed to the next menu. Internally, this information is passed to the main activity, where all variables are configurated. After the session configurations are performed, the therapy can start. For real-time adaptation of the trajectory, the physiotherapist should click in the button *Real Time Settings* and a select the *Reference* option. Depending on the configurated orthosis, a new layout with two options, as shown in Figure **4.12**, will appear.

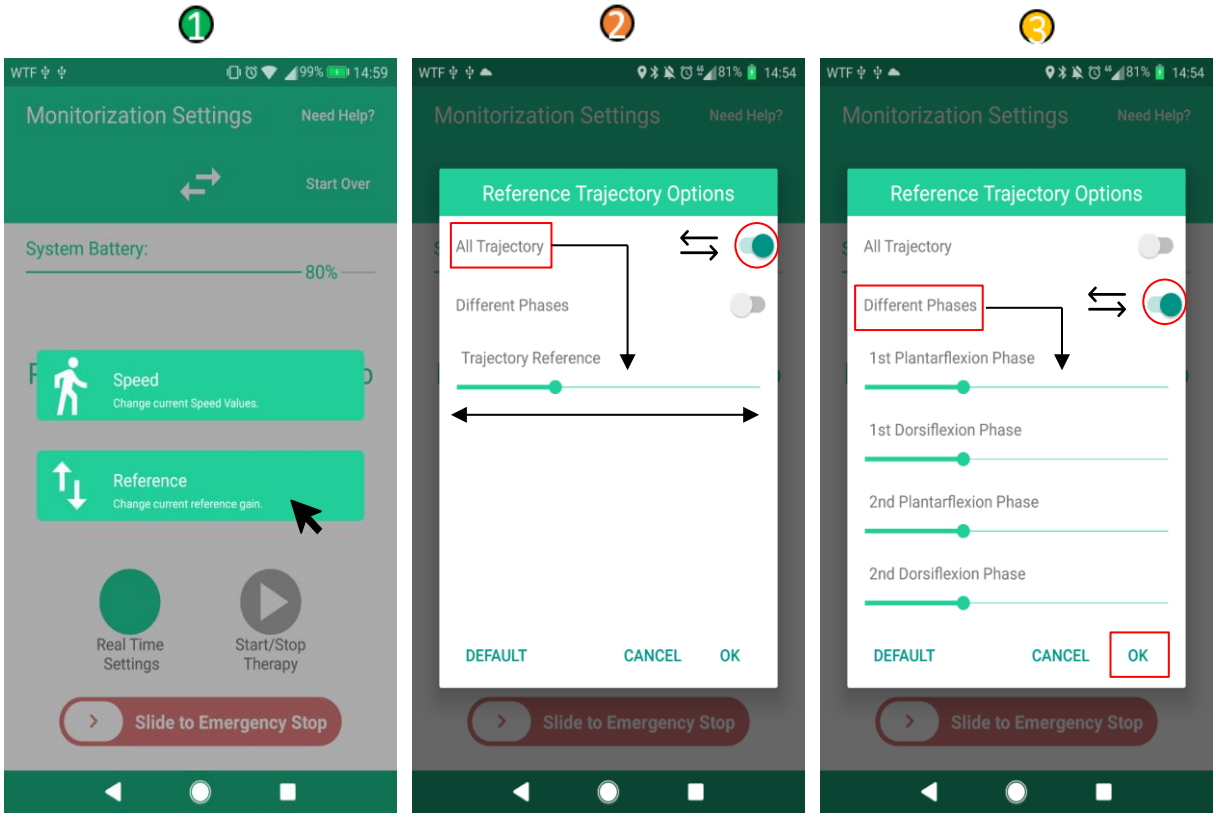

Figure 4.12: Application layout for changing the PID reference: (1) the configuration menu to select the change in speed or reference; (ii) the reference settings considering all trajectory; (iv) the reference settings considering gait phases.

The toggle button to configure the entire trajectory is selected per default. However, the physiotherapist can change it, clicking either in that button or clicking in the button to adapt the trajectory per phases. Depending on the choice, one or more progress bars are shown in order to configure the assistance as required. If the ankle orthosis is selected, four progress bars can be configurated, one for each phase of

the gait cycle, ranging between 60% and 100% of the healthy trajectory. If the knee orthosis is selected instead, two progress bars can be configurated, one for the stance phase and another for the swing phase. In this case, the progress bars range between 75% and 100%. After the trajectory adaptations are concluded, the physiotherapist must click in the OK button, sending the configurations to the main computer that controls the system. Another feature in this layout is a new button, called ***Default***, introduced to instantly request the system to configurate the default trajectory that was chosen in the beginning of the therapy.

4.4 Validation Protocol

In order to validate the control strategy, a set of experiments was carried out. The main goal was to assess the joint angle produced by the orthosis and the real joint angle that the subject is producing. Also, the algorithm latency and the PID response to the trajectory adaptations were evaluated to investigate the time-effectiveness of the proposed strategy.

The following sub-sections will describe the validation protocol followed to perform the experiments with healthy users and the results that were achieved.

A. Subjects

Seven healthy subjects (body mass: 70.9 ± 7.00 kg, height: 179 ± 4.37 cm and age of 25.4 ± 1.13 years) were recruited to perform the experiments. The subjects accepted voluntarily to perform the empirical evaluation, with the main goal of assessing the gait integrity and continuity when the trajectory adaptations are performed. All subjects signed a consent form to be part of the study. Subjects' rights were preserved and, as such, personal information provided was remained confidential. Data was collected at the University of Minho.

B. Protocol and Data Acquisition

Kinematic and kinetic data, as joint angle, joint acceleration and segment acceleration, joint and segment angular velocity, were recorded using the ankle and knee orthoses, once at a time, in sync with Xsens system (Xsens Techonologies B.V., Enschede, The Netherlands). Data was recorded at 100 Hz, for both orthoses and Xsens.

First the subjects were instructed to remain in stand position to put the inertial units in the correct places. As the data of interest is only of the lower limb, the Xsens' lower limb model was used. For that, seven

inertial units were used: one for the pelvis, one for each thigh and shank and one for each foot. Once the sensors are correctly positioned, the system was calibrated, following the steps stated by the manufacturer. Then, the orthosis was placed in the respective joint and the connections of the entire system were inspected. Figure **4.13** displays the experimental set up for the control strategy validation.

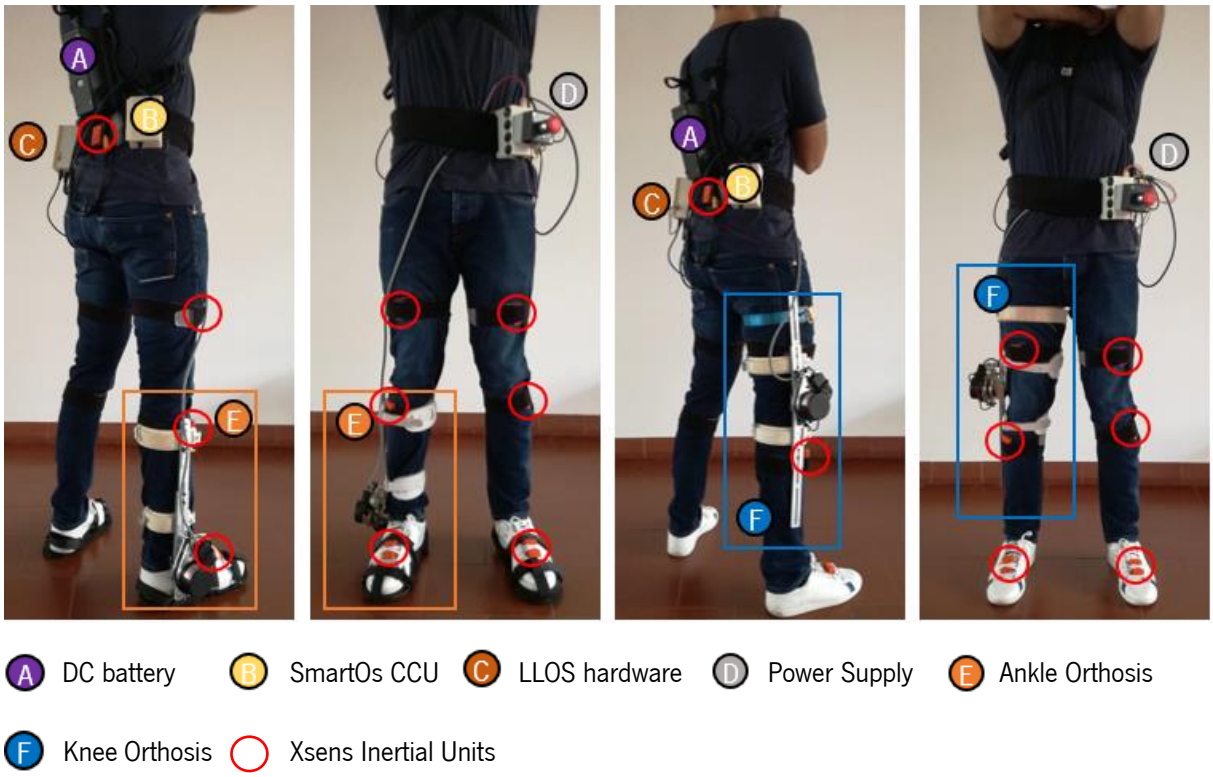

Figure 4.13: Experimental setup for the control validation for both ankle and knee orthoses.

Subsequently, the subjects were instructed to perform a familiarization trial, walking with the orthotic system with 100% of the healthy trajectory control. Then, a 4-minute or 5-minute trial, for the knee and ankle orthosis, respectively, was performed. The experimental trial was continuous since one of the goals was to assess the trajectory adaptation and the PID response in real-time conditions.

For the ankle orthosis, five conditions were assessed: **(i)** 100% of healthy trajectory, **(ii)** 60% of healthy trajectory, **(iii)** 80% of healthy trajectory, **(iv)** 90%, 100%, 60% and 60% for each phase described in the sub-section **4.2.1** and **(v)** 100%, 60%, 90% and 80% for each phase described in the same sub-section. Each condition had a duration of 1-minute and the subjects did not have knowledge of them.

For the knee orthosis, four conditions were evaluated: **(i)** 100% of healthy trajectory, **(ii)** 90% of healthy trajectory, **(iii)** 100% and 75% of healthy trajectory for stance and swing phases, respectively, as described in the sub-section **4.2.2** and **(iv)** 100%, 95% of healthy trajectory for stance and swing phases, respectively. Once more, each condition had a duration of 1-minute.

For each orthosis, three trials of 1-minute condition were performed for 1.0 and 1.6 km/h, which are the main velocities of the system.

During the experiments, the subjects were instructed to comment the assistance, evaluating the comfort during the trajectory adaptation, i.e., if it is comfortable and suited to their normal walk and if they feel that they are contradicting the orthosis movement or not.

C. Data Processing and Analysis

Data from the orthosis sensors, i.e., reference trajectory, real trajectory and PID output, and from the Xsens system, i.e., the joint and segments angles, accelerations, angular velocities and angular accelerations, were filtered using a fourth order zero-lag low-pass Butterworth filter with a cut-off frequency of 5 Hz, as proposed by Winter [65]. A gait cycle normalization was performed for each 1-minute condition, for both assisted and non-assisted limb in order to evaluate the level of walking symmetry.

The mean error, evaluated with the root-mean squared technique (RMSE), presented in Equation **(4.3)**, was calculated stride to stride, condition to condition and trial to trial. The error was calculated following the root-mean squared technique since this method is more sensitive to outliers, giving relatively high weight to large errors when compared to the mean error.

$$\mathrm{RMSE} = \sqrt{\frac{1}{N}\sum_{i=1}^{N}(y_i - \hat{y}_i)^2} \qquad \text{Equation (4.3)}$$

The error was, then, normalized considering the ROM in order to not create erroneous interpretations of low errors, and evaluated for each condition that was tested.

With the Xsens data, features that are representative of the gait were extracted and evaluated with a hypothesis test, following a *t-student* distribution. For the current analysis, a level of significance of 5% was chosen, meaning that the hypothesis test was performed with a level of confidence of 95%.

According to Patterson *et al.* [66], the level of symmetry can be evaluated considering five spatiotemporal parameters (SP): **(i)** the step length, **(ii)** the swing time, **(iii)** the stance time, **(iv)** the double support time and **(v)** the ratio between swing and stance time. In the following dissertation, the second, third and fourth parameter reported by [66] were evaluated and another one was introduced: the total ROM. For each spatiotemporal parameter, normalized by stride for each subject and condition, the symmetry ratio was evaluated, considering Equation **(4.4)**, and tested for each condition, assuming the null hypothesis (H_0)

that *there are no statistically significant differences for each spatiotemporal parameter considering the assisted and non-assisted limb*.

$$Symmetry\ ratio = \frac{SP_{assisted}}{SP_{non\text{-}assisted}} \qquad \text{Equation (4.4)}$$

4.5 Results and discussion

The main goal of this control approach was to create a position tracking control strategy that was fitted to the user's needs, creating different trajectories tailored to the end-user's degree of impairment. The current position control strategies are used in rehabilitation to promote a repetitive gait training, imposing to the user a predefined gait trajectory. Indeed, this strategy gains importance due to the degree of impairment of many neurological affected persons. However, to be a truly rehabilitating therapy, this strategy should be adapted to promote a user-oriented therapy, where the physiotherapist can adjust properly the trajectory considering the motion impairment.

The trajectory adaptation is performed in real-time using a user-friendly mobile application, being mandatory that the algorithm latency is as low as possible, promoting a smooth adaptation and fitted to the system's timing. Latency was calculated using a timer in the high-level of the SmartOs system, where it was evaluated the elapsed time after a request to adapt the trajectory was sent. It was found that, for both orthoses, the **algorithm is fairly fast**, being imperceptible, in temporal terms, for the users when the orthoses perform the trajectory adaptation. Table **4.2** show the results of the algorithm latency considering the type of trajectory adaptation for each orthosis.

Table 4.2: Trajectory adaptation algorithm latency for ankle and knee orthoses

Type of orthosis	*Type of trajectory adaptation*	*Latency*
Ankle	Entire trajectory	≈ 7.00 µs
	Per phases	≈ 207 µs
Knee	Entire trajectory	≈ 7.00 µs
	Per phases	≈ 17.0 µs

As the algorithm latency is small in comparison to the sampling time of high- and low-level control systems, which are, respectively, 10 ms and 1 ms, the real-time trajectory adaptation promotes the **continuity** of the walking pattern, which was required for this control approach.

The following discussion will be divided into two parts, A and B, considering both ankle and knee orthoses. Here it will be discussed the trajectory adaptation in real-time considering the conditions that were evaluated.

4.5.1 Ankle Orthosis

In a general way, the controller was able to perform the adaptations in real-time without interfering with the continuity and integrity of the walking pattern, as it can be seen in Figure **4.14**. This requirement was accomplished since the trajectory adaptations were performed in each **stride initialization**, without promoting changes instantaneously.

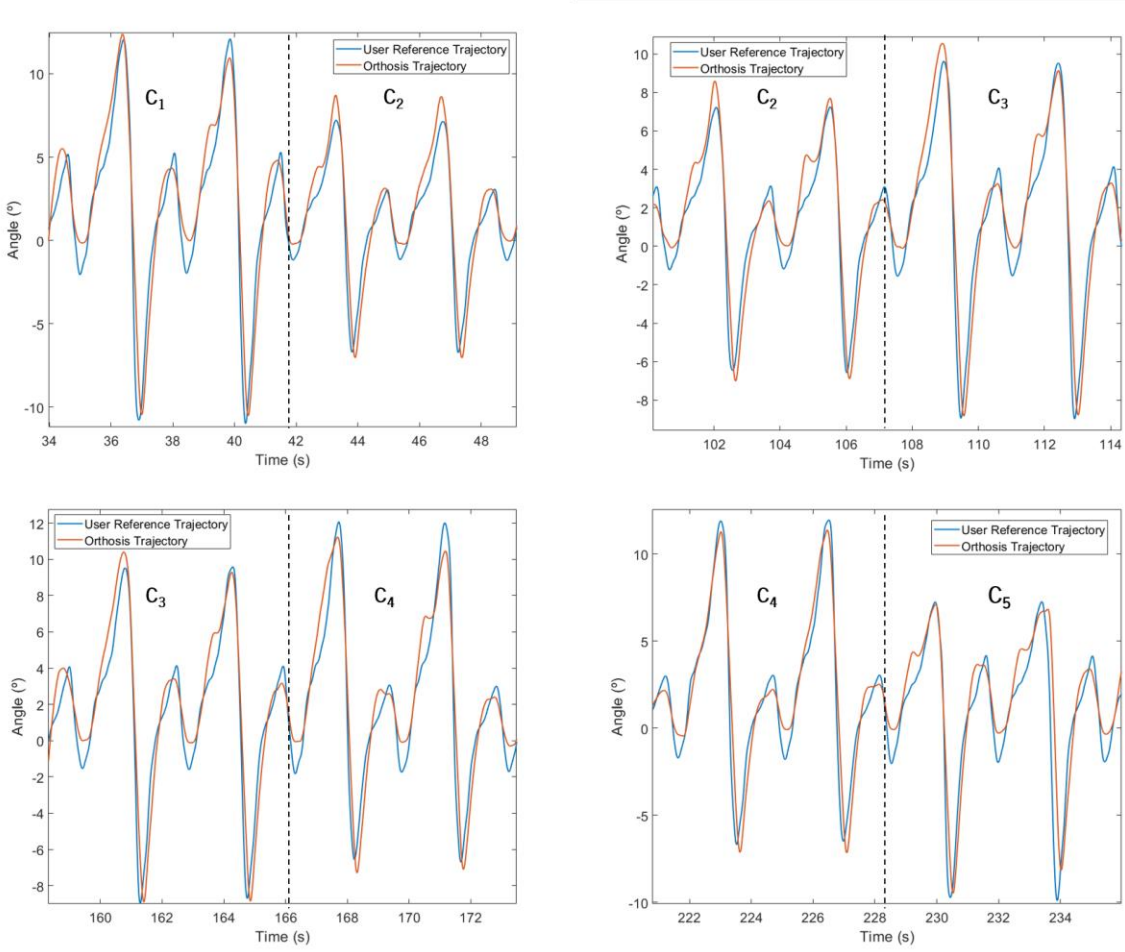

Figure 4.14: Trajectory adaptations evaluated as described in sub-section **4.4.1 - B** for one subject. C1, C2, C3, C4 and C5 represent the five conditions that were tested.

Considering Figure **4.14**, that shows the trajectories transitions during one experimental trial, it can be seen that, indeed, the trajectory adaption, marked by a dashed line, does not interfere with the correct functioning of the system, although the subjects were able to identify the adaptations since the imposed trajectory was different between conditions. Also, it can be seen that the orthosis behaviour, that translates into the subject's behaviour, changes stride to stride, producing an error. Thus, a gait cycle normalization between each condition is important, to analyse the subject's behaviour regarding a mean stride. Figure **4.15** display the stride normalization considering the trials and subjects universe for each 1-minute condition, for 1.0 km/h and 1.6 km/h. The first condition, described as **(i)** in sub-section **4.4.1 – B**, was used as a "**control condition**", in which the users walked with the orthosis at 100% of the healthy trajectory proposed by Winter [65].

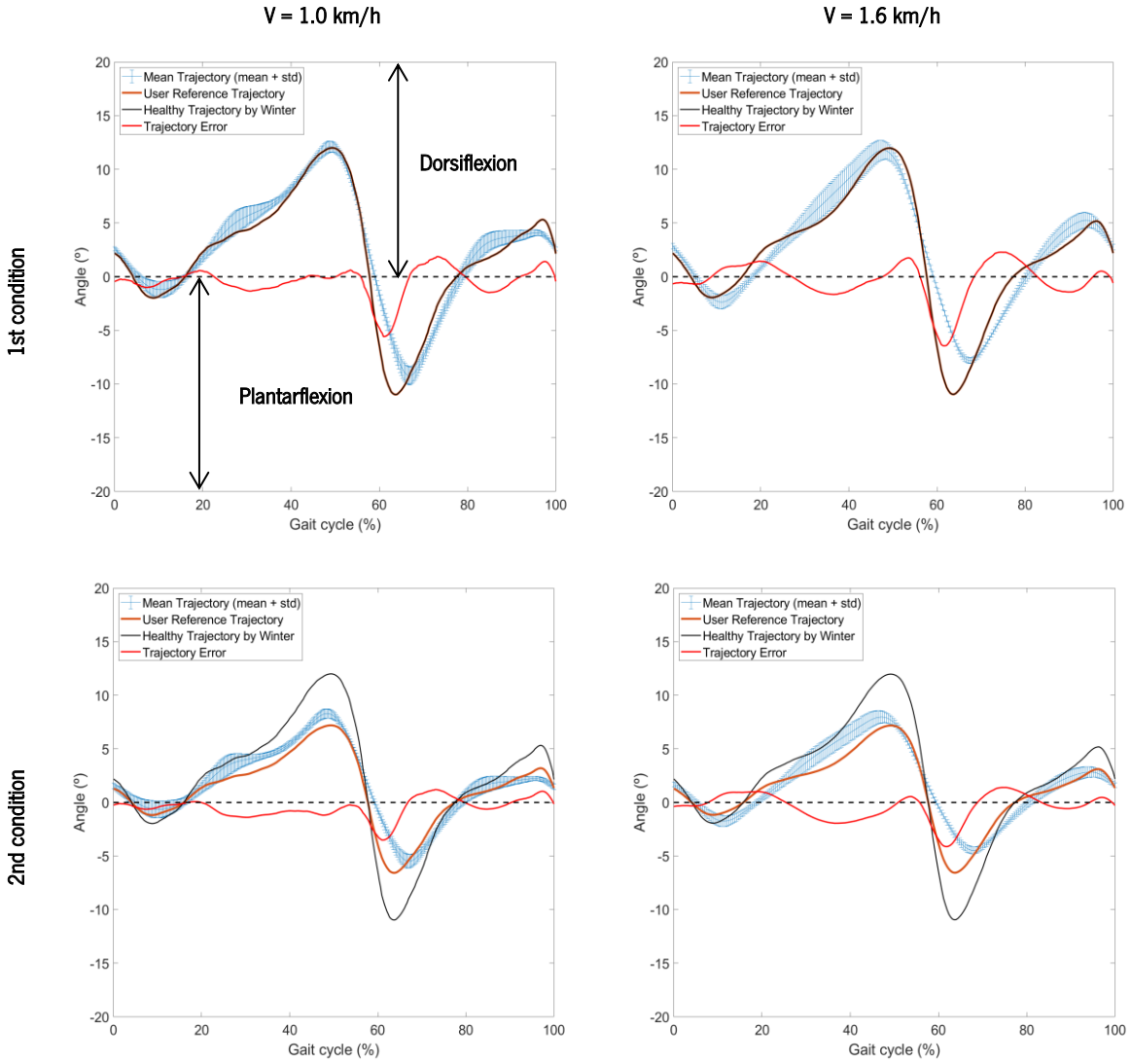

(continue)

(continuation)

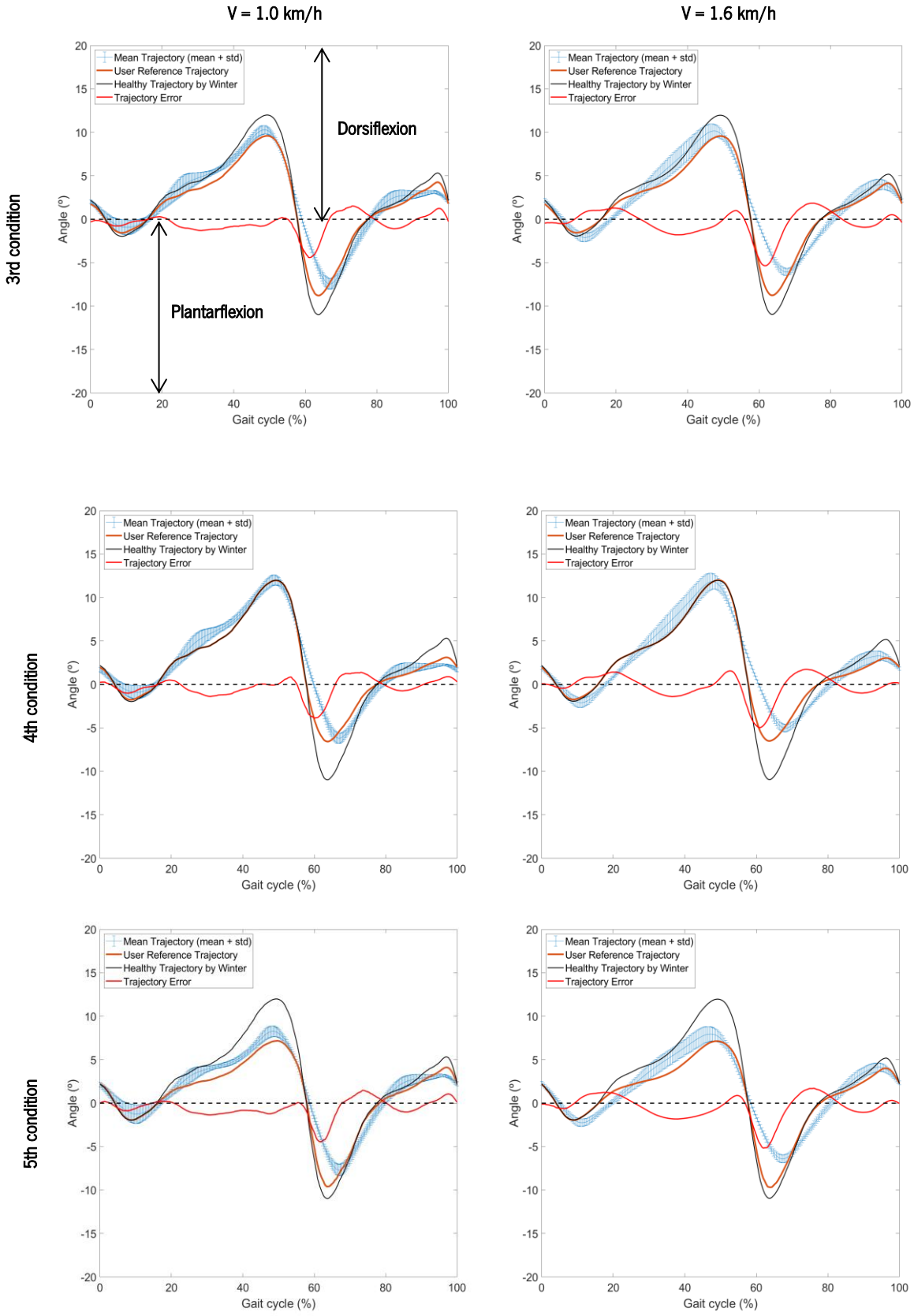

Figure 4.15: Stride normalization regarding the trial's and subject's universe for the ankle joint and walking at 1.0 km/h (in the left) and 1.6 km/h (in the right) for the tested conditions.

Findings of Figure **4.15** show, in a general way, that the users followed the orthosis pattern for all conditions and speeds. This observation was more evident during the first phase of dorsiflexion for the first and fourth condition, particularly in the trajectory's extreme, where the absolute error was close to zero. By the other side, the error between reference and user's trajectory was more evident in the second phase of plantarflexion, statement valid for all conditions and for the two speeds. Moreover, in the first phase of dorsiflexion, for the second, third and fifth condition, the mean error was also higher, especially for 1.6 km/h. This result shows that, as healthy users, **there is interaction between subjects and orthosis**. If the analysis is made considering also the orthosis' speed, it can be observed that for a higher velocity, the error is slightly larger regarding the reference trajectory. Regarding all subjects, there is a smaller variation between the subjects' behaviour (or orthosis real angle) for most of the phases, except the first phase of dorsiflexion, in which seems to exist a slightly larger variation among subjects since the standard deviation is higher. Also, the last phase of dorsiflexion, when the subject is preparing itself for a new gait cycle, the subject's trajectory is more curvilinear and closer to the reference trajectory.

Figure **4.16** displays box plots of RMSE and normalized RMSE regarding the five conditions for 1.0 km/h and 1.6 km/h.

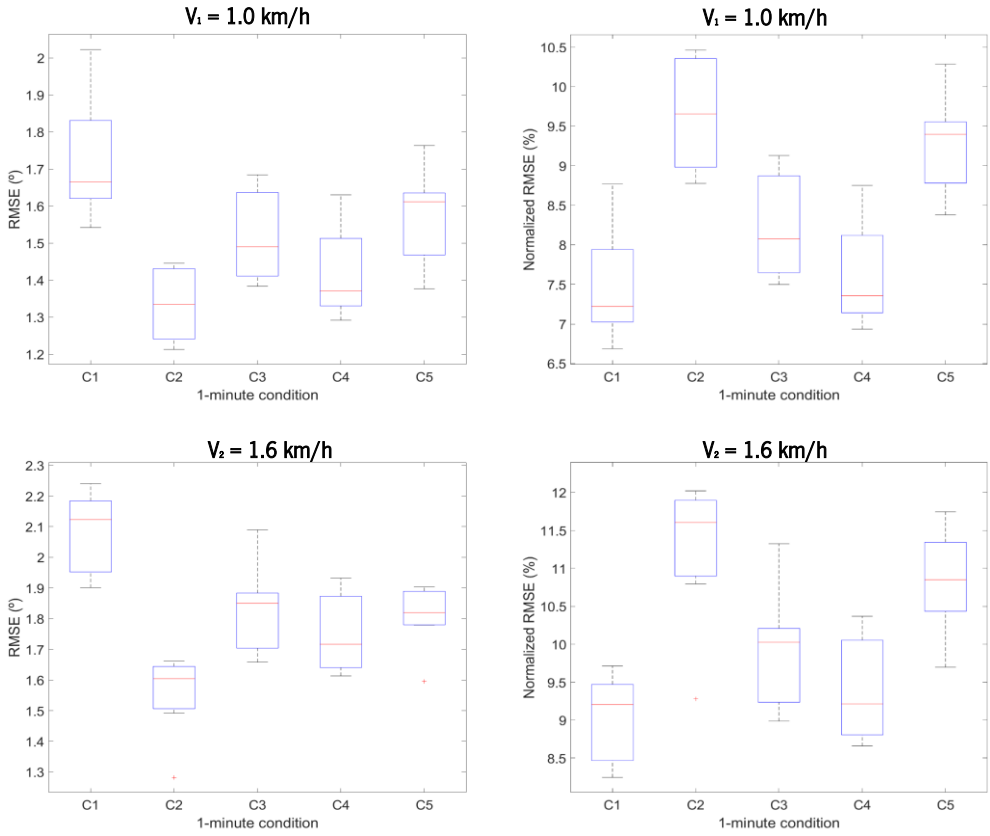

Figure 4.16: RMSE for the five conditions evaluated for the ankle orthosis. In the left, it is presented the absolute RMSE and, in the right, the normalized RMSE by ROM. C1, C2, C3, C4 and C5 represent each one of the five conditions.

By analysing Figure **4.16**, it can be observed that the RMSE decreases when the trajectory adaptations praise lower ROM, i.e., from second condition forward. This error is **less than 2 degrees** for both speeds which, in absolute terms, is not considered a high error. Normalizing the RMSE regarding the ROM for each condition, the value starts to increase in the second trajectory condition as the total ROM is lower, when compared to the healthy trajectory proposed by Winter [65]. This finding shows that RMSE when compared to the subject's ROM, can be significant. However, the median normalized squared error does not overcome 12% of the ROM for all conditions, even when the total ROM is slightly smaller, as in condition 2, where the ROM is 40% lower than the healthy trajectory ($\approx 14.4^{\circ}$ compared to $\approx 24^{\circ}$).

Another conclusion is that the RMSE increases as the speed increases. The subjects followed more the orthosis pattern when they walk at slow speeds. Nevertheless, the **"human healthy" factor** is being considered in the error calculations. Although the orthosis is imposing a trajectory, the healthy subjects are free to interact with the system. When healthy users use the system, their interaction can be, sometimes, higher than the orthosis contribution.

Three subjects reported that when the orthosis assists with a lower ROM, they felt more **freedom** to walk, as the orthosis was giving lower assistance. The apperception of a lower assistance results from differences in the PID response between conditions, producing a lower response when the reference ROM is lower. Consequently, in the actuator, the PID response is translated into a slightly lower torque. Overall, the results show that the subjects followed the orthosis pattern, without contradicting too much the system, producing a smaller error.

As a secondary outcome, the level of gait symmetry was evaluated for the five conditions tested in this control strategy. This evaluation aims to observe if the healthy subjects were able of changing the non-assisted leg gait pattern, contributing to a symmetrical gait. For that, the data recorded with the Xsens system was used for both right and left legs. Table **4.3** presents the results for the five conditions evaluated for the control strategy validation. Assuming the gait as truly symmetric, the ratios presented in Table **4.3** should be equal to 1, according to Equation **(4.4)**.

By analysing Table **4.3**, there were no statistically significant differences in the stance time between the right and left leg (p-value > 0.121), obtaining a ratio close to 1. However, the same was not valid for the swing phase. It is observable that the **swing time of the assisted leg is higher** than the non-assisted leg, either for 1.0 km/h and 1.6 km/h, and the differences are statistically different (p-value < 0.0214), excepting in condition 3 of 1.0 km/h which the p-value was higher than the level of significance (p-value = 0.0899). When the users walked with the orthotic system, it was observable an asymmetry between

time of swing, since the users were not truly synchronized with the system, performing an earlier toe-off. This observation agrees with the results found for the time ratios.

Table 4.3: Hypothesis test for a set of spatiotemporal parameters evaluated for each condition and speed of 1.0 km/h and 1.6 km/h. The mean ratios calculated through Equation **(4.4)** and the standard deviation are presented

Velocity	Conditions	ROM Mean (STD)	Stance time Mean (STD)	Swing time Mean (STD)	ST/SW Ratio Mean (STD)
1.0 km/h	C_1	0.770 (0.132)	1.01 (0.0566)	1.19 (0.101)	0.856 (0.103)
	C_2	0.532 (0.0781)	0.974 (0.0688)	1.14 (0.0772)	0.858 (0.0948)
	C_3	0.612 (0.0902)	0.969 (0.0925)	1.10 (0.137)	0.888 (0.134)
	C_4	0.701 (0.162)	0.992 (0.0640)	1.12 (0.101)	0.898 (0.131)
	C_5	0.659 (0.188)	0.989 (0.0563)	1.14 (0.121)	0.878 (0.129)
1.6 km/h	C_1	0.815 (0.154)	0.965 (0.0579)	1.19 (0.120)	0.824 (0.124)
	C_2	0.544 (0.0822)	0.956 (0.0645)	1.16 (0.0654)	0.829 (0.100)
	C_3	0.697 (0.0829)	0.963 (0.0553)	1.16 (0.105)	0.836 (0.117)
	C_4	0.685 (0.0652)	0.972 (0.0503)	1.14 (0.0745)	0.855 (0.0958)
	C_5	0.627 (0.0766)	0.974 (0.0707)	1.14 (0.0809)	0.859 (0.0194)

Regarding the ST/SW ratio, although this value is high and close to 0.9, the differences were, once more, considered statistically different (p-value < 0.0464). However, in condition 3 and 4, for 1.0 km/h, the values found were closer to 0.9, allowing accepting the null hypothesis with a p-value of 0.0727 and 0.0855, respectively. Regarding the ROM, the differences were also statistically different (p-value < 0.00790), for both 1.0 and 1.6 km/h, excepting in condition 1 of 1.6 km/h (p-value = 0.0953). Therefore, an asymmetry in ROM was verified.

In conclusion, the ratios evaluated regarding the stance and swing phases were conclusive. Although the differences in swing ratio were considered statistically different, the values for the three features are comparable to those found in [66] for a healthy gait. Regarding the ROM, the assisted leg presented an inferior angle in comparison with the unassisted leg. Also, considering this feature, the gait was closer to symmetrical when the strategy was used with 100% of the healthy trajectory. This result was found since the strategy was validated with healthy subjects. It is noteworthy that this strategy is intended to be used in hemiparetic gait.

4.5.2 Knee Orthosis

The same analysis was performed for the knee orthosis. In a general way, the same conclusions were obtained for this orthosis, i.e., the algorithm was able to produce the trajectory adaptations in real-time without interfering with the walking pattern. Once more, this was achievable since the trajectory adaptations were only performed, if a request command was sent, in the following stride, not producing an unexpected change in the joint pattern. This observation is visible in Figure **4.17**, that displays the knee trajectory of one subject and one trial.

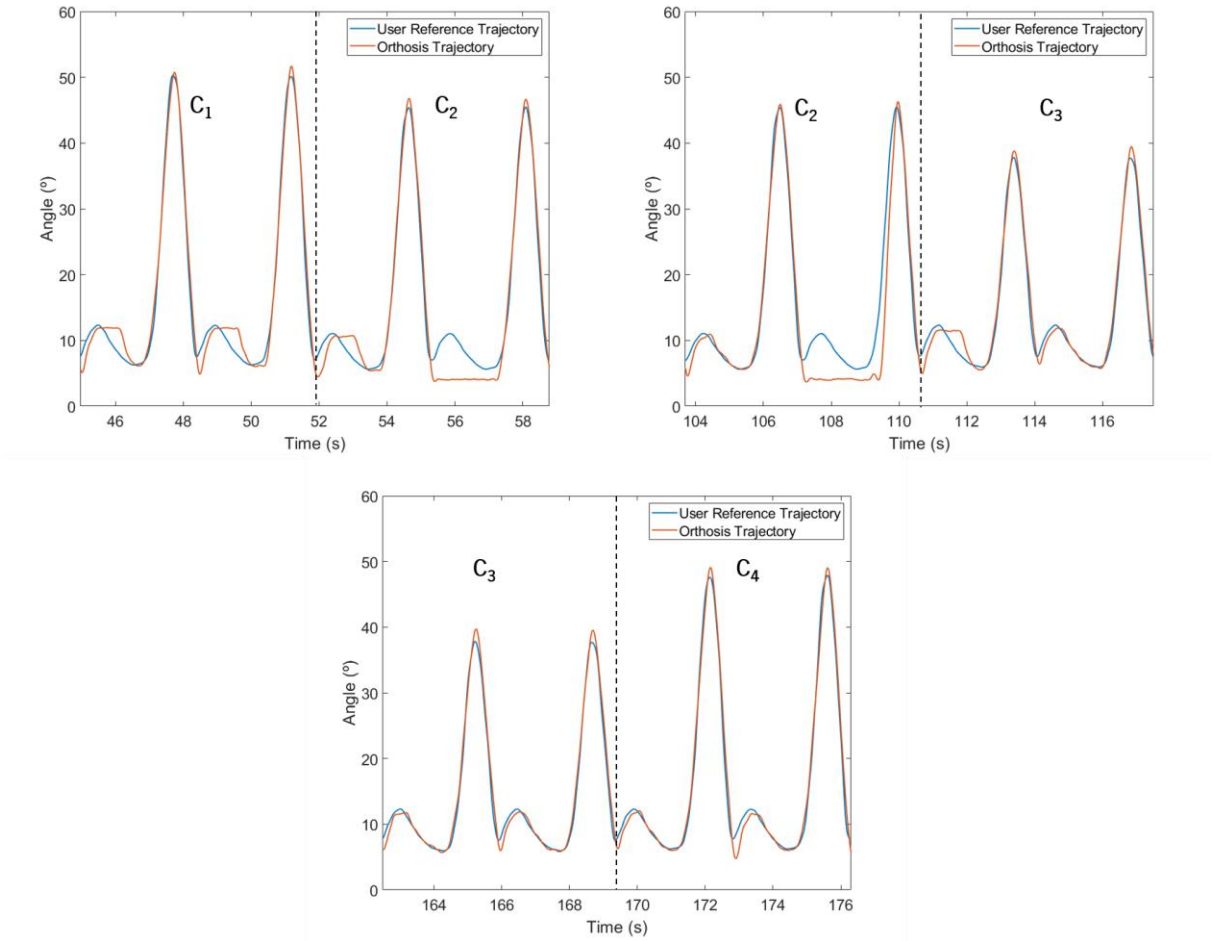

Figure 4.17: Trajectory adaptations evaluated as described in sub-section 4.4.1 - B for one subject. C1, C2, C3 and C4 represent the configurations that were tested.

Considering Figure **4.17**, the orthosis was able to promote the trajectory's adaptations as it was required, allowing the effectiveness of the current control strategy. However, as it can be observed, there were some strides of the second condition in which the orthosis was not able to produce the correct pattern for the stance phase. This observation was expected since a **security procedure** was applied internally to prevent the mechanical blockage of the system: for real angles below 5º, the PID response was set to zero and, consequently, the motor's torque was null. After the reference trajectory reached a certain

threshold, the PID returned to normal, giving commands to the actuator considering the error between the reference trajectory and the subject's real angle. The subjects reported that they felt the transitions between the assistance as it was expected since the ROM variation is higher. However, in the third condition, five of the seven subjects reported that the orthosis held the articulation movement. This condition produced a trajectory that is considered a small trajectory for **healthy subjects** walking at low speeds. As such, this observation will not be valid when dealing with neurologically non-intact subjects since the trajectory is adapted regarding their degree of impairment.

In order to evaluate the subjects' behaviour, a mean stride was calculated for each condition and speed, considering the heel strike event for the reference trajectory. Figure **4.18** displays the stride normalization per condition and velocity regarding the subjects' universe. The mean trajectory and the standard deviation are presented with a blue line, the healthy trajectory proposed by Winter as black, the users' reference trajectory as orange and the error as red.

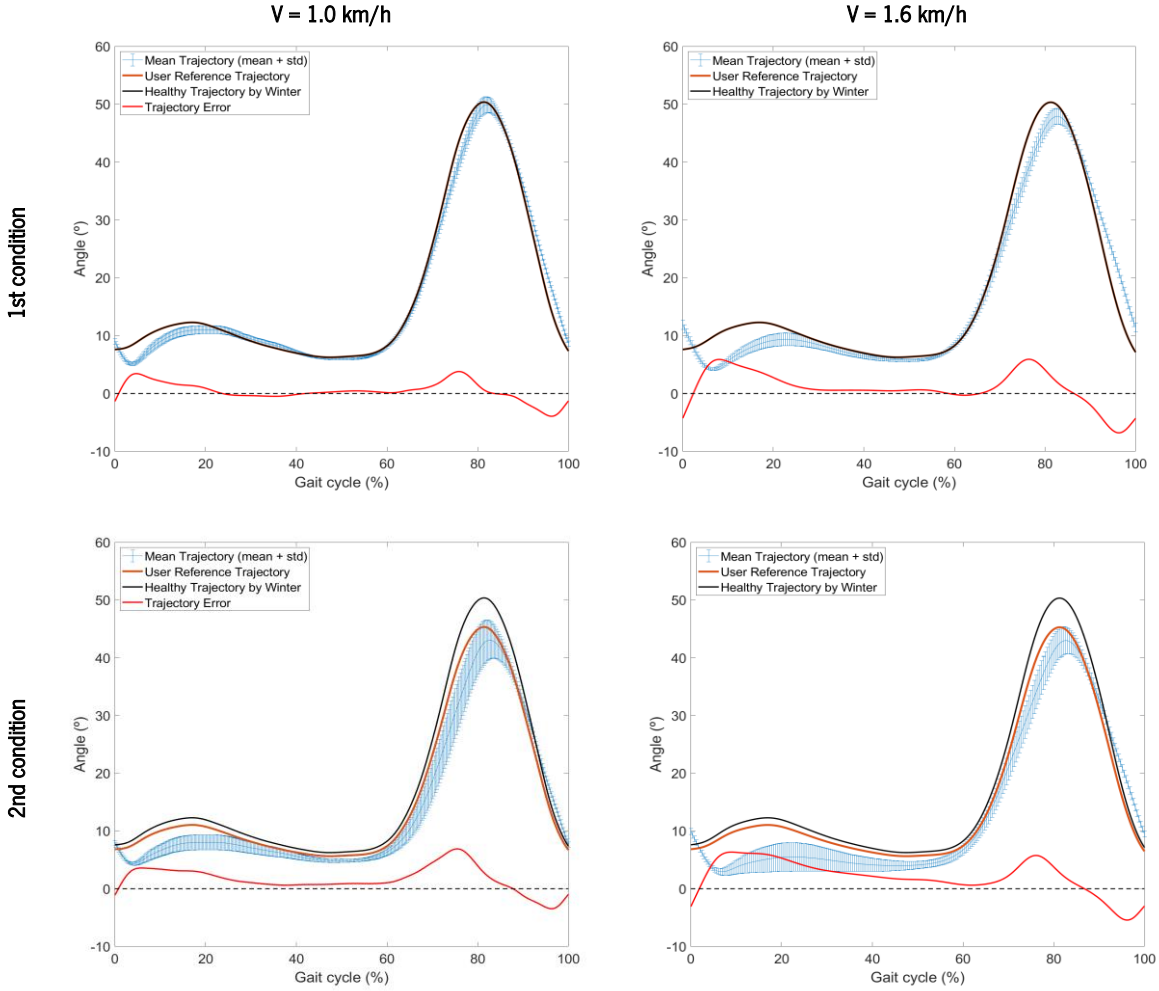

(continue)

(continuation)

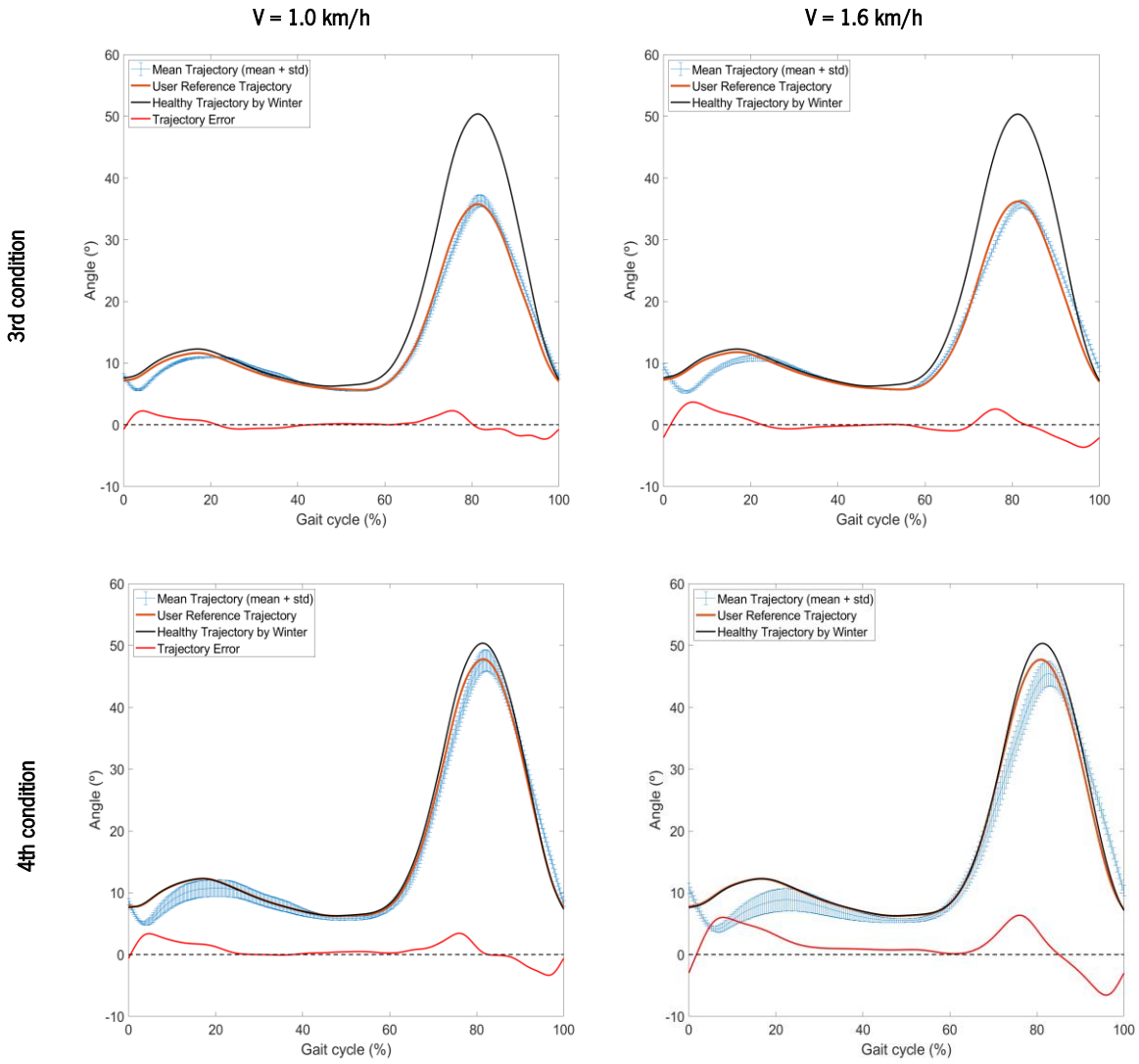

Figure 4.18: Stride normalization regarding the trial's and subject's universe for the ankle joint and walking at 1.0 km/h (in the left) and 1.6 km/h (in the right) for the second, third and fourth condition.

Analysing Figure **4.18**, it can be observed that, in a general way, the subjects followed the orthosis reference pattern. This observation was more evident in the first and third condition, in which both mean error and variation between subjects was smaller. Regarding the third condition, despite of not being considered a normal walking pattern for healthy subjects, the error was smaller for both stance and swing phases. The error was more perceptible when trajectory was adapted for the second condition, i.e., 90% of the healthy trajectory. This is true since the PID response was set to zero under certain values of angle, as explained above, producing the effect as the knee orthosis was blocked in the stance phase.

The mean error was calculated following Equation **(4.3)**. It was found an error per condition with median values below **9%** of the total ROM. Figures **4.19** displays the box plots of RMSE for the four conditions evaluated in this control strategy and considering the subjects' universe.

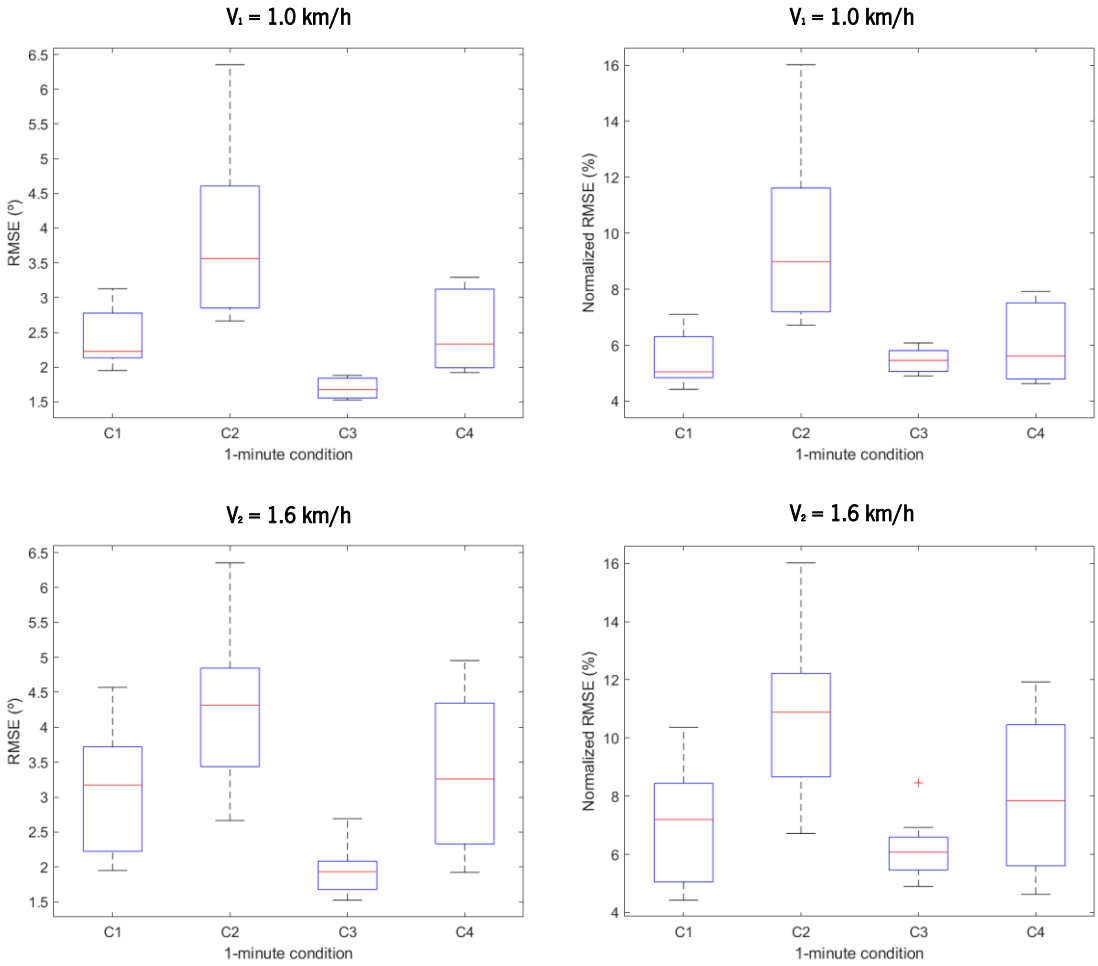

Figure 4.19: RMSE for the four conditions evaluated for the knee orthosis. In the left, it is presented the absolute RMSE and, in the right, the normalized RMSE by ROM.

From Figure **4.19**, it was observed that the RMSE is higher in comparison with the ankle orthosis, with median values that range between 2º and 4.5º. Nevertheless, considering the normalized ROM, the error is not considered high since it represents no more than 16% of the total ROM. As expected, considering the normalized stride, the error was lower in the third condition, with a median normalized RMSE below 6% of the ROM. In this condition, the subjects reported that SmartOs assistance did not allow a natural walking pattern and they felt they were contradicting more the system. Nevertheless, the orthosis was able to impose the trajectory, as it was supposed. This is an important feature, not for healthy subjects, but for hemiparetic patients whose degree of impairment is such that the walking pattern is highly corrupted. As the orthosis is imposing a trajectory adapted and tailored to the end-user's needs, it will allow an **effective gait training** for the first rehabilitation sessions.

Additionally, the gait symmetry was evaluated using the Xsens data. The stance time, swing time, ROM and ratio between stance and swing times were the features evaluated for both assisted and non-assisted legs, as for the ankle orthosis. Table **4.4** present the ratios between the assisted and non-assisted legs for each feature evaluated with Equation **(4.4)**.

Table 4.4: Hypothesis test for a set of spatiotemporal parameters evaluated for each condition and speed of 1.0 km/h and 1.6 km/h

Velocity	Conditions	ROM Mean (STD)	Stance time Mean (STD)	Swing time Mean (STD)	ST/SW Ratio Mean (STD)
1.0 km/h	C_1	0.910 (0.120)	1.07 (0.0552)	1.02 (0.0649)	1.05 (0.116)
	C_2	0.849 (0.105)	1.07 (0.0587)	0.969 (0.0996)	1.12 (0.165)
	C_3	0.767 (0.112)	1.08 (0.0425)	0.927 (0.0479)	1.17 (0.0858)
	C_4	0.911 (0.0989)	1.08 (0.0607)	0.973 (0.107)	1.12 (0.172)
1.6 km/h	C_1	0.806 (0.108)	1.01 (0.0838)	1.01 (0.0475)	0.998 (0.0990)
	C_2	0.789 (0.107)	1.04 (0.0225)	1.02 (0.0410)	1.03 (0.0599)
	C_3	0.688 (0.105)	1.05 (0.0346)	0.963 (0.0730)	1.09 (0.0865)
	C_4	0.781 (0.105)	1.04 (0.0434)	1.01 (0.0436)	1.03 (0.0850)

Results of Table **4.4** show that the knee orthosis allows a more symmetric gait in comparison to the ankle orthosis. This difference is more evident analysing the ratios between stance and swing timings for all conditions evaluated. It is observable that this feature is closer to 1, having just one condition in which the registered differences are considered statistically significant (p-value < 0.0276) that is condition 3, in which the subjects walked with the knee orthosis programmed to perform 75% of healthy trajectory for the swing phase. As the ROM in swing is lower, the swing phase is also lower, explaining the lower value obtained for the swing's ratios in this condition. Regarding this feature, the gait can be considered symmetric for all conditions (p-value > 0.227) except while walking at 1.0 km/h in condition 3, in which was found statistically significant differences with a p-value of 0.00680.

Regarding the stance timing, although the differences between the right and left leg were considered significant (p-value < 0.0176), the ratios' mean value was closer to 1. Nevertheless, for the first and fourth condition, a perfect symmetry was obtained, with differences not considered significant (p-value > 0.0575).

At last, the ROM was the trajectory feature that presented the highest difference between the two legs. It is observable that the ROM of the right leg is significantly lower in comparison with the left leg (p-value < 0.00890). However, this observation was not valid for the first and fourth condition when walking at 1.0 km/h (p-value > 0.0542). Therefore, the gait in terms of ROM is considered asymmetric.

4.6 General conclusions

This chapter presents an adaptive trajectory tracking control strategy for future application in the Human-in-the-loop strategy. Here, it was presented an user-oriented assistive strategy that allows the real-time adaptation of a position reference trajectory to be tailored to the users' needs. Results show that the trajectory adaptation is performed with insignificant latency (in a few microseconds), while ensuring the continuity and integrity of the gait pattern, as it was demanded. As a second outcome, it was evaluated if the healthy users could adapt the walking pattern of the unassisted leg to see if they could produce a more symmetrical gait. The symmetry ratios found were not so different from the healthy gait, except for the ROM feature and the swing time, that showed, in a general way, a significant difference between the assisted and unassisted leg. It is noteworthy that this study was performed with neurological intact individuals, that have a normal gait pattern. In a future perspective, this strategy will be validated in a clinical context where the gait pattern can be adjusted to each patient regarding their needs and degree of impairment.

The following chapter presents another user-oriented strategy in which the assistance is based on the users' effort and active participation on the therapy. The strategy allows the modulation of the joint's compliance in real-time, allowing the passage of a *quasi*-passive assistance to a fully trajectory control assistance. The user-oriented trajectories created in this chapter can be used in the following assistive strategy. In this way, the assistance is fully user-centered, allowing a real-time stiffness modification and a trajectory adaptation regarding the user's necessities.

5. Adaptive User-Oriented Impedance Control

5.1 Introduction

Impedance control is another control strategy frequently addressed in gait assistance and rehabilitation. This control strategy is considered an alternative to the EMG control law since it promotes an user-oriented assistance based on the subject's intention and effort [40]. It is an assisted-as-needed (AAN) strategy, allowing an assistance adjustment based on the level of disability of each impaired person, promoting a gait rehabilitation sustained in effort and interaction. It differs from the position tracking control strategy since it makes use of the subject's intention to produce an adequate assistance. With an adaptive impedance control law, it is possible to adjust the stiffness, producing a stiffer assistance for high levels of impedance, and a more compliant one when low levels of impedance are applied [40].

In this chapter, an adaptive impedance control strategy, already implemented in the knee orthosis [43], is presented and validated with neurologically intact subjects for the ankle orthosis that compose the SmartOs system. The strategy follows the same principal as presented for the knee orthosis. For each subject, an empirical study was carried out, calculating the *quasi*-stiffness of the joint with a similar approach investigated by Dollar *et al.* [67]. These values were inserted into the impedance control law, and the human-orthosis interaction was adapted along with gait cycle.

5.2 Adaptive Impedance Control

The adaptive impedance control strategy already implemented in the SmartOs system for the knee orthosis is considered an assisted-as-needed and *quasi*-hybrid strategy, divided into the three hierarchical control levels, presented and discussed in Chapter 3. It is an AAN control strategy since its main goal is to provide an assistance based in the subject's intention, and *quasi*-hybrid because it allows the passage between a passive mode, characterized by a mechanical and compliant movement, to a full-assistive strategy, characterized by a high-impedance and stiff movement.

The control is performed considering the subject's effort, measured through a strain gauge placed next to the orthosis joint. The subject applies a force in the orthosis to perform the intended movement and, consequently, promotes a deformation in the sensor. This deformation is, then, converted to torque, considered the **interaction torque**, which is proportional to the user's interaction with the orthotic system.

As a truly AAN control strategy, the reference torque needed to provide the assistance is evaluated regarding the error between the reference and the measured trajectory, respectively θ_{REF} and θ_{SYS}. This

approach is similar to that found in [42] and equal to that presented in [43]. To compute the AAN reference torque, this error is multiplied by the stiffness value (k), evaluated during the various phases of the gait cycle. Figure 5.1 shows the block diagram of the adaptive impedance strategy.

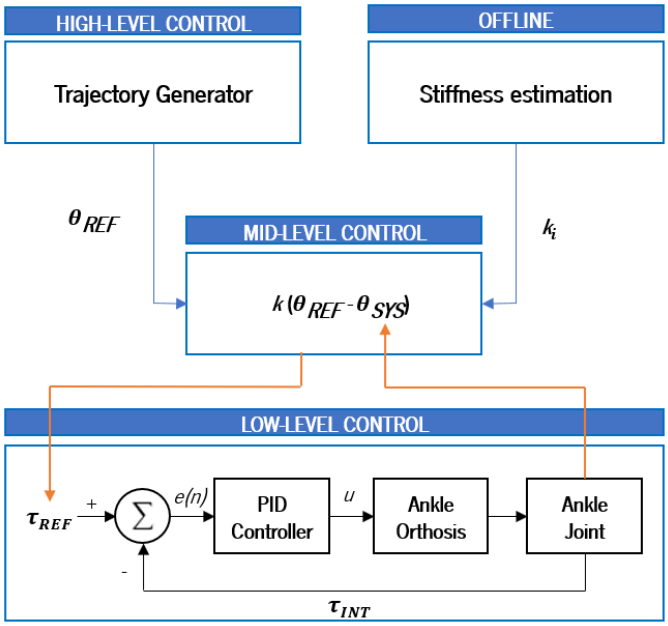

Figure 5.1: Block diagram of the adaptive impedance control strategy implement in the SmartOs system.

After the AAN reference torque being calculated, this reference is sent to a PID controller. Table 5.1 presents the proportional, integrative and derivate coefficients that are used in the PID controller.

Table 5.1: Controller's coefficients used impedance control law

Controller's Coefficients	*Adopted values*
K_p	120
K_i	1.5
K_d	1.5

This assistive strategy is also configurated with the mobile application. In order to allow an interconnection of this assistive strategy with the one presented in Chapter 4, the mobile application was updated. In this way, the session therapy can be sustained in participation, effort and also with a reference trajectory that can be real-time tailored to the users' needs. A new box was introduced in the fifth layout of Figure 5.2 with the name *User Trajectory*, that allows the subject or the physiotherapist to change the reference trajectory of the control law in order to fit the current necessities. The default trajectory is 60% of the healthy trajectory but clicking in this box, a progress bar will appear, and the user can change the default

trajectory according to his/her needs. The process is similar to that explained in the previous chapter. Figure 5.2 presents the modifications introduced in the mobile application.

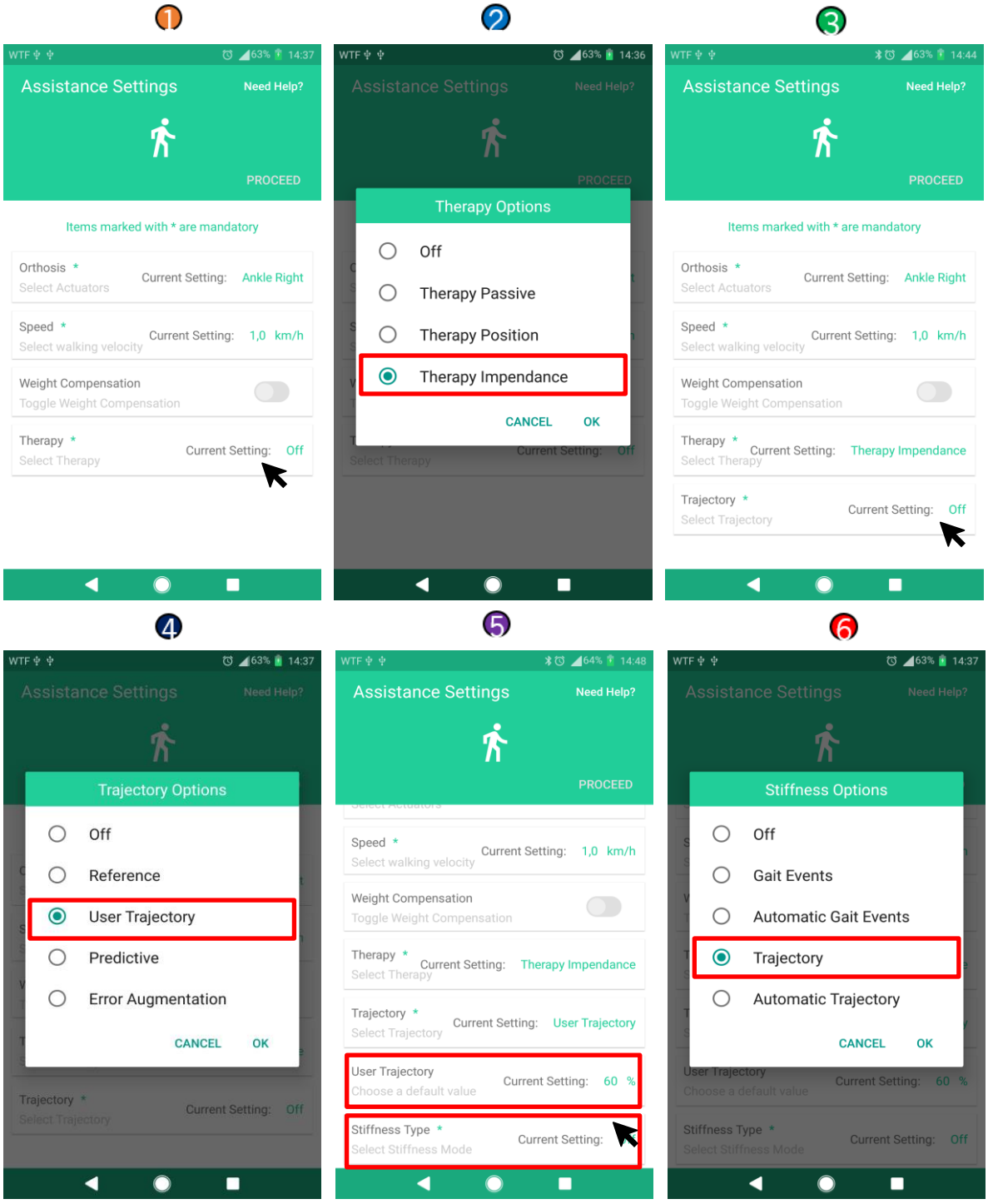

Figure 5.2: SmartOs mobile application modifications for the adaptive impedance control.

For selecting the impedance control-based strategy, the physiotherapist must choose the option **Therapy Impedance** (layout 2). Once this step is accomplished, the physiotherapist must choose the correct reference gait pattern that is most suited for his/her patient. A new option was introduced in this layout,

the **User Trajectory** (layout 4). If this option is chosen, a command will be sent to the orthosis to apply the assistive strategy that is sustained in effort, participation, and where the reference trajectory is adapted to each user. Afterwards, the same protocol of Chapter **4** is valid: the physiotherapist must choose a default value, with a minimum of 60% of healthy trajectory presented by Winter [65]. Finally, the physiotherapist must select how it will change the stiffness values. In this case, as the stiffness values will be changed considering the reference trajectory, the physiotherapist must click in **Trajectory**. Afterwards, it will appear a layout with progress bars, allowing the setting of the initial values of *quasi-*stiffness. These values can be modified according to five gait phases, as shown in Figure **5.3**, between heel strike (HS) and flat foot (FF), FF and heel off (HO), HO and toe off (TO), TO and mid-swing (MSw) and, finally, between MSw and HS. After this configuration is set, the physiotherapist can send the configurations to the SmartOs CCU.

Additionally, it is possible to adapt the virtual stiffness values and the reference trajectory in real-time, clicking in **Stiffness** and in **Reference** buttons, respectively. If an adaptation in the reference trajectory is required, the layout 2 or 3 of Figure **4.12** of Chapter **4**, will appear. If an adaptation in the stiffness is required, the progress bars in layout 1 of Figure **5.3** will appear.

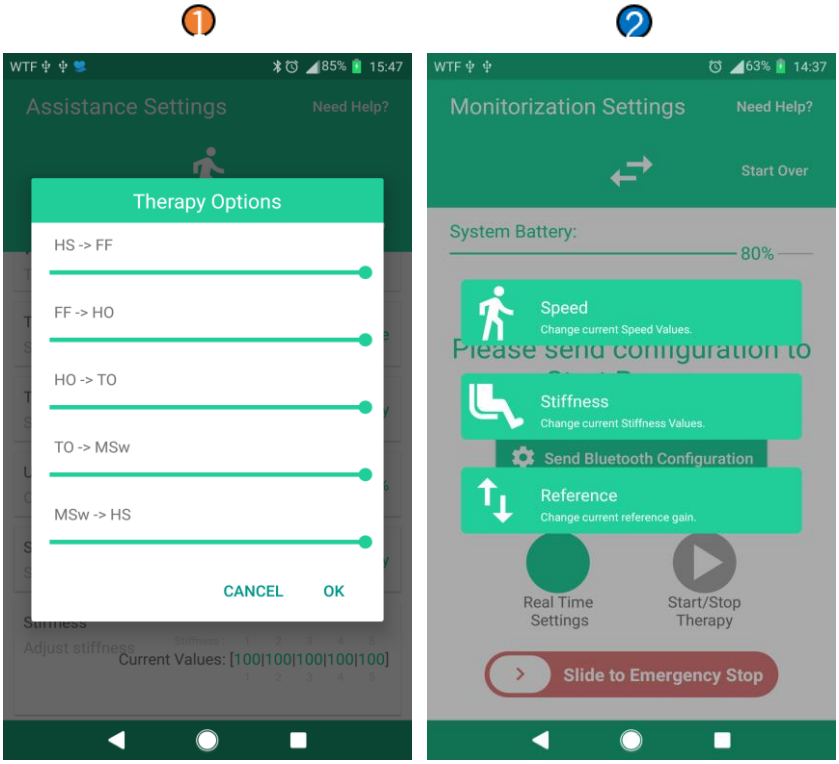

Figure 5.3: Layout with possible gait phases to adapt the virtual stiffness (left) and layout for real time modifications, both stiffness and reference (right).

The stiffness of a joint is considered the first derivate of torque in relation to the angle position [67]. The ankle joint pattern is characterized by four typical passages into the neutral angle, i.e., zero degrees, which leads to infinite values of stiffness during these passages. Dollar *et al.* [67] presented a simple approach for estimating the ankle joint stiffness for the different gait phases instead of following the definition of calculating the derivative sample to sample. The stiffness was estimated in [67] with a **linear regression model** that approximates the slope of the torque *vs* angle curve for different gait phases during the stance phase, calculating the ***quasi*-stiffness**. In this approach, the *quasi*-stiffness was evaluated just in the stance since the articulation torque is null during the swing. The author praised the simplicity over the complexity and found a linear model that presented a reasonable coefficient of determination.

A similar approach was followed in the present dissertation but considering the curve **human-orthosis interaction torque** *vs* **angle position**. The human-orthosis interaction torque was considered an indicator of the subject's effort, as in [40] and explained above, being, as well, an indicator of the subject's motion intention. To evaluate the interaction torque during the gait cycle, the orthosis was used in a passive mode, i.e., where the reference interaction torque, τ_{REF} in Figure **5.1**, is considered zero and there is no motion if the user does not interact with the assistive device. The *quasi*-stiffness was estimated by determining the best linear model that fits the curve human-orthosis interaction torque *vs* angle trajectory, following the least-square method.

According to the least-square method, the best approximation to a certain curve is the one that produces the **minimal deviations**, sample to sample, regarding a set of data. If we consider the diviations in relation to the ground truth (y_i) as an error e_i, the algorithm creates the curve in which the sum of square e_i is minimum [68], shown in Equation **(5.1)**.

$$\sum_{i=1}^{n} e_i^2 = \sum_{i=1}^{n} [(y_1 - f(x_i)]^2 \qquad \text{Equation (5.1)}$$

In Equation **(5.1)**, f: $\mathbb{R} \rightarrow \mathbb{R}$ is the fitting curve which, in this case, considering a linear model, is a function of two variables and with a degree n of 1, as shown in Equation **(5.2)**.

$$f(x) = mx + b \qquad \text{Equation (5.2)}$$

In order to find the best curve that minimizes the square error, the partial derivatives of Equation **(5.1)** in relation to m and b must be zero. If we consider E as Equation **(5.1)** and solving the partial derivatives,

we found the two equations needed to solve the system of linear equations, Equation **(5.3)** and **(5.4)**, to calculate the best values of *m* and *b*, considering the giving data set.

$$\frac{\partial E}{\partial m} = 2\sum_{i=1}^{n}(-x_i)\cdot[y_i-(mx_i+b)] \qquad \text{Equation (5.3)}$$

$$\frac{\partial E}{\partial b} = 2\sum_{i=1}^{n}[-y_i-(mx_i+b)] \qquad \text{Equation (5.4)}$$

Expanding Equation **(5.3)** and **(5.4)**, the best values of *m* and *b* can be found, solving the system of linear equations.

$$m = \frac{n\sum x_i y_i - \sum x_i \sum y_i}{n\sum x_i - (\sum x_i)^2} \qquad b = \frac{\sum y_i \sum x_i^2 - \sum x_i y_i}{n\sum x_i - (\sum x_i)^2}$$

The stiffness was considered to be **the slope of each linear curve** for each phase of the human-orthosis interaction torque *versus* angle curve. As such, the coefficient *m* was assumed to be the best linear approximation. It was calculated for six phases of the gait cycle: **(i)** from HS to FF, **(ii)** from FF to MSt, **(iii)** from MSt to HO, **(iv)** from HO to TO, **(v)** from TO to MSw and **(vi)** from MSw to a new HS. The gait phases were segmented offline through measure of the angular velocity, in rad/s, recorded with an IMU placed on the foot. The angular velocity was, then, an input of the finite state machine algorithm, presented in [69], to segment the trajectory into the respective phases.

The linear model was evaluated for each phase considering the coefficient of determination (R^2), calculated considering the ground truth value, i.e., the interaction torque, and the predicted values given by the linear model.

5.3 Quasi-stiffness estimation

5.3.1 Experimental protocol

To estimate the *quasi*-stiffness, an experimental study was performed with neurologically intact subjects walking with the orthotic system at *quasi*-passive mode. All subjects signed a consent form to be part of the study. Subjects' rights were preserved and, as such, personal information provided was remained confidential. Data was collected at the University of Minho.

A. Subjects

Three healthy subjects (body mass: 60.0 ± 13.1 kg, height: 163 ± 12.0 cm and age of 25.0 ± 2.00 years), without clinical history or evidence of motor disorders that could affect their ability to walk normally, accepted to participate, voluntarily, in an empirical study to evaluate the interaction human-orthosis and to estimate the *quasi*-stiffness during the gait cycle. All anthropometric data needed to perform the empirical study were measured.

B. Data Acquisition

Kinematic and kinetic data, namely the foot angular velocity (from wearable IMUs), the ankle angle (from an embedded potentiometer) and the interaction torque (from an embedded strain gauge), were acquired with an orthotic system for ankle assistance in the passive mode, at a sampling frequency of 100 Hz. Data were acquired for three gait speeds, 1.0 km/h, 1.3 km/h and 1.6 km/h. Figure **5.4** displays the experimental setup used to evaluate the human-orthosis interaction torque and estimate the *quasi*-stiffness for each phase.

C. Data Processing and Analysis

For each gait speed, the kinematic (angle and gyroscope) and kinetic data (human-orthosis interaction torque) were filtered using a zero-phase fourth-order low pass Butterworth filter with a cut-off frequency of 5 Hz [65]. Data was time divided into gait cycles considering the angular velocity recorded by an IMU placed on the foot [69]. The values of *quasi*-stiffness were normalized considering the user's body mass. Additionally, due to systems constraints, these values were normalized to a scale between 0 and 1, in which the maximum value of *quasi*-stiffness found for each trial was considered 1 Nm/°kg.

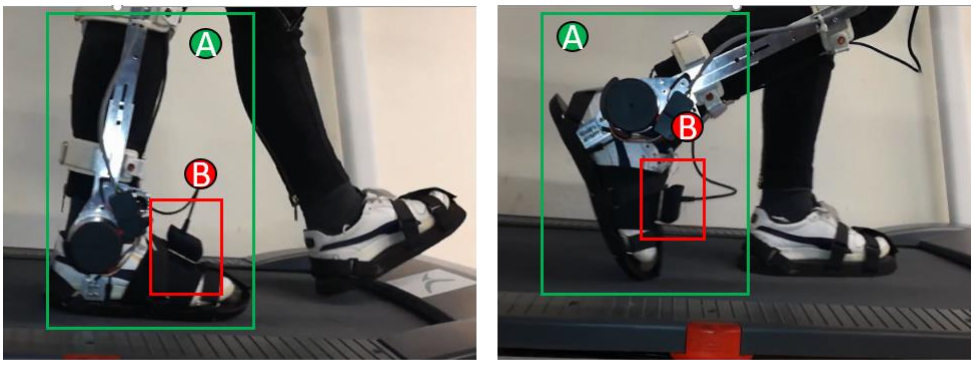

Figure 5.4: Experimental setup for quasi-stiffness estimation.

5.3.2 Results and Discussion

In order to evaluate where the subjects need more help to perform the correct gait pattern, the *quasi*-stiffness of the joint was estimated with a linear model for each gait phase, choosing the slope of the best fitting curve.

In a general way, considering the three gait speeds, the linear model presented reasonable results in predicting the human-orthosis interaction torque for a specific angle. If the analysis is made considering the two main gait phases, i.e., stance and swing, the mean coefficient of determination (R^2) is, respectively, near 50% and 70%. This result shows that, indeed, the linear model is more suitable to the swing phase, as the model can explain almost 70% of the ground truth data. It was found increased values of *quasi*-stiffness for HO → TO phase and, for most of the tested configurations, it is the phase where the value of *quasi*-stiffness was higher. Furthermore, the *quasi*-stiffness present higher values for *single support* phase in comparison with the *double support* phase. In the *single support* phase, that begins when the heel leaves the ground [64], i.e., in HO, the subject stands all his/her weight into just one leg, the one that is initializing the stride.

As it was reviewed in the *state-of-the-art*, the fact of using the orthotic device in a passive mode, it introduces an increased effort in the subject. As a *quasi*-passive device, the orthosis is almost purely mechanical, presenting inertia to the movement. Also, its mass, although not considerable, affects the gait pattern and, perhaps, augments the energy that the users is spending. Therefore, it is reasonable that in a *single support* phase, the subject requires more effort and applies more strength to overcome the inertia that the system offers. Therefore, the main goal of this assistive strategy is to encourage the subject to apply strength and effort, applying to their participation, at the same time the orthosis helps the patient in the most difficult gait phases, as reported to be the HO → TO phase.

Figure 5.5 display an example of the linear model prediction in comparison with the ground truth for one representative subject. In this figure, it is possible to observe the curve human-orthosis interaction torque, measured with the strain gauge, *vs* ankle angle (above) and the result given by the linear model (below) for 1.0, 1.3 and 1.6 km/h.

By analysing Figure 5.5, it can be seen that the linear approximation can be considered a reasonable approach since the curve maintains a similar shape. However, the coefficient of determination was not high enough in the stance phase to consider the linear model a very good approximation of the ground truth. Nevertheless, in this phase, the subjects support their weight in both legs so, in theory, it should be easier for them to overcome the friction that the system is promoting.

V_1 = 1.0 km/h

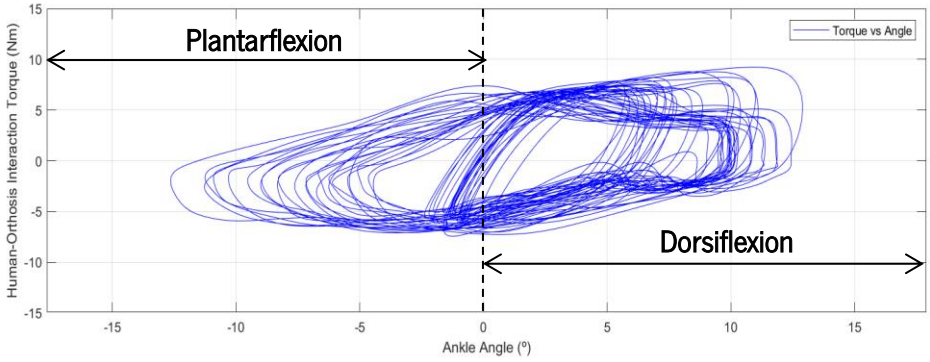

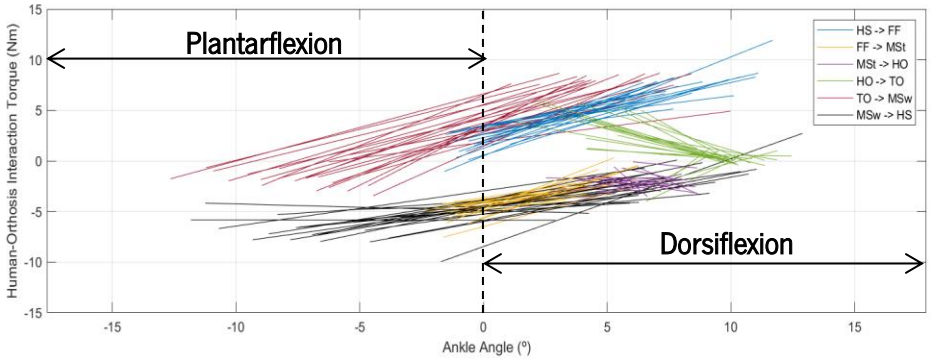

V_2 = 1.3 km/h

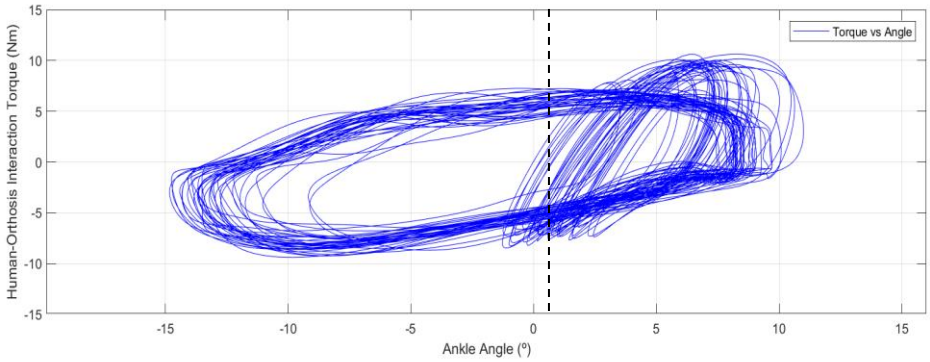

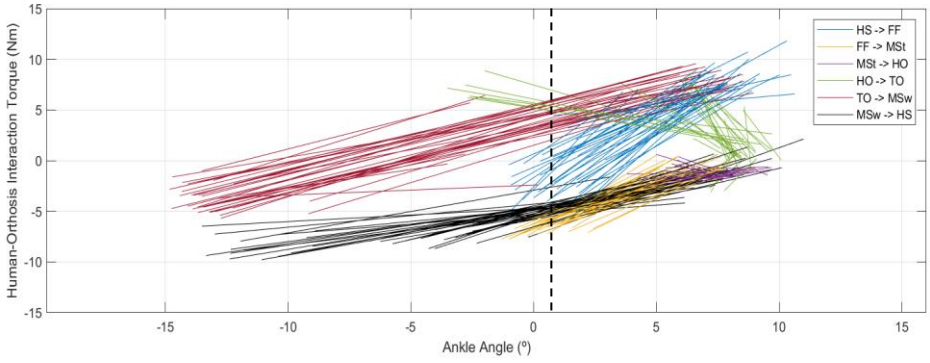

(continue)

(continuation)

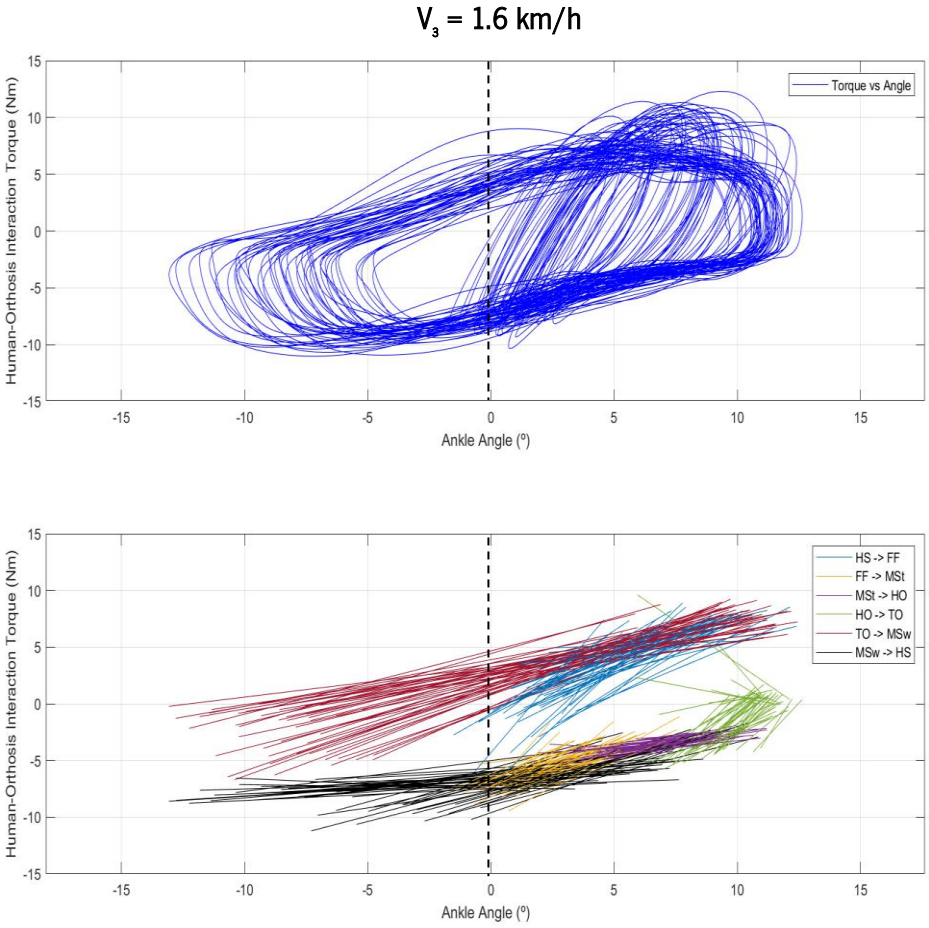

Figure 5.5: Linear approximation of the curve human-orthosis interaction torque vs angle (below) for 1.3 and 1.6 km/h against the real curve (above).

According to the proposed strategy, the values were normalized between 0 and 1 Nm/°kg. Table **5.2** display the results for each velocity, namely the normalized *quasi*-stiffness values considering the gait phases, the normalized *quasi*-stiffness divided into stance and swing phases, the normalized *quasi*-stiffness divided into *single* and *double support* phases and the respective coefficient of determination for stance and swing phases.

Analysing Table **5.2**, it is observable that, for all velocities, the *quasi*-stiffness values were bigger for the phases in which the subject was in *single support*. This result is more evident in the slowest velocity, 1.0 km/h, in which the maximum value was found in the **MSw → HS**. Nevertheless, the subphase **HO → TO** present a high value as well, which indicates that these gait phases are the most critical for subjects. Therefore, the orthosis should be stiffer, assuming mostly the control and helping the user to perform the correct trajectory.

Table 5.2: Quasi-stiffness values normalized by gait phase, stance and swing, single and double support, and the coefficient of determination for stance and swing (continue)

Velocity	*Gait Phase*	*Normalized quasi-stiffness [Nm/°kg]*	*Normalized mean quasi-stiffness per stance and swing [Nm/°kg]*	*Normalized mean quasi-stiffness per double and single support [Nm/°kg]*	Coefficient of Determination per stance and swing
1.0 km/h	HS → FF	0.644 ± 0.383	0.514 ± 0.284	0.398 ± 0.0904	0.439 ± 0.111
	FF → MSt	0.479 ± 0.286			
	MSt → HO	0.136 ± 0.0523			
	HO → TO	0.798 ± 0.172			
	TO → MSw	0.743 ± 0.198	**0.782 ± 0.0545**	**0.676 ± 0.123**	**0.733 ± 0.105**
	MSw → HS	**0.821 ± 0.254**			
1.3 km/h	HS → FF	0.251 ± 0.141	0.363 ± 0.329	0.410 ± 0.180	0.427 ± 0.151
	FF → MSt	0.295 ± 0.130			
	MSt → HO	0.0707 ± 0.0355			
	HO → TO	**0.836 ± 0.232**			
	TO → MSw	0.584 ± 0.328	**0.557 ± 0.0375**	**0.644 ± 0.229**	**0.728 ± 0.250**
	MSw → HS	0.531 ± 0.275			

Note: Abbreviations' meaning can be found here.

(continuation)

Velocity	*Gait Phase*	*Normalized quasi-stiffness [Nm/°kg]*	*Normalized mean quasi-stiffness per stance and swing [Nm/°kg]*	*Normalized mean quasi-stiffness per double and single support [Nm/°kg]*	*Coefficient of Determination per stance and swing*
1.6 km/h	HS → FF	0.519 ± 0.352	**0.566 ± 0.281**	0.469 ± 0.288	0.467 ± 0.235
	FF → MSt	**0.842 ± 0.126**			
	MSt → HO	0.194 ± 0.0525			
	HO → TO	**0.708 ± 0.412**			
	TO → MSw	0.489 ± 0.0552	0.469 ± 0.0277	**0.604 ± 0.184**	**0.675 ± 0.194**
	MSw → HS	0.450 ± 0.128			

Note: Abbreviations' meaning can be found here.

This result is in accordance with the users' perception since they reported more difficulty in performing the TO event with the orthosis in passive mode. For 1.6 km/h, the higher value of quasi-stiffness was found while the user is in *double support*. This result was not expected since, in this phase, the users have their foot flat on the floor and the weight is well distributed in both legs. Therefore, it should be easier for them to overcome the inertia and friction that the system causes. As a consequent of this result, the *quasi*-stiffness during the stance phase was higher, when compared to the swing phase. Nevertheless, a high value in the **HO → TO** subphase was also found, which underlines the necessity of a stiffer movement in this sub-phase.

Regarding the remaining phases of swing, it was found that the quasi-stiffness decreases as higher the velocity is. This result can be related with the fact that with a higher velocity, the segments acceleration is also higher, helping the subject to overcome the mechanical friction the orthosis is offering. During swing, the biological torque of the ankle joint is practically zero. The swing movement is, therefore, a result of the knee joint movement that propels the limb forward [64]. In this sense, as a result of this higher acceleration and the fact of 1.3 and 1.6 km/h being a more comfortable speed, the *quasi*-stiffness was lower.

5.4 Adaptive Impedance Control Strategy Validation

To validate the impedance control strategy for the ankle orthosis, a set of experimental sessions were carried out with healthy subjects that had a prior habituation of walking with the orthotic device into the passive and positions assistive modes. In fact, the three modes of control have a variable in common:

the interaction torque. In the position mode, the orthotic device imposes a trajectory into the subject. This way, the interaction torque that the subject is performing can be used to evaluate if the user is following or contradicting the system. In the passive mode, the interaction torque is measured as a metric to evaluate the subject's effort as the orthosis is not giving any assistance. Therefore, the subject assumes the total control of the system. Finally, in the impedance control, the interaction torque is used as the variable of control, allowing an assistance based on the user's effort and participation. In this strategy, the orthosis increases the assistance as the user interacts. As such, it is important that the subject have knowledge in the first two control approaches in order to have a perception how this new strategy is requiring interaction with the system.

5.4.1 Validation Protocol

A. Subjects

Seven non-neurological subjects (body mass: 70.4 ± 11.9 kg, height: 170 ± 10.1 cm and age of 24.4 ± 1.40 years) with a prior habituation of walking with the orthotic device in the passive and position modes, accepted to participate voluntarily into the experiments with the purpose of validating the adaptive impedance control in the ankle orthosis. All anthropometric data required to proceed with the control validation were measured and collected prior to the beginning of the session. All subjects signed a consent form to be part of the study. Subjects' rights were preserved and, as such, personal information provided was remained confidential. Data was collected at the University of Minho.

B. Data Acquisition

Kinematic and kinetic data from the orthosis' embedded potentiometer and strain gauge were acquired at a sampling frequency of 100 Hz. The setup used was similar to the one described in Figure **4.3** (Chapter **4**), excepting the use of the Xsens system that, for this validation, was not considered required.

For the experiments, the subjects were instructed to walk in a continuous trial for 4 minutes. The trial was divided into two segments of 1-minute and one segment of 2-minutes. In the first minute of trial, the subjects walked with the virtual stiffness set at the maximum value of 1 Nm/°kg. In the following two minutes, the virtual stiffness was changed to the values found with the linear model. Finally, in the last minute, the subjects were instructed to stand the foot and to minimize their interaction with the system. The reference trajectory was set to 100% of the healthy one.

C. Data Processing and Analysis

Data were filtered with a zero-lag fourth order Butterworth filter with a cut off frequency of 5 Hz. As this strategy is dependent on the subjects' effort, the strides were segmented in time, considering the heel strike event, subject to subject and trial by trial.

5.4.2 Results and Discussion

In a general way, the impedance control law provided a reasonable walking assistance. The subjects reported that, with the impedance control law, the orthosis movement was **smoother** and **fluid**, even if the virtual stiffness values were modified. They felt that **their participation was crucial** for the movement since they noticed that when their participation was practically null, the orthosis did not foster a proper assistance. Also, in this control, the PID's delay was minimal in comparison with the trajectory tracking control. In fact, the delay decreased from a mean of 250 ms, presented in the previous chapter, to a minimum of 19.0 ms (± 4.40 ms) for 1.0 km/h and 23.0 ms (± 2.60 ms) for 1.6 km/h. This value presents some fluctuations, between subjects and speed, that is entirely due to the different interaction that each user produces.

Figure **5.6** displays a part of the continuous trials for each velocity, allowing the visualization of the virtual stiffness modification all over the gait cycle, according to the information listed in Table **5.2**.

In fact, the *quasi*-stiffness was studied for six different sub-phases of the gait cycle, as the algorithm presented in [69] allows. Nevertheless, it was decided to use five values of *quasi*-stiffness that are coincident with the extreme points of the curve's sub-phases presented in Chapter **4**, represented by **1** – from HS to FF, **2** – from FF to HO, **3** – from HO to TO, **4** – from TO to MSw and **5** – from MSw to HS.

As the *quasi*-stiffness values were modified in real time, the subjects were able to identify the changes in the orthosis behaviour. Some of the subjects felt the system was stiffer after the modifications in the *quasi*-stiffness values, in a way that they felt they had to perform more strength to maintain the same walking pattern. Other participants reported that they felt the system more compliant in a way that they easily performed the ankle motion. In fact, decreasing the values of *quasi*-stiffness can produce two effects in the orthotic system that, at a first view, can be seen as oppositions: **(1)** the system is more passive so it gives less assistance and, consequently, it easily allows the user command to perform his/her preferred walking pattern, increasing the user's freedom of motion; **(2)** the system is more passive so it gives less assistance and, consequently, can be considered stiffer in a way that, as the motors do not give assistance, the orthosis is almost purely mechanical. If so, the user can feel the orthosis offering

more inertia to the movement. Indeed, both options were reported by the users when they walked with the orthotic device. Nevertheless, with the values of *quasi*-stiffness closer to 1 Nm/°kg or adjusted according to the linear model, **they felt more comfortable** with this assistive strategy in comparison with the trajectory tracking control since they were able to command the orthosis and not the opposite. This is valid since the subjects were healthy individuals. For future analysis, the effect of this assistive strategy in the patient's rehabilitation should be studied.

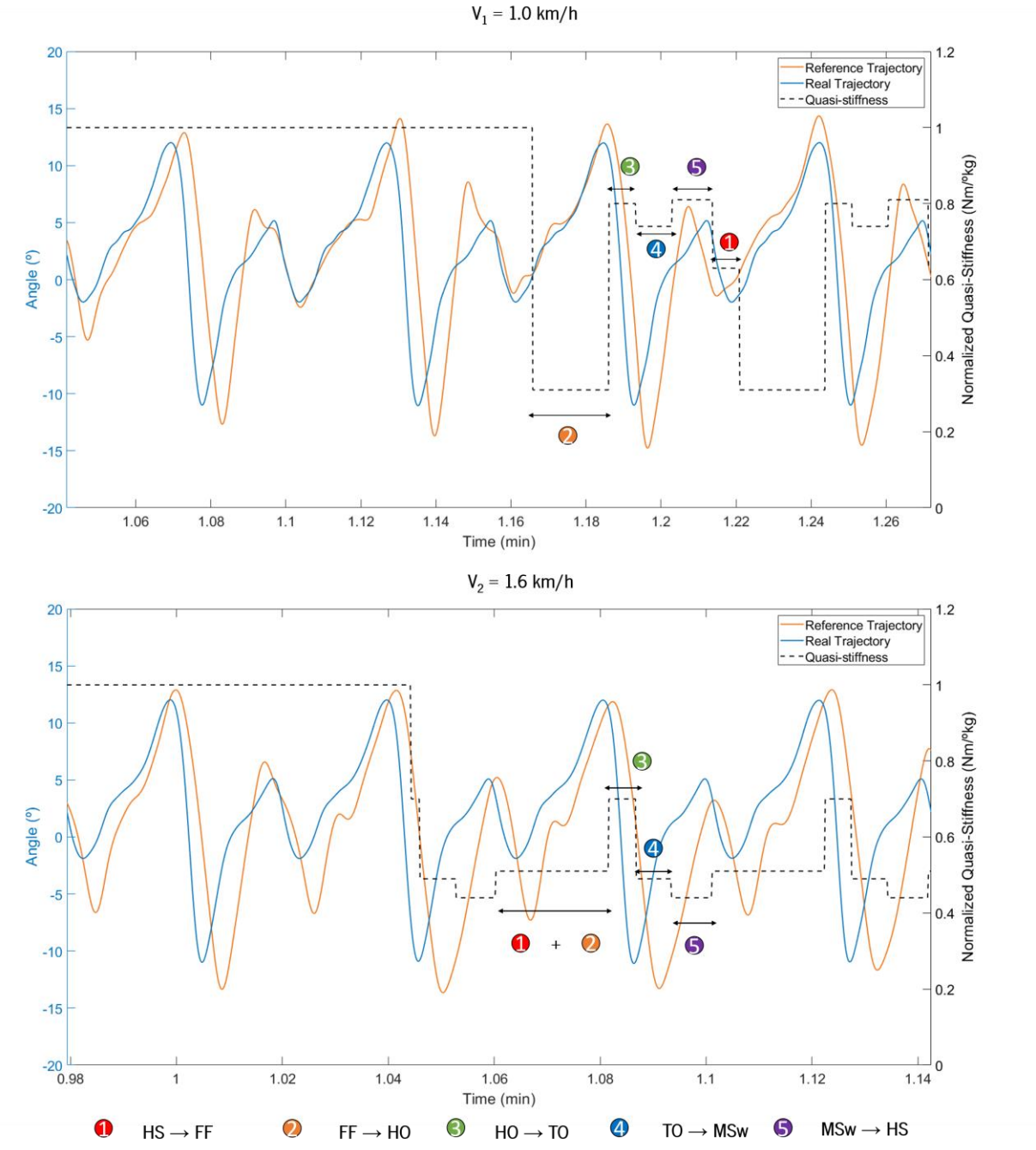

Figure 5.6: Quasi-stiffness variation all over the gait cycle for 1.0 km/h (above) and 1.6 km/h (below).

For visualization and analysis purposes, Figure **5.7** displays the mean trial for one representative subject walking with the orthotic system at both 1.0 and 1.6 km/h.

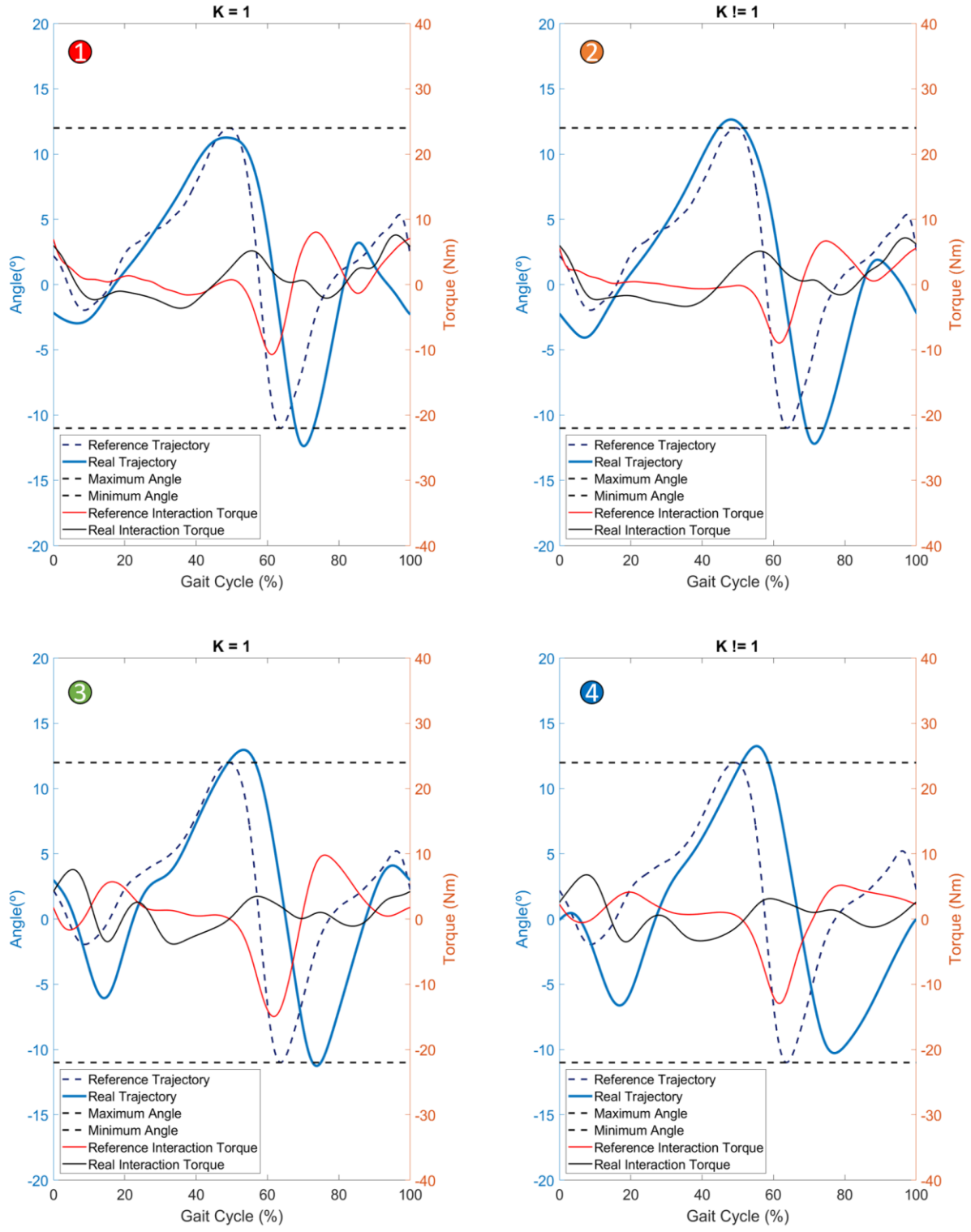

Figure 5.7: Real trajectory with the orthotic system close to a position control and after modifications in the values of quasi-stiffness for 1.0 km/h (above) and 1.6 km/h (below).

The trajectory performed by the healthy subject is closer to the reference one, especially during the main sub-phases of dorsiflexion and plantarflexion. With exception for the layout 4 of Figure **5.7**, the user was able to overcome the reference angle during the TO event (≈ 60% of the gait cycle). As the user is not totally synchronized with the orthotic device, and more evident in 1.6 km/h, the error between the reference and real angle was not totally zero. As such, the orthosis assists more during those phases. It was verified the existence of a minimum delay when compared with the trajectory tracking control. It was verified a delay below 23 ms, that represents a decreasing of 90.8% in comparison to the trajectory tracking control presented in the previous chapter. This reasonable result is entirely due to the subjects' interaction with the system. Nevertheless, the users reported the necessity of existing a biofeedback system to help them to be even more synchronized with the system.

An interesting point is that although the TO was found to be the critical event while walking with the orthotic device, for most of the subjects, this event was accomplished with success, maintaining the reference angle or, in some cases, overcoming the reference angle. This observation indicates that, indeed, the **user performed a higher interaction** with the system.

5.5 General conclusions

This chapter presented an assistive strategy for the SmartOs based on the subjects' effort and active participation. The assistive strategy was adapted to the ankle orthosis, and the mobile application was changed to promote an interconnection of this assistive strategy and the previous one exploited in Chapter **4**. Also, it was presented an empirical study of *quasi*-stiffness variation over the gait cycle for three gait speeds using a linear model for the *quasi*-stiffness estimation. It was found that the users perform more interaction in the TO event, that was found to be the critical event. From the experimental validation, it was found that this assistive strategy is effective, allowing the users to perform a correct gait pattern at the same time they interact with the system.

Both this strategy and the one previously validated in Chapter **4**, allow the SmartOs to provide user-oriented assistance and have the potential for future use in the Human-in-the-loop strategy. The next step is to evaluate the energetical impact of using the SmartOs in its end-users.

6. TOWARDS HUMAN-IN-THE-LOOP CONTROL

6.1 Introduction

As introduced in Chapter 3, the SmartOs system was developed aiming an effective assistance for persons with motor impairments, having always in thought the end-user's needs. Assistive strategies, involving trajectory tracking control, joint impedance modulation, EMG-based control, among others, have been proposed to control powered devices. However, none of them have introduced the energy as a metric to adapt the assistance.

Recently, researchers are directing their investigations to a new field of control, the Human-in-the-loop control, where a physiological signal, as the energy expenditure, is being used to adjust the assistance for each user, promoting an assistance that is efficient in energy consumption. However, this new control strategy requires the energy expenditure estimation, which has been based on **non-wearable and non-ergonomic** devices as gas analysers that, for clinical use, are not suitable. Therefore, new ways of estimating the energy that the user is spending are being studied, applying machine learning-based regression models to solve this issue.

In this chapter, the application of the human-in-the-loop control approach is studied. For this purpose, an empirical study with the trajectory tracking control was carried out for three gait speeds (slow, median and fast), with two main purposes: **(i)** verify if exists significant differences in the subjects' energetic effort for the three velocities and **(ii)** if (i) is true, then evaluate if the use of a powered device augments the energy consumption compared to walk without the system. Additionally, machine learning-based regression models were implemented to estimate the energy consumption using wearable sensors, as EMG and IMUs.

6.2 Theoretical concepts

As reported in Chapter 2, some literature works assessed the energy expenditure of subjects while walking with the powered device. In most of these studies, the energy consumption was compared between the powered assistance *vs* the powered-off assistance. This comparison is valid, and it shows that, indeed, the use of these powered assistive devices reduced the energy expenditure. However, the study of how these systems increase or decrease the subjects' effort when compared to the normal walking is not often an outcome of studies. As an example, from the twelve studies presented in the *state-of-the-art*, just in [28], [48], [50], [51], the energy expenditure of the end-user was evaluated and compared with the

normal gait, i.e., walking without the device. Indeed, most of the experiments were performed with healthy subjects and it is known that healthy subjects adapt their walking pattern to minimize the energy consumption [72], [73]. Therefore, it is important to continuously assess energy expenditure, allowing the adjustment of the device's assistance to promote a reduction in the metabolic cost.

6.2.1 Indirect Calorimetry

Generally, these studies are performed with a standard device for quantifying the exchanges of oxygen and carbon dioxide with a technique called **indirect calorimetry** [70]. Indirect calorimetry is considered the standard technique for energy expenditure calculation. According to [70], it reflects the metabolism of tissues, allowing the evaluation of the respiratory exchange ratio. The first modelling of the energy expenditure was stated by Lusk, in 1924. All over the century, many authors have proposed changes to the first equation, being Brockway's [71] the most accepted and used in the literature in the current decade. As shown in Equation **(6.1)**, the energy expenditure, in J/s, is evaluated concerning the flow of oxygen and carbon dioxide production, but also concerning the nitrogen that result of the combustion of carbohydrates, lipids and proteins [70].

$$-\Delta \mathrm{H} = x_1 \dot{V}O_2 + x_2 \dot{V}CO_2 + x_3 N \qquad \text{Equation (6.1)}$$

According to [72], the nitrogen parcel can be discarded since it just represent 4% of the total real energy expenditure and its exclusion produces an error equivalent to 1% of the total amount of energy. Therefore, Equation **(6.1)** can be rewritten as follows, according to Brockway's [71] coefficients.

$$EE\ [W] \approx 16.58\ \dot{V}O_2 + 4.51\ \dot{V}CO_2 \qquad \text{Equation (6.2)}$$

The calculated energy can be divided into three main components, important to sustain vital activities and daily live activities. The energy used to sustain the vital functioning is called **basal energy expenditure** (BEE). This component represents more than 60% of the total amount of energy, as presented in [72]. Another component, that represents almost 30% of the total energy, is responsible for the energy used in physical activities, usually termed AEE (**activity energy expenditure**). The remaining 10% is called diet-induced thermogenesis, being the energy used during the postprandial metabolism [72].

When evaluating the energy expenditure of a specific physical activity, it is good practice subtracting the BEE to the total amount of energy, as most of the studies in the literature perform. In this way, it is possible to evaluate the amount of energy that is being spent for that specific activity without considering

the energy required for vital functioning. For this, the steady state, in which the exchange of oxygen and carbon dioxide vary less than 10% in a consecutive 3-minutes [73].

Although indirect calorimetry is a standard technique and reflects well the energy expenditure of users, its use in clinical context is not the most ergonomic. Different approaches for estimating the energy expenditure relying on machine learning algorithms have been validated against indirect calorimetry. Regression models, perceptron neural networks or convolutional neural networks (CNN), have been used to estimate the energy expenditure. In this dissertation, two different machine learning algorithms, one feedforward neural network, and a long short-term memory (LSTM) neural network, were exploited to estimate the steady-state energy expenditure of users walking with the orthotic device.

6.2.2 Machine Learning-based models

Neural networks have been created with the purpose of modelling complex problems, as the humans' brain do, allowing a statistical generalization. The neural networks were mostly developed for supervised machine learning, approximating a function *f(x)* to a set of input features, *x*, in order to obtain *y*, the target value or class [74].

A feedforward neural network is a type of artificial neural network. It can be a single perceptron, having just an input layer and an output layer, or a multilayer perceptron, as presented in Figure **6.1**, having one or more hidden layers. These architectures are considered feedforward since the information is passed unidirectionally through the input layer to the output layer, without having feedback of information.

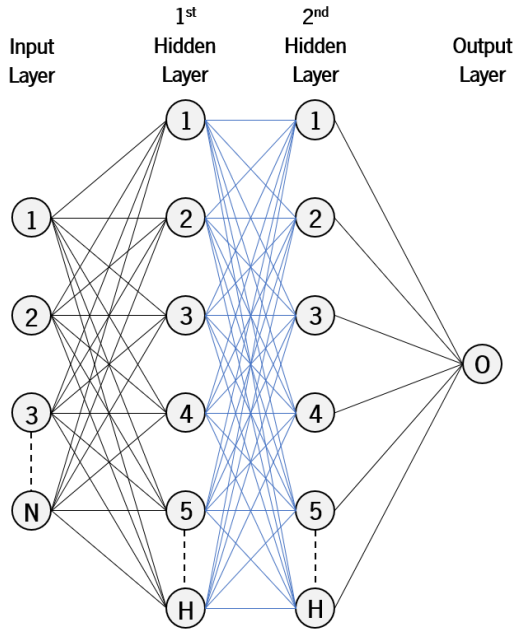

Figure 6.1: Feedforward neural network representation for regression with two hidden layers of H neurons.

It can be used for either classification or regression problems, differing in the output layer. Usually, if the neural network is used for regression, the output layer presents just one node, as presented in Figure **6.1**. If it is used for classification problems, the output layer presents as much nodes as the number of categories [75]. Each layer of the network is composed by neurons, or nodes, which are computational units that have one or more input connections, a transfer function and an output connection. For example, in Figure **6.1**, the numbered circles of the first hidden layer are considered nodes. A node can be seen as a neuron of the human brain, but with mathematical representation. Each input of the node is multiplied by a weight **w**, as presented in Figure **6.2**, and then it is evaluated the composite sum. Before entering into the node, it is added the bias **b**, allowing the better adjustment of the input features to the output [74]. The goal of neural networks is to optimize these weights **w**, allowing a proper fitting of the input data into the target, until the loss of the network, usually the mean squared error (MSE) function for regression problems [74], is the minimum possible.

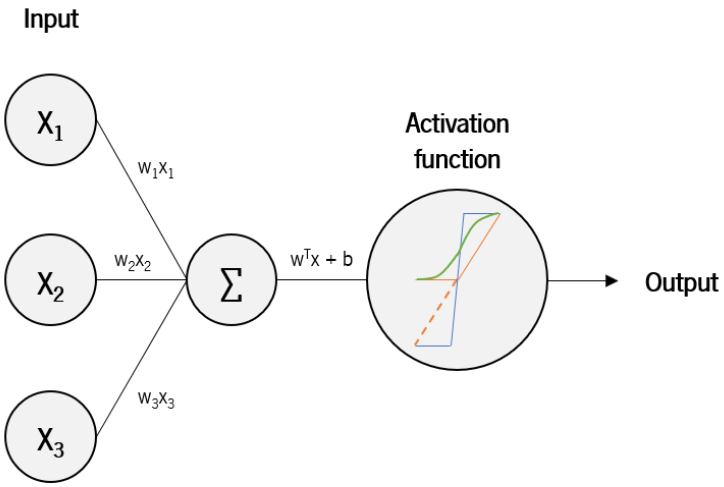

Figure 6.2: Computational unit or neuron of a network architecture.

The activation function is an important feature of the neural networks. Without the activation functions, neural networks would be similar to linear regression models. In Figure **6.2**, it is represented the most used activations functions in neural networks: the sigmoid functions, in red, that rescales the output between 0 and 1; the rectified linear unit (ReLu), represented in orange, that computes the maximum between the weighted sum and 0; the linear activation function, also represented in orange with a dashed line, that does not perform any rescale of the input; and the hyperbolic tangent, represented in blue, that squashes the output between -1 and 1 [74]. This behaviour of nodes is repeated all over the layers that compose the neural network, allowing the network to learn complex problems.

The LSTM network, or long short-term memory, is a type of recurrent network. A recurrent network (RNN) differs from a feedforward neural network since the flow of information is not unidirectional, and it exists feedback of information. The prediction relies on the current inputs and also in information about previous inputs, known as hidden states, endowing the network with memory [76]. In each node, the current input is concatenated with the output of the previous hidden state, helping the network to predict the present output [77]. Figure **6.3** displays a graphical resume of the recurrent neural network's behaviour.

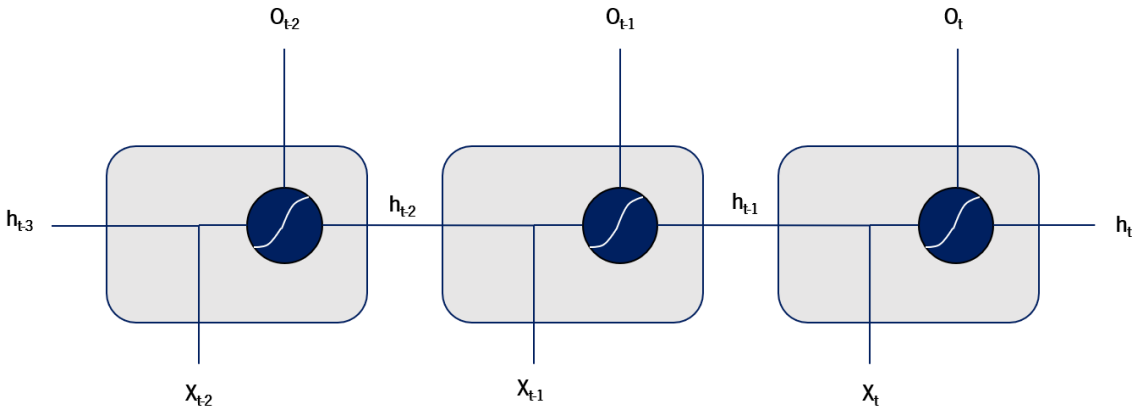

Figure 6.3: Recurrent neural network behaviour: X is the input, O is the output and h is the hidden state (network's memory).

The problem in simple recurrent networks is that they are not suited for long-term dependencies. When the gap between an important information to predict the output and the current input is too big, the RNN are not suitable [77]. LSTMs were developed in an attempt to solve this problem. Each cell of this neural network consists of three gates, a forget gate, an input gate and an output gate. Also, it is composed off a cell state that allows the information to flow within the LSTM cell and between LSTM cells. Figure **6.4** displays a diagram of a LSTM cell.

The first gate is the forget gate. With this gate, the neural network is able to decide which information is important or not to be passed all over the cell. The input data, X_t, is concatenated with the previous hidden state and passed into a sigmoid activation function. As this transfer function, represented in Figure **6.4** as red, squashes the output between 0 and 1, the non-relevant information, with an output close to 0, is forgotten. By the other side, the relevant information, with an output close to 1, get through the cell. The second gate is the input gate. The resultant of the current input and the previous hidden state, then enters into the input gate, where it passes, again, in a sigmoid transfer function, that determines what values of the cell state should be updated, and it passes through a hyperbolic tangent function, represented in blue in Figure **6.4**, that calculates the values pointed as candidates to be updated in the cell state. The last gate, the output gate, is responsible for calculating the next hidden state to be propagated all over the time steps. Once more, the current input and the previous hidden state are concatenated and passed

into a sigmoid transfer function that, together with the updated cell state, origins the LSTM cell's output [77]. With these features, the LSTM neural networks are often used in the prediction of sequential data, as speech recognition, and time-series data [74].

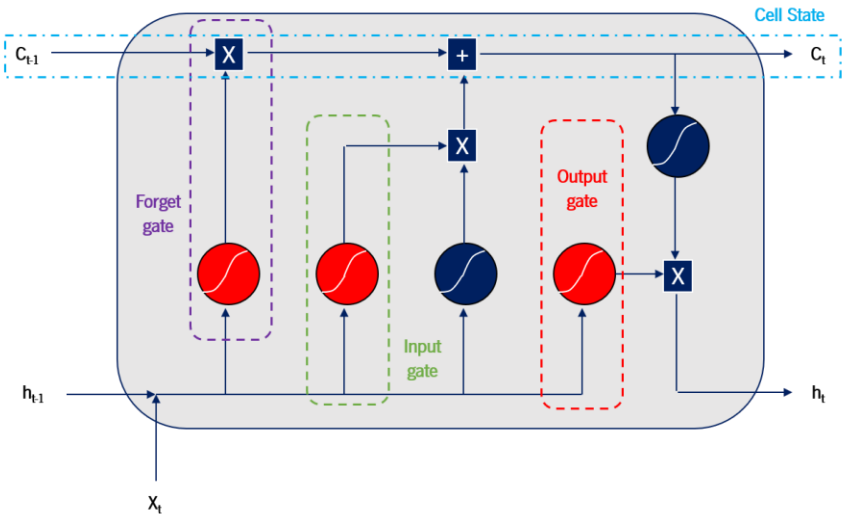

Figure 6.4: LSTM cell configuration.

Both MLP and LSTM neural networks, and neural networks in general, present some parameters that, when adjusted properly, allows an effective training of the model. The main parameters of a neural network are the number of units that is used, the number of epochs, the learning rate and the batch size [75].

The number of units, presented earlier, affects the complexity of the model and its capacity of generalization. Generally, if the number of units is set to a very high number, the model tends to overfit, i.e., it learns very well the training set and predicts poorly the test set [75].

The number of epochs also affects the capability of the model. An epoch is considered a total pass into the training dataset. If this parameter is big, this represents that the neural network is being allowed to see and learn the training set many times, leading to overfitting. By the other side, if this parameter is very low, the model will not learn enough, leading to underfitting [75].

Regarding the learning rate, this parameter influences the gradient magnitude in the training process. If this value is very high, the model will not converge to the optimal minimum. If this value is too low, the model will take too long to converge, or it could be stuck in a local minimum [75].

Regarding the batch size, dividing the training data into groups of equal size will allow the network to learn more information, augmenting its capacity, and it will reduce the computational burden. However, this value should be carefully tuned since very low batch size could lead to a poor generalization [75].

In general, neural networks are a very powerful tool for data modelling, but its parameters should be carefully chosen in order to allow a model generalization that either predicts well the training data and the test data.

6.3 Experimental Protocol

An experimental study was performed with healthy subjects walking with the ankle orthotic system with the trajectory tracking control strategy, for two main purposes: first, to evaluate the energy consumption that the SmartOs' use can introduce in the normal walking; and second, to explore machine learning-based regressor models to estimate the energy expenditure for a set of wearable sensors.

A. Subjects

Eight healthy subjects (four females and four males, body mass: 68.3 ± 10.1 kg, height: 171 ± 7.65 cm and age of 24.3 ± 1.75 years), without clinical history or evidence of motor disorder that could affect their ability to walk normally, accepted to participate, voluntarily, in the empirical study. All subjects signed a consent form to be part of the study. Subjects' rights were preserved and, as such, personal information provided was remained confidential. Data was collected at the LABIOMEP – Porto Biomechanics Laboratory.

B. Data Acquisition

In order to evaluate the energy expenditure, the COSMED K4b^2 (Rome, Italy) was used to calculate the flow of oxygen and carbon dioxide during the experiments. It was ensured that the mask was well fitted to the subject to prevent miscalculations of the gas exchanges. This sensor was synchronized with a Polar H10 (Polar Electro Oy, Kempele, Finland), that was used to monitor the heart rate. Data were collected breath-by-breath.

For machine learning purposes, the subject was instrumented with the Xsens system (Xsens Techonologies B.V., Enschede, The Netherlands) to measure the segments acceleration and angular velocity of the feet, shanks, thighs, and waist. Also, an IMU was placed on the chest, specifically in the sternum, allowing the acceleration and angular velocity evaluation of the torso. The IMUs were placed in each segment in the *medialis* side, as illustrated in Figure 6.5. Data was collected at 100 Hz.

Moreover, muscular activity was measured at 1000 Hz using four EMG surface electrodes (Delsys Trigno Avanti, Massachussets, USA), placed on the *tibialis anterior* (TA), *gastrocnemius lateralis* (GL), *bicep femoris* (BF) and *vastus lateralis* (VL) muscles.

Figure 6.5 illustrates the sensors on body placement.

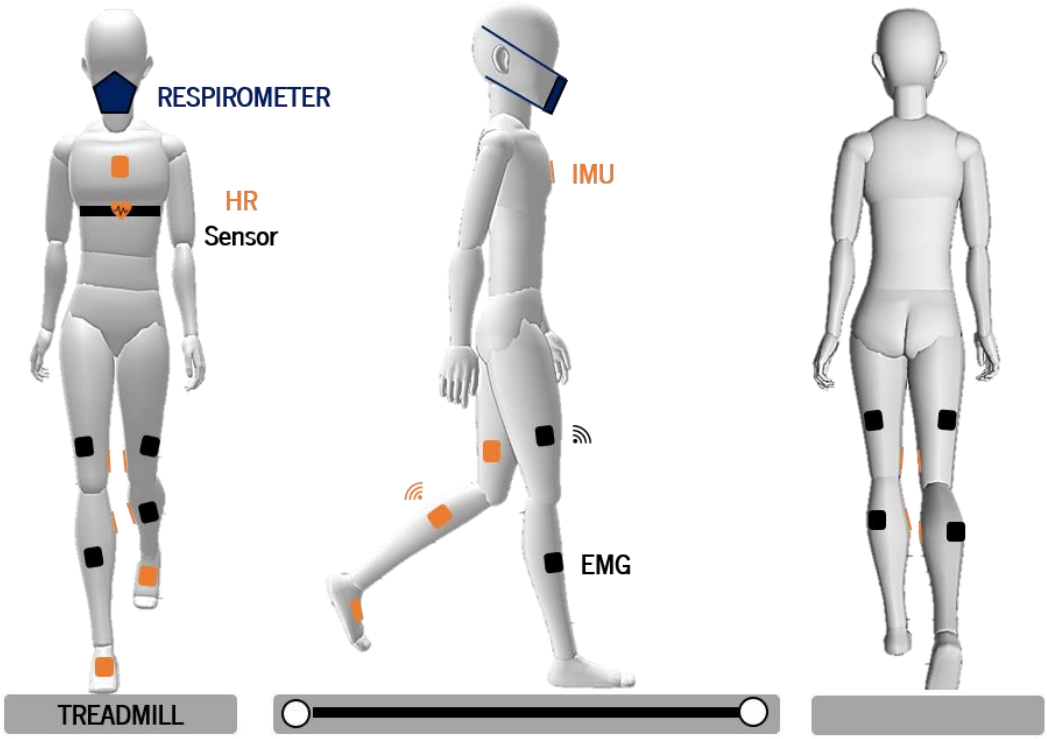

Figure 6.5: Sensors placement for the experiments.

The subjects performed six trials for three gait speeds (0.8 km/h, 1.2 km/h and 1.6 km/h). Each trial consisted of 12 minutes: 3 minutes of standing, to measure the basal energy expenditure; 6 minutes of walking on an AMTI (Advanced Mechanical Technology, Inc., Watertown, Massachusetts, USA); and 3 minutes in standing position for recovering. Between each trial, the subjects rested for a period of 10-minutes. This procedure was repeated twice, one time without the orthotic device and another time with the orthotic system in assistive mode, as shown in Figure 6.6.

C. Data Processing and Analysis

Kinetic data (segments' acceleration and angular velocity), measured with the Xsens system, were filtered with a first order, zero-lag Butterworth filter with a cut-off frequency of 0.1 Hz to preserve only the low frequencies responsible for the movement transitions.

The muscular activity, measured with the Delsys system, was filtered with a band-pass filter of first order between 20 Hz and 500 Hz to preserve the fundamental frequencies. A low-pass Butterworth filter of 0.05 Hz was applied to the EMG signals to calculate the surrounding signal and a normalization for each muscle was performed considering the maximum voluntary contraction (MVC), making MVC as 1V.

The respiratory data, measured with the COSMED K4b^2, was used to calculate the energy expenditure following Equation **(6.2)**. A 95% confidence interval was calculated to eliminate possible outliers. This way, each sample that overcome the confidence interval, was set to the maximum/minimum extremes. The basal energy expenditure was calculated as the mean value of the first 3 minutes of standing. The same was applied for the walking condition and for the recover condition. In the walking condition, the steady state was assumed to be reached at the last 3 minutes of data. Therefore, calculating the mean value of the steady-state for each condition, a step-like signal of energy expenditure was created.

Figure 6.6: Setup for the experimental study to evaluate the energy consumption with and without an orthotic device and for machine learning purposes.

6.4 Energy Expenditure on SmartOs

A comparative study was performed between the energy expenditure monitored during assisted and non-assisted walking at different gait speeds, to evaluate the energy expenditure of subjects while walking with the orthotic device. The mean energy expenditure was evaluated considering all subjects and compared, using for that the t-*student* test, assuming the level of significance of 5% (α = 5%).

In a general way, the orthotic system promoted an **augmentation of energy expenditure**. Although the five studies of literature reported that their devices allowed a decrease in the energy expenditure, this result was expected since the device is imposing a trajectory to healthy subjects that, perhaps, is not the most suitable for each one. The orthotic device can be seen as a perturbation into the subjects' normal walking.

Therefore, **this statement proves the need to introduce the Human-in-the-loop strategy**. The mean energy expenditure considering all subjects can be observed in Figure **6.7**.

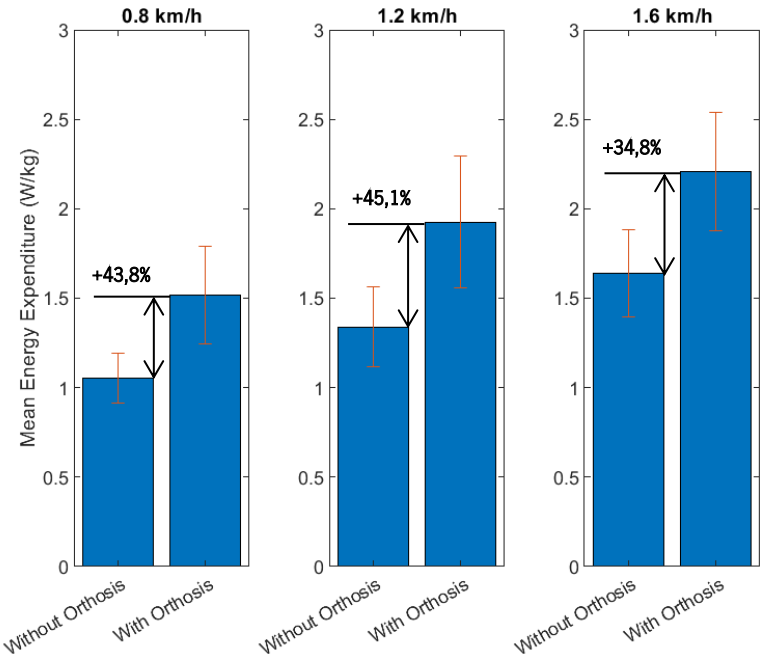

Figure 6.7: Comparison of the mean energy expenditure [W/kg] between walking with and without the orthotic system, considering the subjects' universe.

Figure **6.7** shows that the energy expenditure of users increases as the speed increases. For 0.8 km/h, the users revealed a mean energy expenditure of 1.05 W/kg walking normally, taking the effect of basal energy expenditure, **that increased 43.8% with the orthotic system** ($EE \approx$ 1.51 W/kg). For 1.2 km/h, an **increment of 45.1%** was verified when the subjects walked with the orthotic system. The energy expenditure increased from a mean of 1.33 W/kg to 1.93 W/kg. For 1.6 km/h, the energy expenditure increased from 1.64 W/kg to 2.21 W/kg, which corresponds to an augmentation of **34.8%**.

The orthotic system resulted in an increased energy expenditure, but this increment was not the same for the three velocities. It is noteworthy that this increment was slower as the speed increases to a more comfortable speed (1.6 km/h). This observation is valid since the orthosis' speeds are considered slow for humans to walk. Generally, the humans walk at self-comfortable speed, often called the preferred walking speed, which is normally between 4 km/h to 5 km/h. As such, as the speed is close to a normal velocity, the energy expenditure while walking with and without the orthosis is also closer.

Another conclusion can be retrieved. There are differences between the energy expenditure all over the velocities while the users walk with the orthotic system. The ANOVA was performed to verify if these differences are significant. Considering the three groups of samples that were tested, i.e., the energy

expenditure for the three gait speeds, a F value of 9.09 was found. As the critical $F_{2,21,0.05}$ is 3.47, the differences can be considered significant (p-value = 0.00140).

6.5 Estimating Energy Expenditure

In order to estimate the energy expenditure, a prior study was conducted to check the correlations between the predictors (kinetic and EMG data) and the variable to be predicted (energy expenditure), using the Pearson correlation coefficient. Analysing the correlations between features and ground truth signal, the best predictors can be evaluated to potentiate a better estimation.

6.5.1 Predictor selection

With the Pearson's correlation coefficient, the linearity between the predictors and the variable to be predicted is analysed [78], following Equation **(6.3).**

$$\mathrm{PCC} = \frac{\sum_{i=1}^{n}(x_i - \bar{x})\,(y_i - \bar{y})}{\sqrt{\sum_{i=1}^{n}(x_i - \bar{x})^2}\cdot\sqrt{\sum_{i=1}^{n}(y_i - \bar{y})^2}} \qquad \text{Equation (6.3)}$$

The Pearson correlation coefficients found between the processed EMG signals and the ground truth signal were positive and above 0.700, as shown in Figure **6.8 – 1**. This result demonstrates that the EMG translates well the variation of the energy expenditure. Also, it is observable that the two muscles of the shank, i.e., the TA and GL muscles, present the higher correlations, with mean values near to 0.800. If the composite sum of EMG is calculated for both legs, i.e., the resulting sum of TA, GL, BF and VL, the correlation is also higher, rounding a positive correlation of 0.800. In fact, performing the EMG composite sum, as presented in the [58], allowed the reduction of some noise due to different activations' power, and allowed an overview of the muscle activation for both legs.

The same conclusion was obtained for the acceleration and angular velocity of the sagittal plane. Correlations above 0.700 were found for segments' acceleration (Figure **6.8 – 2**) and angular velocity (Figure **6.8 – 3**). Once more, both predictors, after processed, fit well the energy expenditure variation for each subject. Also, it was observed that, as near the floor the segments become, the correlation between predictors and energy expenditure gets higher. This can be explained because, and especially during standing position, the signal gets cleaner as the segments become closer to the ground because they are not so affected by the subjects' balance.

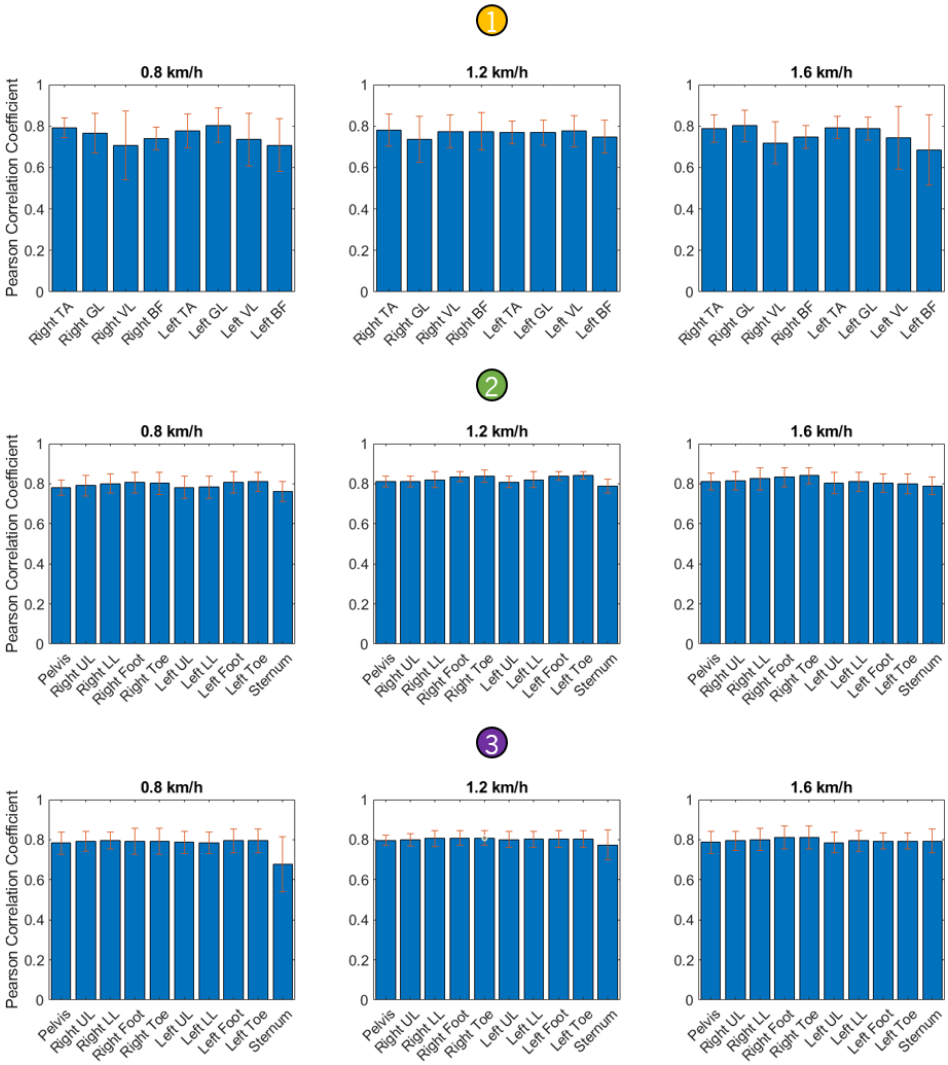

Figure 6.8: Pearson correlation coefficient between EMG (1), acceleration (2) and angular velocity (3) and energy expenditure.

Regarding the heart rate signal (Figure **6.9**), a positive high correlation was found for 1.2 km/h and 1.6 km/h. For the lowest speed, 0.8 km/h, the correlation was not strong. This low value was found because some of the subjects reported a negative correlation, contradicting others with a positive one. Also, between those with a positive correlation, some subjects presented a week result. In fact, 0.8 km/h is a very slow speed that, perhaps, do not require a high cardiac effort.

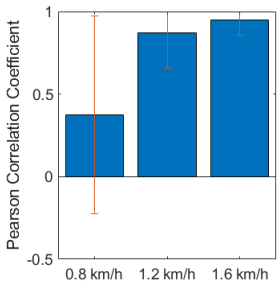

Figure 6.9: Pearson correlation between heart rate and energy expenditure.

Figure 6.10 presents the EMG composite sum, the acceleration and angular velocity variation for the right leg, as well as the heart rate and the energy expenditure, for one subject walking with the orthotic device at 0.8, 1.2 and 1.6 km/h. All predictors experienced the same pattern variation as the energy expenditure, explaining the high correlations. The acceleration does not present the gravity effect and, thus, is zero during the standing position. By opposite, the EMG signals presents an initial value different from zero since the muscles are activated during the standing position.

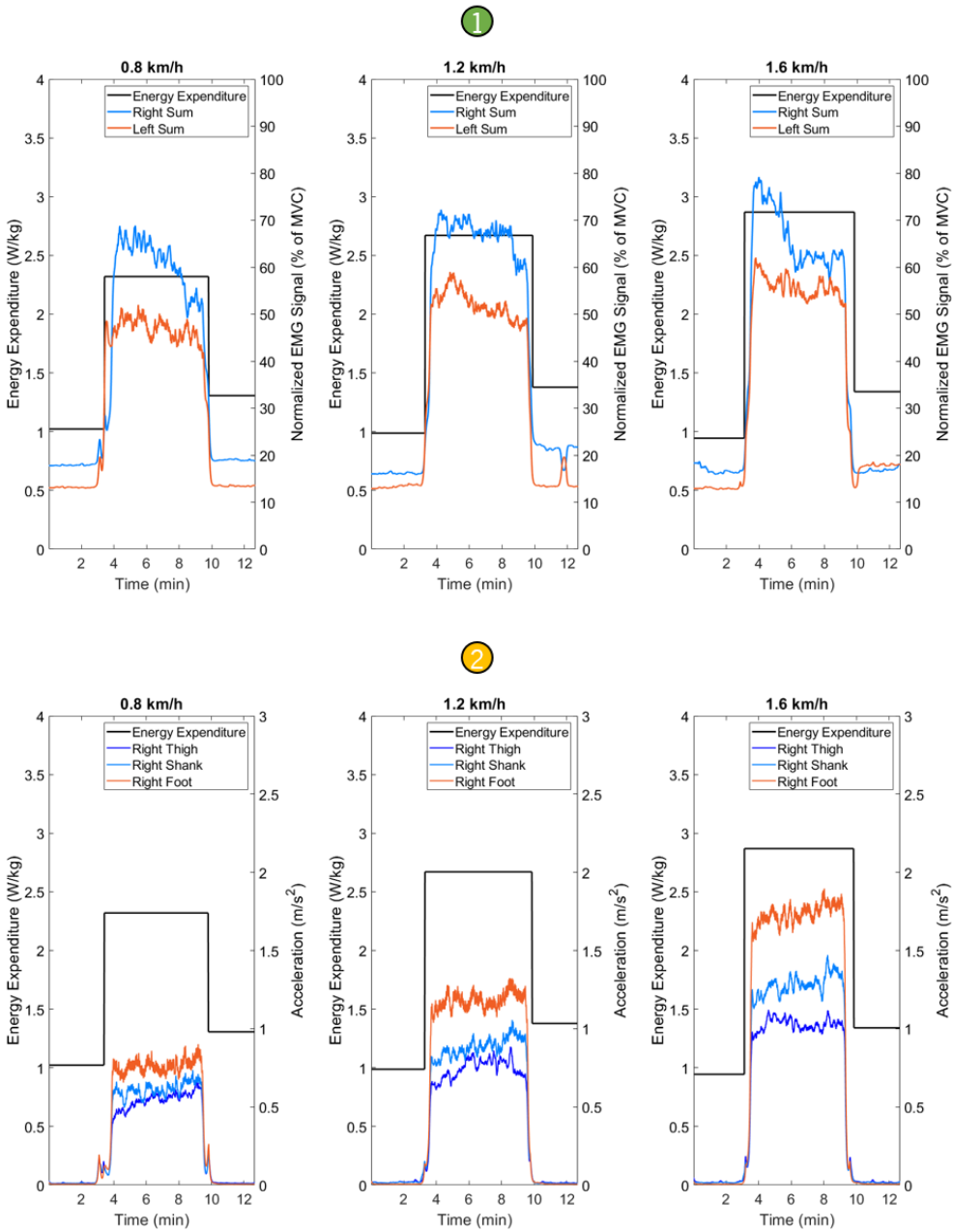

(continue)

(continuation)

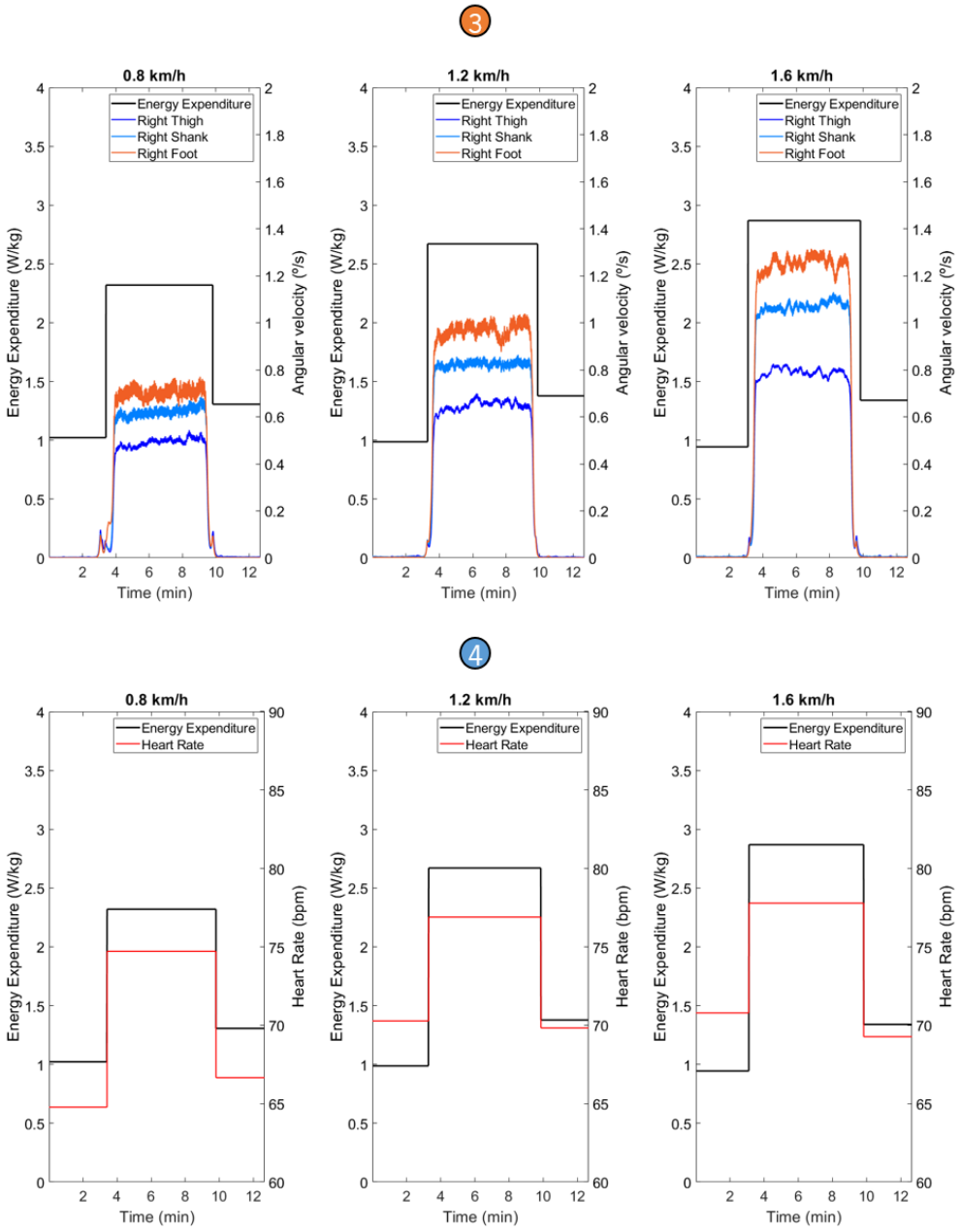

Figure 6.10: EMG (1), acceleration (2), angular velocity (3) and heart rate (4) signals for lower limbs.

The final predictors for estimating the energy expenditure from the neural networks were chosen considering the correlation results. Therefore, fifteen predictors were selected for estimating the energy expenditure. The acceleration and angular velocity of the both lower limbs segments (12), the composite sum of muscles activation for both legs (2), and the heart rate were chosen as the biomechanical features. The signals were interpolated in order to have the same size for the models input. Adding to these, the anthropometric data, as the gender, body mass, height and age, were also used as an input, as well as

the walking speed. The anthropometric data was used since the energy expenditure is user-dependent, as stated in [56]. The speed was used in order to have a general network that can distinguish the energy expenditure for different speeds. As such, a total of twenty features were selected.

6.5.2 Machine Learning Algorithms

For both MLP and LSTM neural networks, the dataset was divided into train and test subjects. The subjects were permuted, having all subjects in the test dataset at least one time. Therefore, four datasets were created, choosing randomly 6 subjects for training and 2 subjects for test.

For the MLP, a configuration with one hidden layer was performed. The machine learning package from MATLAB allows the self-management of training and validation data. As such, the training data was split into two separated folds: one corresponding to 80% of all training data was used for the training process; the other that contained the remaining 20% of data was used to validate the model during the training process, allowing an early stop if the model is overfitting. Table **6.1** resumes the training configurations used with the MLP neural network.

Table 6.1: Experimental set for MLP neural network

Configurations	*No. Epochs*	*No. Neurons*	*Batch size*	*No. Validation samples*	*Training algorithm*
1	10 000	10	10 000	50	GD
2	2000	10	10 000	30	GD
3	2000	10	10 000	30	Adam
4	2000	10	5000	30	GD
5	2000	10	5000	30	Adam
6	2000	100	10 000	30	GD
7	2000	100	10 000	30	Adam

Note: GD – Gradient descent; Adam – stochastic gradient descent with adaptive learning rate

For the LSTM network, a different validation was performed. The MATLAB package for LSTM allows the user to give data to be used for validation during the training process. Thus, a 6-fold cross-validation technique was used. The training dataset was divided into 6-folds, where 5 of them were used for training the model, and the other was used to validate it during the training process at every epoch, as shown in

Figure 6.11. This approach attempts to avoid the overfitting, allowing the construction of a more generalized model.

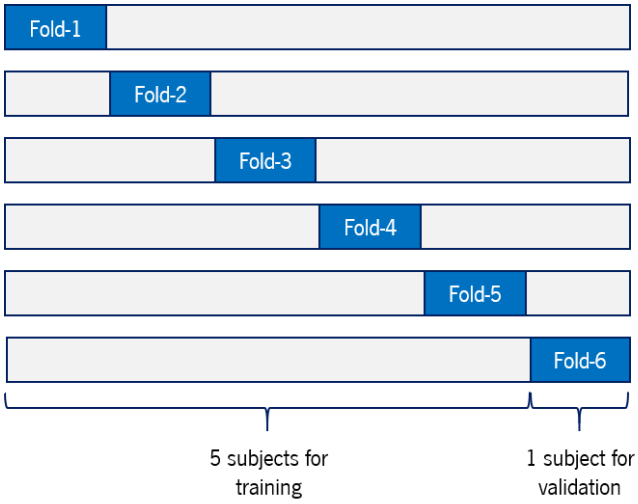

Figure 6.11: K-Fold cross-validation for the LSTM neural network.

Table 6.2 resumes the different configurations that were tested for the LSTM neural network. As LSTMs are highly computational and the training dataset, in terms of sample, overcomes 11 million points, the batch size remained in 10 000 points, as observed for the MLP.

Table 6.2: Experimental set for LSTM neural network

Configurations	*No. Epochs*	*No. Neurons*	*Batch size*	*Validation Checks*	*Training algorithm*
1	100	10	10 000	1 subject per epoch	SGD
2	100	100	10 000	1 subject per epoch	SGD
3	100	10	10 000	1 subject per epoch	Adam
4	100	100	10 000	1 subject per epoch	Adam

Note: SGD – Stochastic gradient descent; Adam – stochastic gradient descent with adaptive learning rate

For both neural networks, the loss was computed with the mean squared error, as shown in Equation **(6.4)**. Therefore, the weights of the neural networks were optimized in order to minimize the loss.

$$\mathrm{MSE} = \frac{1}{N}\sum_{i=1}^{n}\left(y_i - \hat{y}_i\right)^2 \qquad \text{Equation (6.4)}$$

To evaluate the model's performance, the RMSE, introduced in the previous chapters and evaluated through Equation **(4.3)**, the Pearson's correlation coefficient calculated through Equation **(6.3)**, and the Spearman's correlation coefficient, calculated using the following Equation **(6.5)**, were assessed. Also, the normalized RMSE based on the total variation of energy observed for each subject and trial was performed, allowing the error quantification in terms of percentage.

$$\mathrm{SCC} = 1 - \frac{6\sum d_i^2}{N(N^2 - 1)} \qquad \text{Equation (6.5)}$$

The results were also compared with a linear regressor model, based on the least squares method, that was presented in [58].

6.5.3 Results and Discussion

Towards a Human-in-the-loop strategy into the SmartOs orthosis, two machine learning architectures were exploited to estimate the energy expenditure of users while walking with the SmartOs-ankle orthosis in the assistance mode. In a general way, the machine learning algorithms were able to estimate the energy expenditure of users while they walked with the orthotic device. It was found a RMSE below 0.400 W/kg for all the tested algorithms, which is less than those reported in the literature. Furthermore, the LSTM neural network was the machine learning algorithm that presented the best results, with an error close to 0.200 W/kg for the best model, which represents 11% of the total range of energy observed in the test dataset.

Table **6.3** presents the MLP neural network performance metrics for the best model found for each dataset, considering the configurations described in Table **6.1**.

By analysing Table **6.3**, the dataset 4, with the third configuration described in Table **6.1**, presented the best test results. The best configuration consisted in a shallow MLP with 10 neurons in which the learning rate was adapted during the training process. The feedforward neural network presented a mean error of

0.342 (± 0.141) W/kg for the test subjects and correlations above 0.800, which highlights the capacity of this model to predict energy expenditure using biomechanical data.

Table 6.3: Performance metrics for the test subjects of the MLP neural network for the four datasets

Dataset	*Best Configuration*	*Performance metrics*			
		RMSE	NRMSE	PCC	SCC
1	2	0.512 (0.0851)	29.3 (8.63)	0.977 (0.00810)	0.774 (0.0478)
2	2	0.376 (0.193)	21.5 (13.9)	0.993 (0.00470)	0.865 (0.0512)
3	3	0.564 (0.179)	26.6 (4.51)	0.983 (0.00410)	0.876 (0.0594)
4	**3**	**0.342 (0.141)**	**20.9 (11.8)**	**0.988 (0.00720)**	**0.891 (0.0220)**

Although the RMSE is a low value, this value was found to be almost 21% of the total amount of energy for the test subjects. This result means that, although the absolute error is low, this error can be significant regarding the total range of energy observed. Further studies should perform an extensive search of the best parameters that potentiate a decrease in this metric, improving the model's ability of estimating the energy expenditure.

Regarding the correlations, the Pearson and Spearman correlation coefficients were high and positive, which shows that the neural network was able to distinguish if the subjects were walking with the orthotic device or if they were in standing position. Figure 6.12 present the results of the test subjects used to evaluate the best model's performance for the three gait speeds.

Analysing Figure 6.12, the neural network was able to catch the important information in the selected predictors that potentiate a good estimation of energy expenditure with a minimum RMSE. Furthermore, the neural network was able to distinguish the three walking speeds, producing an estimation that increases as the speed increases, as stated for the ground truth signal. However, it was not able to differentiate the small differences between the initial standing position and the final recover, as displayed in Figure 6.12, since the energy expenditure estimation remained the same for both stages.

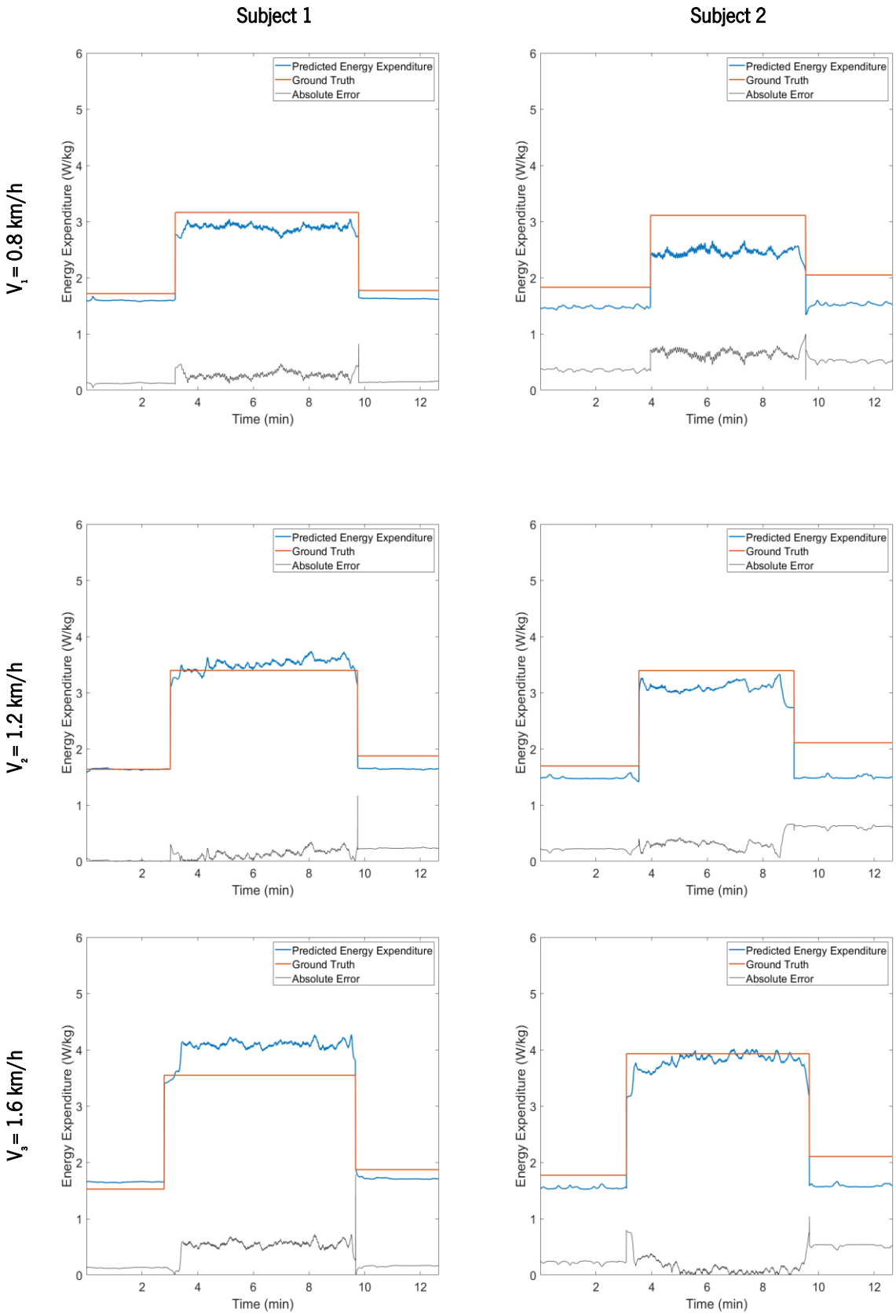

Figure 6.12: Energy expenditure estimation for the test subjects of the best feedforward neural network model.

The LSTM neural network was another machine learning approach exploited in this chapter. This neural network allowed a RMSE decreasing in comparison with the MLP, potentiating a better estimation of the energy expenditure. The best model was found for the same dataset as the MLP, with one LSTM layer with 10 units. Table **6.4** presents test performance metrics obtained for the best configuration found for each dataset used.

Table 6.4: Performance metrics for the LSTM configuration regarding the four datasets

Dataset	*Best Configuration*	*Performance metrics*			
		RMSE	NRMSE	PCC	SCC
1	1	0.249 (0.139)	13.0 (3.99)	0.982 (0.00800)	0.849 (0.0650)
2	3	0.246 (0.0716)	13.4 (5.16)	0.993 (0.00480)	0.871 (0.0364)
3	3	0.551 (0.137)	27.5 (8.42)	0.987 (0.0111)	0.871 (0.0651)
4	**3**	**0.193 (0.0579)**	**11.0 (1.92)**	**0.991 (0.00750)**	**0.858 (0.0281)**

Analysing Table **6.4**, the LSTM presented best performance metrics for both datasets in comparison with the MLP neural network. The correlation coefficients found presented high values and were positive, highlighting that the machine learning-based model was able to correctly estimate the energy expenditure for the test subjects. Furthermore, the normalized RMSE decreased to 11%, which represents a drop of almost 47% in comparison to the best model found for the MLP. Figure **6.13** displays the same two subjects of test that were presented for the MLP configuration.

Analysing Figure **6.13**, it is observable that the LSTM model promoted a better estimation of the energy expenditure, especially in subject 2 for 0.8 km/h, where the drift observed in the MLP neural network is no longer observed. Moreover, in subject 1 and while walking at 1.6 km/h, the LSTM model showed an improvement in comparison with the MLP neural network, since it did not overestimate so much the energy expenditure. However, for this same subject and trial, the LSTM neural network was not able to correctly estimate the basal energy expenditure.

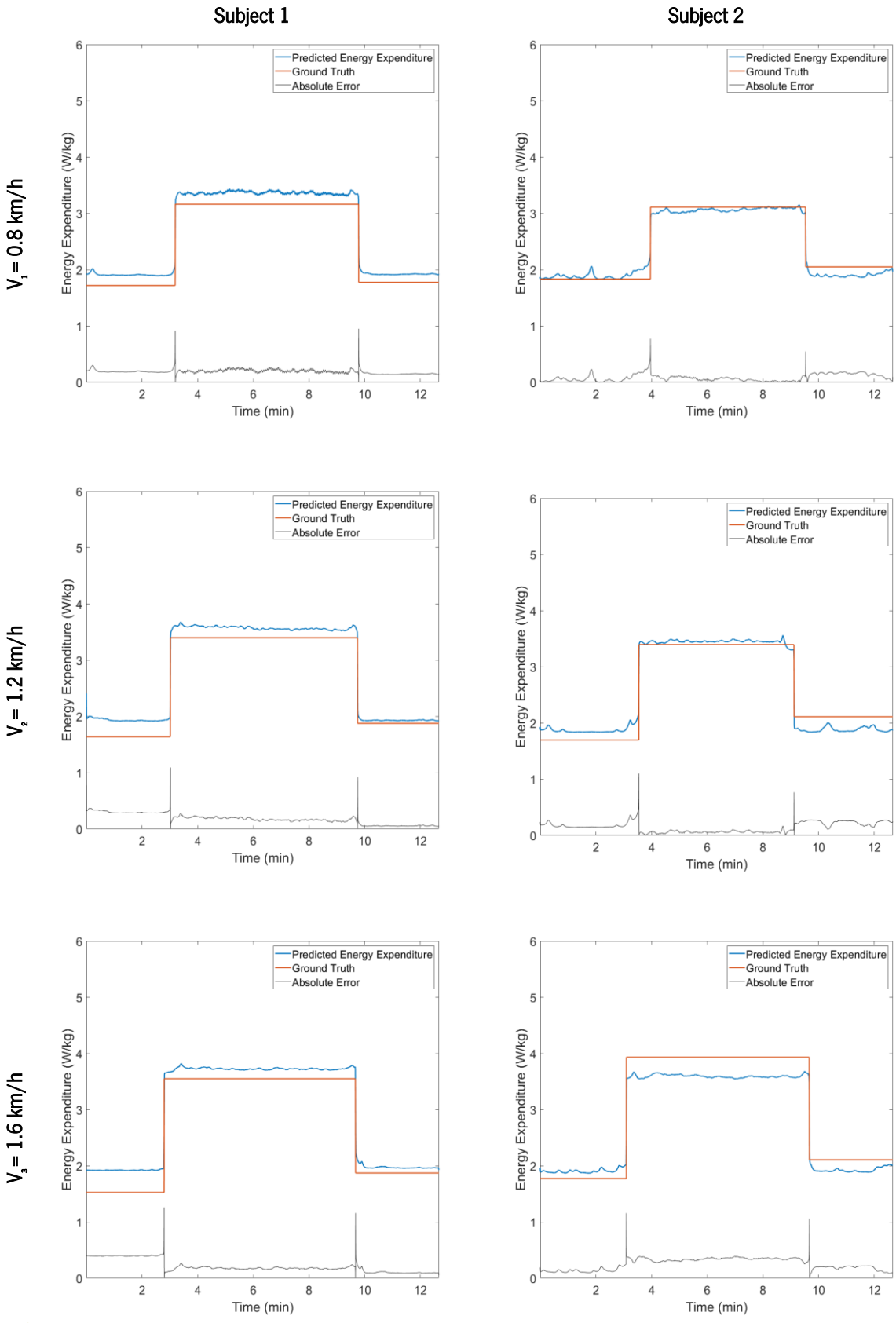

Figure 6.13: Energy expenditure estimation for the test subjects of the best LSTM model.

The linear regression model evaluated in [58] was also assessed in this dissertation for comparative terms. The linear regression model was also able to predict the steady-state energy expenditure with a mean RMSE of 0.332 (±0.173) W/kg. However, the best fit was not found for the same dataset combination as the MLP or the LSTM neural networks. Table **6.5** presents the results of the linear regression model for the best test set.

Table 6.5: Performance metrics for the four datasets of the linear regression model

Dataset	*Performance metrics*			
	RMSE	NRMSE	PCC	SCC
1	0.565 (0.171)	31.4 (9.79)	0.980 (0.0109)	0.850 (0.0705)
2	**0.332 (0.173)**	**18.0 (10.7)**	**0.988 (0.00450)**	**0.885 (0.0148)**
3	0.777 (0.539)	33.9 (19.1)	0.987 (0.00570)	0.874 (0.0644)
4	1.65 (0.0756)	98.3 (18.4)	0.984 (0.00790)	0.897 (0.0115)

Analysing Table **6.5**, for the same dataset where both MLP and LSTM presented the best results, the linear regression model was not able to estimate correctly the energy expenditure of the test subjects. Indeed, a RMSE of 1.65 W/kg was observable for this dataset. This was observable because, perhaps, the model did not have the capacity of catching the important information in the predictors that lead to a correct estimation in the energy expenditure. In fact, for this dataset, the predictors for all subjects may present a similar pattern but, as the energy expenditure is user-dependent, it led to an overestimation of the ground truth signal. However, both Pearson and Spearman correlation coefficients presented a high value, which indicates that, although the linear regression model for this dataset was not able to estimate the energy expenditure value, it was able to identify correctly when the subjects were walking or were in standing position. Nevertheless, it was found a dataset, trained with different subjects, in which the linear regression model presented a RMSE of 0.332 W/kg for the test subjects. This result represented a mean normalized RMSE of 18%, which is a reasonable result considering this approach. Figure **6.14** shows the

energy expenditure estimation for the test subjects of the best dataset found using the linear regression model reported in [58].

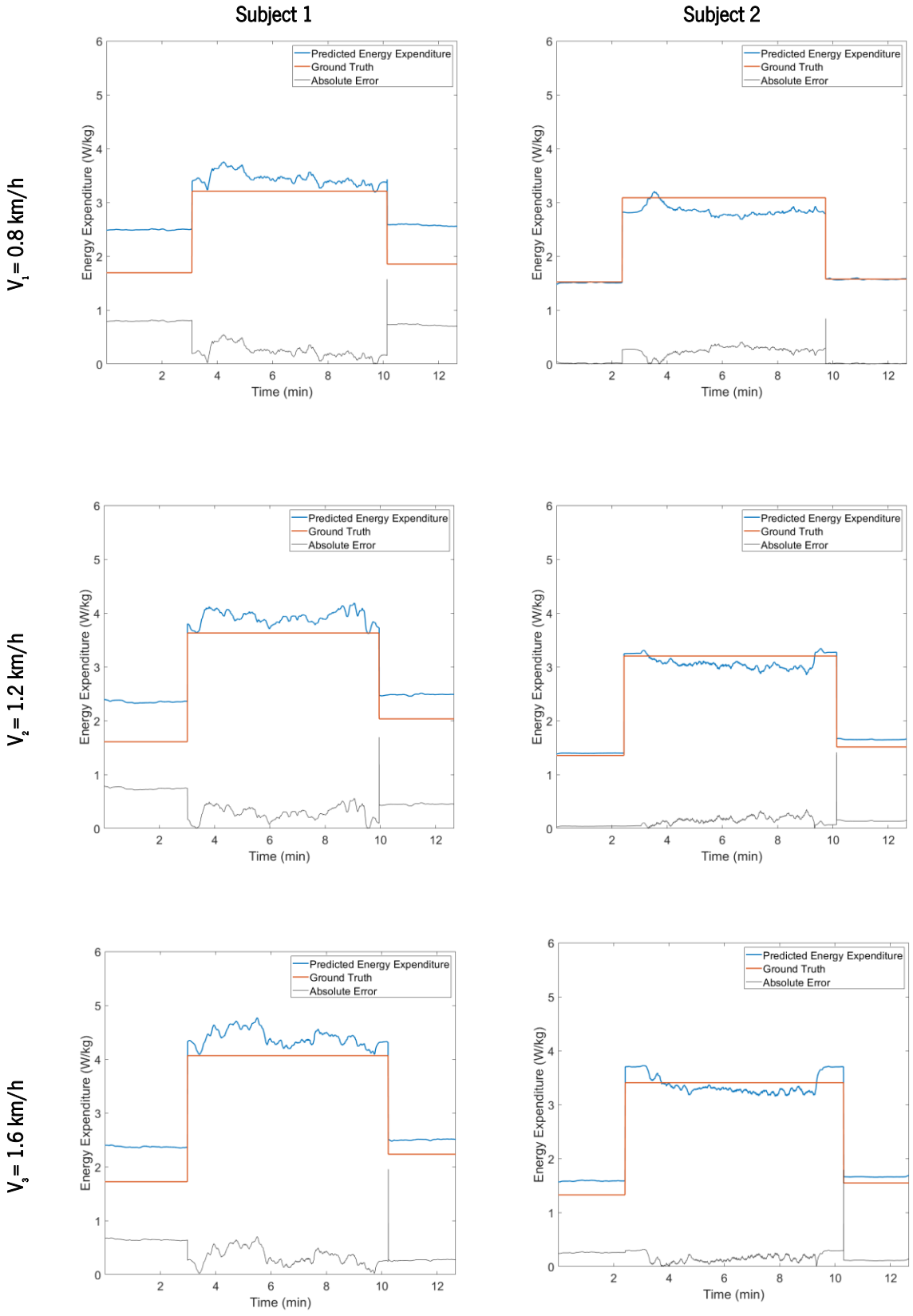

Figure 6.14: Energy expenditure estimation of the test subjects for the best linear regression model.

Analysing Figure **6.14**, for dataset 2, the linear regression model estimated the energy expenditure with a reasonable accuracy, especially for subject 2, in both standing or walking. Regarding subject 1, the linear regression model estimated better the energy expenditure while the subject was walking, since the absolute error produced was smaller.

6.6 General conclusions

In this chapter, the first steps towards a Human-in-the-loop control approach were presented. First, the impact of using an orthosis in healthy subjects was assessed. For that, the energy expenditure was evaluated, collecting the pulmonary dynamics using a gas analyser. With this empirical study, it was proved the necessity of introducing Human-in-the-loop in the SmartOs since all subjects experienced an augmentation of energy expenditure while they were assisted with the ankle orthosis. However, for introducing this control approach in the SmartOs, and in order to be suited for impaired persons, new approaches of estimating the energy expenditure without relying in the gas analyser were evaluated. The use of machine learning techniques, as a feedforward neural network and a LSTM neural network, were studied to evaluate their potential use in estimating the energy expenditure. The results highlight the use of these approaches for Human-in-the-loop strategy, and especially the LSTM neural network, since a reasonable estimation was obtained with a mean normalized RMSE of 11% for the best dataset.

7. CONCLUSIONS

In this dissertation, the first steps towards the introduction of Human-in-the-loop strategy into a Smart Wearable Orthotic System – SmartOs – were addressed. As a first goal, the implementation and/or validation of two different user-oriented control strategies for future use in the clinical context, that promote a therapy sustained in both repetitive gait training and active participation, was performed. As a second goal, an empirical study to check the energetic impact of using the orthotic device into healthy subjects was conducted. In an attempt to avoid the use of non-ergonomic and clinical non-suitable sensors for estimating the energy expenditure, two different machine learning-based regressor algorithms were implemented and tested for further use in Human-in-the-loop control.

First, a literature analysis was conducted to assess the current state of powered orthoses. It was concluded that, during these last years, many orthoses have been developed to aid persons with motor impairments. Different control strategies, such as trajectory tracking control, EMG-based control, impedance control, among others, have been proposed to control these powered devices. However, the powered orthoses still do not endow strategies able to promote an user-oriented assistance, tailored to the end-user needs. To tackle this problem, the investigators have focused their attention on the use of energy expenditure as way to promote a more personalized and effective assistance for persons with impaired gait. A new strategy - Human-in-the-loop – is getting its first steps towards a personalized assistance, making use of energy expenditure to adapt certain assistance parameters, as the torque peak magnitude. Currently, the energy expenditure measurements required the use of indirect calorimetry, which is the most reliable technique in these days. However, this technique makes use of gas analysers, which are not the most ergonomic and suitable sensors for clinical context. It requires a specialized team for working with these sensors, besides being a noisy and expensive technique.

SmartOs is a modular, bioinspired, time-effective orthotic system intended for human locomotion assistance and rehabilitation. It is composed of two orthotic devices, the PKO and PAFO, and different sensory modules that allow an effective gait monitorization. Moreover, the orthotic devices are controlled using a user-friendly mobile application, where the main configurations, as the assistive strategy, and the monitorization modules, can be activated. This dissertation uses the potentialities of SmartOs system, mainly for the implementation of two user-oriented control strategies.

For the first control strategy, the Adaptive User-Oriented Trajectory Tracking Control, an algorithm to create user-oriented assistances for both PKO and PAFO orthotic devices was developed. This strategy allows the angular trajectory modification in real-time in sub-phases of the gait cycle, using the user-

friendly mobile application. This strategy was tested in two lower-limb orthotic devices, the PKO and PAFO, and the results prove its necessity in the clinical context. The orthoses were able to modify its assistance with a low latency (in a fraction of microseconds), and the users were able to follow its assistance. As a second outcome, the gait symmetry was evaluated while the users walk with the orthotic device. It was found that, in terms of range of motion and swing time, the orthosis does not promote a symmetrical gait. For other symmetry evaluation metrics, such as the stance time, and the ratio between stance and swing times, the orthosis showed to provide a *quasi*-symmetrical gait. However, this result was more visible in the PKO.

For the second strategy, named Adaptive User-Oriented Impedance control, the validation of an algorithm to change the joint's stiffness all over the gait cycle was performed. The strategy was already applied to the PKO and, thus, the same strategy was followed for the PAFO device. An empirical study evaluating where the subjects feel more necessity of assistance was conducted with the orthotic device in a passive mode. It was found that the toe off event is the most critical phase of the gait cycle and where the subjects need more help. A linear model that approximates the human-orthosis interaction torque *vs* angle curve per gait phases was constructed, and the slope of the best fit was used as the joint's stiffness. The validation with healthy subjects showed that the orthosis was able to adapt the joint's compliance in real-time, promoting an assistance based on the user's effort and active participation.

Lastly, the impact of using the SmartOs-ankle orthosis into healthy subjects was assessed. For that, a comparative study was performed with the subjects walking with and without the orthotic device, evaluating the pulmonary dynamics. Oxygen consumption and carbon dioxide production was measured through indirect calorimetry to calculate the energy expenditure of users. As the orthosis promoted an augmentation of energy expenditure, the need for introducing the Human-in-the-loop strategy was highlighted. As this strategy relies on non-ergonomic sensors, as stated in the *State-of-the-art*, an attempt of estimating the energy expenditure through wearable sensors was performed using two machine learning algorithms. The results, obtained with a MLP and a LSTM, prove that these techniques are suitable for energy expenditure estimation. These machine learning-based regression models were confronted with a linear regression model and it was found that the LSTM is the best approach.

In general, the main goals of this dissertation were accomplished with success. Both PKO and PAFO now have two user-oriented assistive strategies that allow them to deliver an assistance tailored to the end-user needs. With that, and with the machine learning model for estimating the energy expenditure, the

first steps towards the Human-in-the-loop strategy were successfully accomplished. Thus, the research questions formulated in Chapter 1 can be answered.

RQ 1: *Can the energy expenditure be used to study the gait efficiency enabled by powered assistive devices, and to exploit the Human-in-the-loop control?*

This RQ was answered in Chapter 2. After a revision in the literature, it was found that the energy expenditure is being monitored to evaluate the impact of using an orthotic device into the subject's assistance. Moreover, this measure has been explored in Human-in-the-loop control, where the orthotic-based assistance is changed in real-time, producing an effective but also efficient assistance. As most of the current orthoses are controlled with torque trajectory control, the main parameters being changed are the torque peak magnitude, the torque peak timing and the actuation onset.

RQ 2: *Is it possible to adapt the existing control strategies as a way to introduce the Human-in-the-loop control in the SmartOs?*

This RQ was answered in Chapter 4 and 5. The SmartOs consists of two orthotic devices, the PKO and the PAFO, for a time-effective rehabilitation of persons with motor impairments. For introducing the Human-in-the-loop control in the SmartOs, two control approaches were introduced and validated with healthy subjects. The first strategy, the Adaptive User-Oriented Trajectory Control, presented in Chapter 4, enables creating different position trajectories tailored to the user's needs, in real-time, for both PKO and PAFO devices. The second control strategy, already validated in the PKO device, was extended to the PAFO device. Moreover, the interconnection between the two assistive strategies was ensured, allowing the delivering of an assistance based on effort and active participation with a reference trajectory tailored to each end-user needs. Thus, it is possible to adapt the existing control strategies as a way to introduce the Human-in-the-loop control in the SmartOs.

RQ 3: *Are there differences in the user's energy expenditure when assisted by the SmartOs at slow walking speeds?*

This RQ was answered in Chapter 6. The SmartOs was designed for persons with motor impairments, who usually walk at slow speed. Thus, SmartOs only allows slow walking speeds that are not comfortable for healthy subjects. An empirical study was conducted with the orthotic device for the three main gait speeds – 0.8 km/h, 1.2 km/h and 1.6 km/h. This study shows that the orthosis promoted an augmentation of energy expenditure for all speeds in comparison to walk without the device. Regarding the energy expenditure for the three speeds, there are differences between them, and the differences are considered statistically significant (p-value = 0.00140).

RQ 4: *Are the machine learning-based models able to evaluate the energy expenditure in the SmartOs, minimizing the use of non-ergonomic systems?*

This RQ was answered in Chapter **6**. The machine learning algorithms consisted of an effective solution for estimating the energy expenditure with an error that can be overcome with more available data for training the model. In this dissertation, two machine learning-based regression models were tested, one MLP with one hidden layer of 10 neurons, and one LSTM neural network with 10 units, and it showed a reasonable performance in estimating the energy expenditure of users while walking the orthotic device. Therefore, the use of non-suitable techniques as indirect calorimetry can be replaced by machine learning-based empirical models fed by motion data from wearable sensors.

7.1 Future work

As future work, a more extensive validation of the presented assistive strategies should be carefully performed, including the evaluation with patients with motor impairments. Moreover, in an attempt of creating a more robust model, more data for the Human-in-the-loop purpose should be collected using the presented control strategies, creating different orthosis-based assistances regarding the position trajectory and the interaction stiffness. Also, an extensive search of different configurations for the neural networks should be performed, ensuring the creation of the best model that predicts well the energy expenditure. Once this is performed, the prediction model should be implemented in real-time in parallel with the proposed assistive strategies in order to have an orthotic device that: **(1)** allows an effective estimation of energy expenditure and **(2)** adapts the assistance, in real-time, regarding the energetic demand of each user.

REFERENCES

[1] World Wealth Organization, "World Report on Disability," 2011.

[2] D. Sanz-Merodio, "Development of strategies to reduce energy expenditure for lower-limb active orthoses," 2018.

[3] S. Balasubramanian, "Motor impairments following stroke," no. August, 2015.

[4] D. Longo, A. Fauci, D. Kasper, S. Hauser, J. Jameson, and J. Loscalzo, *Harrison's Manual of Medicine*. 2012.

[5] J. Jonsdottir and M. Ferrarin, "Gait Disorders in Persons After Stroke," in *Handbook of Human Motion*, B. Müller, Ed. Springer, 2016.

[6] L. N. Awad *et al.*, "A soft robotic exosuit improves walking in patients after stroke," *Sci. Transl. Med.*, vol. 9, no. 400, 2017.

[7] T. Yan, M. Cempini, C. M. Oddo, and N. Vitiello, "Review of assistive strategies in powered lower-limb orthoses and exoskeletons," *Rob. Auton. Syst.*, vol. 64, pp. 120–136, 2015.

[8] H. Herr, "Exoskeletons and orthoses: Classification, design challenges and future directions," *J. Neuroeng. Rehabil.*, vol. 6, no. 1, pp. 1–9, 2009.

[9] R. S. Mosher, "From Handiman to Hardiman," *Society of Automotive Engineers Transactions*, vol. 76. pp. 588–597, 1967.

[10] M. R. Tucker *et al.*, "Control strategies for active lower extremity prosthetics and orthotics: A review," *J. Neuroeng. Rehabil.*, vol. 12, no. 1, 2015.

[11] Mihailo Pupin Institute, "History of Robotics Laboratory," *Robotics Laboratory*, 2012. [Online]. Available: http://www.pupin.rs/RnDProfile/history.html.

[12] A. B. Zoss, H. Kazerooni, and A. Chu, "Biomechanical Design of the Berkeley Lower Extremity Exoskeleton (BLEEX)," *IEEE/ASME Trans. MECHATRONICS*, vol. 11, no. 2, pp. 128–138, 2006.

[13] A. AIA, C. H, L. X, O. M, and A. JM, "Survey of On-line Control Strategies of Human-Powered Augmentation Exoskeleton Systems," *Adv. Robot. Autom.*, vol. 05, no. 03, 2016.

[14] Y. Sankai, "HAL: Hybrid assistive limb based on cybernics," *Springer Tracts Adv. Robot.*, vol. 66, no. STAR, pp. 25–34, 2010.

[15] R. Riener, L. Lünenburger, S. Jezernik, M. Anderschitz, G. Colombo, and V. Dietz, "Patient-cooperative strategies for robot-aided treadmill training: First experimental results," *IEEE Trans. Neural Syst. Rehabil. Eng.*, vol. 13, no. 3, pp. 380–394, 2005.

[16] D. Sanz-Merodio, M. Cestari, J. C. Arevalo, and E. Garcia, "Control motion approach of a lower limb orthosis to reduce energy consumption," *Int. J. Adv. Robot. Syst.*, vol. 9, 2012.

[17] A. Esquenazi, M. Talaty, A. Packel, and M. Saulino, "The Rewalk powered exoskeleton to restore ambulatory function to individuals with thoracic-level motor-complete spinal cord injury," *Am. J. Phys. Med. Rehabil.*, vol. 91, no. 11, pp. 911–921, 2012.

[18] H. A. Quintero, R. J. Farris, C. Hartigan, I. Clesson, and M. Goldfarb, "A Powered Lower Limb Orthosis for Providing Legged Mobility in Paraplegic Individuals," *Top Spinal Cord Inj. Rehabiliation*, vol. 17, no. 1, pp. 25–33, 2012.

[19] H. K. Kwa, J. H. Noorden, M. Missel, T. Craig, J. E. Pratt, and P. D. Neuhaus, "Development of the IHMC mobility assist exoskeleton," *Proc. - IEEE Int. Conf. Robot. Autom.*, pp. 2556–2562, 2009.

[20] P. D. Neuhaus, J. H. Noorden, T. J. Craig, T. Torres, J. Kirschbaum, and J. E. Pratt, "Design and evaluation of Mina: A robotic orthosis for paraplegics," *IEEE Int. Conf. Rehabil. Robot.*, 2011.

[21] T. Nakamura, K. Saito, Z. D. Wang, and K. Kosuge, "Realizing model-based wearable antigravity muscles support with dynamics terms," *2005 IEEE/RSJ Int. Conf. Intell. Robot. Syst. IROS*, pp. 2053–2058, 2005.

[22] C. Feng, Y. Yong, Y. Ge, and F. Yu, "WPAL for human power assist during walking using dynamic equation," *2009 IEEE Int. Conf. Mechatronics Autom. ICMA 2009*, pp. 1039–1043, 2009.

[23] C. L. Lewis and D. P. Ferris, "Invariant hip moment pattern while walking with a robotic hip exoskeleton," *J. Biomech.*, vol. 44, no. 5, pp. 789–793, 2011.

[24] J. R Koller, D. H Gates, D. P Ferris, and C. David Remy, "'Body-in-the-Loop' Optimization of Assistive Robotic Devices: A Validation Study," 2016.

[25] A. M. Dollar and H. Herr, "Design of a quasi-passive knee exoskeleton to assist running," *2008 IEEE/RSJ Int. Conf. Intell. Robot. Syst. IROS*, pp. 747–754, 2008.

[26] P. C. Kao, C. L. Lewis, and D. P. Ferris, "Invariant ankle moment patterns when walking with and without a robotic ankle exoskeleton," *J. Biomech.*, vol. 43, no. 2, pp. 203–209, 2010.

[27] P. Malcolm, S. Galle, P. Van Den Berghe, and D. De Clercq, "Exoskeleton assistance symmetry matters: Unilateral assistance reduces metabolic cost, but relatively less than bilateral assistance," *J. Neuroeng. Rehabil.*, vol. 15, no. 1, 2018.

[28] L. M. Mooney and H. M. Herr, "Biomechanical walking mechanisms underlying the metabolic reduction caused by an autonomous exoskeleton," *J. Neuroeng. Rehabil.*, vol. 13, no. 1, pp. 1–12, 2016.

[29] M. Kim *et al.*, "Human-in-the-Loop Bayesian Optimization of a Tethered Soft Exosuit for Assisting Hip Extension," in *Wearable Robotics: Challenges and Trends. WeRob 2018. Biosystems &*

Biorobotics, 2019, vol. 22, pp. 142–146.

[30] E. Martini *et al.*, "Gait training using a robotic hip exoskeleton improves metabolic gait efficiency in the elderly," *Sci. Rep.*, vol. 9, no. 1, 2019.

[31] J. E. Pratt, B. T. Krupp, C. J. Morse, and S. H. Collins, "The RoboKnee: An exoskeleton for enhancing strength and endurance during walking," *Proc. - IEEE Int. Conf. Robot. Autom.*, vol. 2004, no. 3, pp. 2430–2435, 2004.

[32] W. Y. Lai, H. Ma, W. H. Liao, D. T. P. Fong, and K. M. Chan, "HIP-KNEE Control for Gait Assistance with Powered Knee Orthosis," *2013 IEEE Int. Conf. Robot. Biomimetics, ROBIO 2013*, no. December, pp. 762–767, 2013.

[33] R. Jiménez-Fabián and O. Verlinden, "Review of control algorithms for robotic ankle systems in lower-limb orthoses, prostheses, and exoskeletons," *Medical Engineering and Physics*. 2012.

[34] J. Zhang *et al.*, "Human-in-the-loop optimization of exoskeleton assistance during walking," *Science (80-.).*, vol. 356, no. 6344, pp. 1280–1284, 2017.

[35] J. J. Craig, *Introduction to Robotics: Mechanics and Control*, 3rd editio. Pearson Education, Inc., 2005.

[36] Q. T. Dao, M. Hagiwara, and S. I. Yamamoto, "Design and evaluation of the lower-limb robotic orthosis for gait rehabilitation actuated by pneumatic artificial muscle," *ACM Int. Conf. Proceeding Ser.*, pp. 85–89, 2017.

[37] W. Huo, S. Mohammed, and Y. Amirat, "Impedance Reduction Control of a Knee Joint Human-Exoskeleton System," *IEEE Trans. Control Syst. Technol.*, vol. PP, pp. 1–16, 2018.

[38] G. Aguirre-Ollinger, J. E. Colgate, M. A. Peshkin, and A. Goswami, "Active-impedance control of a lower-limb assistive exoskeleton," *2007 IEEE 10th Int. Conf. Rehabil. Robot. ICORR'07*, vol. 00, no. c, pp. 188–195, 2007.

[39] B. M. Fleerkotte, B. Koopman, J. H. Buurke, E. H. F. Van Asseldonk, H. Van Der Kooij, and J. S. Rietman, "The effect of impedance-controlled robotic gait training on walking ability and quality in individuals with chronic incomplete spinal cord injury: An explorative study," *J. Neuroeng. Rehabil.*, vol. 11, no. 1, pp. 1–15, 2014.

[40] S. Hussain, S. Q. Xie, and P. K. Jamwal, "Adaptive impedance control of a robotic orthosis for gait rehabilitation," *IEEE Trans. Cybern.*, vol. 43, no. 3, pp. 1025–1034, 2013.

[41] S. Hussain, S. Q. Xie, and P. K. Jamwal, "Adaptive impedance control of a robotic orthosis for gait rehabilitation," *IEEE Trans. Cybern.*, vol. 43, no. 3, pp. 1025–1034, 2013.

[42] V. Rajasekaran, J. Aranda, and A. Casals, "Adaptive walking assistance based on human-orthosis

interaction," *IEEE Int. Conf. Intell. Robot. Syst.*, vol. 2015-Decem, pp. 6190–6195, 2015.

[43] J. Figueiredo, P. Félix, C. P. Santos, and J. C. Moreno, "Towards human-knee orthosis interaction based on adaptive impedance control through stiffness adjustment," *IEEE Int. Conf. Rehabil. Robot.*, pp. 406–411, 2017.

[44] S. Kramer, L. Johnson, J. Bernhardt, and T. Cumming, "Energy Expenditure and Cost during Walking after Stroke: A Systematic Review," *Arch. Phys. Med. Rehabil.*, vol. 97, no. 4, pp. 619-632.e1, 2016.

[45] L. N. Awad, J. A. Palmer, R. T. Pohlig, S. A. Binder-Macleod, and D. S. Reisman, "Walking Speed and Step Length Asymmetry Modify the Energy Cost of Walking After Stroke," *Neurorehabil. Neural Repair*, vol. 29, no. 5, pp. 416–423, 2015.

[46] A. Danielsson and K. S. Sunnerhagen, "Energy expenditure in stroke subjects walking with a carbon composite ankle foot orthosis," *J. Rehabil. Med.*, vol. 36, no. 4, pp. 165–168, 2004.

[47] M. Franceschini, M. Massucci, L. Ferrari, M. Agosti, and C. Paroli, "Effects of an ankle-foot orthosis on spatiotemporal parameters and energy cost of hemiparetic gait," *Clin. Rehabil.*, vol. 17, no. 4, pp. 368–372, 2003.

[48] K. Seo, J. Lee, Y. Lee, T. Ha, and Y. Shim, "Fully Autonomous Hip Exoskeleton Saves Metabolic Cost of Walking," in *IEEE International Conference on Rehabilitation Robotics and Automation (ICRA)*, 2016.

[49] R. L. Waters and S. Mulroy, "The energy expenditure of normal and pathologic gait," *Gait Posture*, vol. 9, no. 3, pp. 207–231, 1999.

[50] P. Malcolm, W. Derave, S. Galle, and D. De Clercq, "A Simple Exoskeleton That Assists Plantarflexion Can Reduce the Metabolic Cost of Human Walking," *PLoS One*, vol. 8, no. 2, pp. 1–7, 2013.

[51] S. Galle, P. Malcolm, S. H. Collins, and D. De Clercq, "Reducing the metabolic cost of walking with an ankle exoskeleton: interaction between actuation timing and power," *J. Neuroeng. Rehabil.*, vol. 14, no. 1, pp. 1–16, 2017.

[52] Y. Ding *et al.*, "Effect of timing of hip extension assistance during loaded walking with a soft exosuit," *J. Neuroeng. Rehabil.*, vol. 13, no. 1, pp. 1–10, 2016.

[53] B. T. Quinlivan *et al.*, "Assistance magnitude versus metabolic cost reductions for a tethered multiarticular soft exosuit," *Sci. Robot.*, vol. 2, no. 2, 2017.

[54] Y. Ding, M. Kim, S. Kuindersma, and C. J. Walsh, "Human-in-the-loop optimization of hip assistance with a soft exosuit during walking," *Sci. Robot.*, vol. 3, no. 15, pp. 1–9, 2018.

[55] J. F. Norman, S. Bossman, P. Gardner, and C. Moen, “Comparison of the Energy Expenditure Index and Oxygen Consumption Index During Self-Paced Walking in Children with Spastic Diplegia Cerebral Palsy and Children Without Physical Disabilities,” *Pediatr. Phys. Ther.*, vol. 16, no. 4, pp. 206–211, 2004.

[56] T. Beltrame, R. Amelard, R. Villar, M. J. Shafiee, A. Wong, and R. L. Hughson, “Estimating oxygen uptake and energy expenditure during treadmill walking by neural network analysis of easy-to-obtain inputs,” *J. Appl. Physiol.*, vol. 121, no. 5, pp. 1226–1233, 2016.

[57] L. R. Keytel *et al.*, “Prediction of energy expenditure from heart rate monitoring during submaximal exercise,” *J. Sports Sci.*, vol. 23, no. 3, pp. 289–297, 2005.

[58] K. A. Ingraham, D. P. Ferris, and C. D. Remy, “Using Portable Physiological Sensors to Estimate Energy Cost for ‘Body-in-The-Loop’ Optimization of Assistive Robotic Devices,” in *2017 IEEE Global Conference on Signal and Information Processing, GlobalSIP 2017 - Proceedings*, 2018, pp. 413–417.

[59] T. Beltrame, R. Amelard, A. Wong, and R. L. Hughson, “Prediction of oxygen uptake dynamics by machine learning analysis of wearable sensors during activities of daily living,” *Sci. Rep.*, vol. 7, no. September 2016, pp. 1–8, 2017.

[60] J. Zhu, A. Pande, P. Mohapatra, and J. J. Han, “Using Deep Learning for Energy Expenditure Estimation with wearable sensors,” *2015 17th Int. Conf. E-Health Networking, Appl. Serv. Heal. 2015*, pp. 501–506, 2015.

[61] J. S. C. Figueiredo, “Smart Wearable Orthosis to Assist Impaired Human Walking,” University of Minho, 2019.

[62] “EXO-H2,” Arganda del Rey, Madrid, Spain.

[63] J. Cao, S. Q. Xie, R. Das, and G. L. Zhu, “Control strategies for effective robot assisted gait rehabilitation: The state of art and future prospects,” *Med. Eng. Phys.*, vol. 36, no. 12, pp. 1555–1566, 2014.

[64] J. Perry, *Gait Analysis: Normal and Pathological Function*. Thorofare, New Jersey: SLACK Incorporated, 1992.

[65] D. A. Winter, *BIOMECHANICS AND MOTOR CONTROL OF HUMAN MOVEMENT*, 4th Editio., vol. 2nd. Hoboken, New Jersey: John Wiley & Sons, Inc., 2009.

[66] K. K. Patterson, W. H. Gage, D. Brooks, S. E. Black, and W. E. McIlroy, “Evaluation of gait symmetry after stroke: A comparison of current methods and recommendations for standardization,” *Gait Posture*, vol. 31, no. 2, pp. 241–246, 2010.

[67] K. Shamaei, G. S. Sawicki, and A. M. Dollar, "Estimation of Quasi-Stiffness and Propulsive Work of the Human Ankle in the Stance Phase of Walking," *PLoS One*, vol. 8, no. 3, 2013.

[68] K. Molugaram, G. S. Rao, K. Molugaram, and G. S. Rao, "Chapter 5 – Curve Fitting," in *Statistical Techniques for Transportation Engineering*, 2017, pp. 281–292.

[69] J. Figueiredo, P. Félix, L. Costa, J. C. Moreno, and C. P. Santos, "Gait Event Detection in Controlled and Real-Life Situations: Repeated Measures from Healthy Subjects," *IEEE Trans. Neural Syst. Rehabil. Eng.*, vol. 26, no. 10, pp. 1945–1956, 2018.

[70] S. Kipp, W. C. Byrnes, and R. Kram, "Calculating metabolic energy expenditure across a wide range of exercise intensities: The equation matters," *Appl. Physiol. Nutr. Metab.*, vol. 43, no. 6, pp. 639–642, 2018.

[71] J. Brockway, "Derivation of formulae used to calculate energy expenditure in man," *Hum. Nutr. Clin. Nutr.*, vol. 41, no. 6, pp. 463–471, 1987.

[72] R. Das Gupta, R. Ramachandran, and N. Thomas, "Indirect Calorimetry: From Bench to Bedside," *Indian J. Endocrinol Metab.*, vol. 21, no. 4, pp. 594–599, 2017.

[73] M. M. Reeves, P. S. W. Davies, J. Bauer, and D. Battistutta, "Reducing the time period of steady state does not affect the accuracy of energy expenditure measurements by indirect calorimetry," *J. Appl. Physiol.*, vol. 97, no. 1, pp. 130–134, 2004.

[74] I. Goodfellow, Y. Bengio, and A. Courville, *Deep Learning*. .

[75] C. M. Bishop, *Pattern Recognition and Machine Learning*. Springer, 2006.

[76] L. R. Medsker and L. C. Jain, Eds., *Recurrent Neural Networks: Design and Applications*. CRC Press LLC, 2001.

[77] A. Mikami, "Long Short-Term Memory Recurrent Neural Network Architectures for Generating Music and Japanese Lyrics," *Comput. Sci. Dep.*, pp. 1–27, 2016.

[78] M. M. Mukaka, "Statistics corner: A guide to appropriate use of correlation coefficient in medical research," *Malawi Med. J.*, vol. 24, no. 3, pp. 69–71, 2012.